UNIVERSITY OF CALIFORNIA, MERCED

Ecological and Evolutionary Consequences of Extinction Dynamics on Island Communities

A dissertation submitted in partial satisfaction of the requirements for the degree Doctor of Philosophy

in

Quantitative and Systems Biology

by

Irina Birskis Barros

2024

Committee in charge:
Professor Sora L. Kim, Chair
Professor Jessica L. Blois
Professor John N. Thompson
Professor Justin D. Yeakel

The Dissertation of Irina Birskis Barros is approved, and it is acceptable in quality and form for publication on microfilm and electronically:

Prof. Justin D. Yeakel (Principal Advisor)

Prof. Sora L. Kim (Committee Chair)

Prof. Jessica L. Blois (Committee Member)

Prof. John N. Thompson (Committee Member)

University of California, Merced

2024

"Life shrinks or expands in proportion to one's courage."

(Anais Nin)

For all the women scientists who came before me,

and opened doors...

You expanded the (and my) world.

Thank you.

Artwork by Isabella Sinclair (1842-1900). Naturalist and scientific illustrator who published the first book with colored images of Hawaiian flowering plants (*Indigenous Flowers of the Hawaiian Islands*). She was one of the first to be concerned about the effects of invasive species on Hawaiian biodiversity. The plate here depicts Ōhia lehua (*Metrosideros polymorpha*), an endemic plant from Hawaii.

Contents

Acknowledgments

Somehow, for me, writing the three chapters in this dissertation was much easier than writing these acknowledgments. This is because I know that no matter how hard I try, there are no words sufficient to express my gratitude to everyone who helped me on this journey. I also want to say that I have been incredibly lucky throughout my PhD. I have met and worked with not only amazing scientists but also remarkable human beings who, like me, believe that science should be for everyone, everywhere, and who fight for equity in STEM.

With that being said, I want to start by thanking Justin, who stood by me through every step of my PhD. Justin is a genuine scientist, intrigued by every open question and able to think outside the box to explore possible answers. He made me enjoy the entire PhD process, which is no small thing, showing me how to treat science with the simplicity it deserves. He pushed me when needed, but in a way that boosted my confidence to stand on my own feet in science — and I shall continue walking. Thank you, Justin. I could never have asked for a better supervisor.

I owe a debt of gratitude to Ana Paula Assis (Paulinha), without whom this dissertation would not have been possible. Paulinha is one of the most brilliant evolutionary biologists I have ever met, and her passion for science and evolution is contagious! Not only did she help build my foundation in evolutionary biology, but our discussions throughout my PhD have guided me toward the path I want to pursue in academia. She has mentored and encouraged me, and I still have the luck to call her a friend. I do not have enough words to thank you, Paulinha!

I must thank my defense committee — Sora Kim, Jessica Blois, and John Thompson — who have not only helped refine my research but have also genuinely inspired me as a scientist. Thank you, Jessica, for challenging my thinking on how to address ecological and evolutionary questions, showing me how to build strong and logical statements. Thank you, Sora, for always being so willing to help, from discussing the struggles and joys of motherhood in an academic career to brainstorming about isotopes! I also owe an extra thank you to Sora for encouraging me to work on isotopes toward the end of my PhD and for offering all the tools at her disposal to ensure I would succeed in my (crazy) idea to work with honeycreepers. Thank you, John, for being such an amazing mentor since I started as a graduate student back in Brazil. John has always been willing to meet for scientific discussions throughout my academic journey and consistently offered brilliant insights that help me view problems, results, and ideas from perspectives I would not have considered otherwise. Every conversation we had was a valuable learning experience that inspires me to be a better scientist.

I must also thank, Taran Rallings, Megha Suswaram, Ritu VPS, Uttam Bhat, and Anna Almeida - Justin was able to build such an amazing team that made everything so much fun and easier! - I feel incredibly lucky to have had you as

my lab mates. I sincerely thank Sora's lab and Robin Trayler for their patience, kindness, and generosity towards me as a beginner in isotopes; I have learned so much from you! I also want to extend my gratitude to Mike Dawson, Helen James, and Gustavo Burin, who have contributed at different stages of building my research.

I cannot express how grateful I am to have my family as my rock and safety net. Thank you to my mom and dad, Lais and Aguinaldo, and to my brother, Plínio; without you, nothing would be possible. You make me stronger! Of all the blessings in my life, the greatest is having you as my family. I love you all deeply.

Thank you, Yannick, who arrived at the end of my PhD journey, challenging the dimension of time. Thank you, my son, for introducing me to Neverland — a place I visited often to clear my mind and be reminded of what truly matters...

Most of all, I want to thank my husband, Nicolas, who goes above and beyond to ensure that not only my dreams come true but that I continue dreaming. You inspire me every day, and your love fuels my motivation to be better. I truly have no words to thank you enough. Meu coração é seu!

Artwork by Maria Sibylla Merian (1647-1717), a naturalist and scientific illustrator who traveled alone at her own expense with her daughter to South America to explore the biological diversity of Suriname. She expanded knowledge of natural history and was one of the first to observe and document the process of insect metamorphosis.

Abstract

Islands have long captivated evolutionary and ecological biologists, especially since Darwin's pivotal insights on natural selection during his visit to the Galapagos Islands. While islands account for only 6% of the Earth's land area, they harbor 20% of global species diversity, hosting many endemic species and unique morphological diversity, providing textbook examples of adaptive radiation. However, island biodiversity has been severely affected during the Anthropocene, with three out of four island species becoming extinct, with the disappearance of the dodo (*Raphus cucullatus*) in the 17th century being one of the first recognized human-caused extinctions on islands. The extinction of a species can profoundly affect an entire ecosystem, leading to changes in both ecological and evolutionary dynamics. Focusing on the evolution of morphological traits, I combined theoretical and empirical approaches to explore the ecological and evolutionary consequences of extinctions on island communities. In Chapter 1, I explored the interplay between colonization, extinction, and coevolution, and how these intersecting dynamics shape species' traits and the structure of mutualistic networks on islands. For that, I used a stochastic mathematical model, integrating Island Biogeography Theory with coevolutionary dynamics. My results show that as extinction rates increase, the number of interactions needed for a species to achieve maximum persistence on the islands also rises, but only up to a threshold. Moreover, islands with higher extinction rates have species with greater trait similarity. In Chapter 2, I used data from historical Hawaiian honeycreepers, a group of Hawaii-endemic birds that have lost several species in the last century. I test whether greater morphological variation and larger niche breadth increases resilience to extinction in each species. Using geometric morphometrics and stable isotope ratios, I show that within guilds, species that have gone extinct exhibited lower morphological variation. Lastly, in Chapter 3, I used phylogenetic comparative methods to investigate the evolution of beak shape in the Hawaiian honeycreepers and the loss of unique adaptive peaks with species extinctions. I show that the extinction of Hawaiian honeycreepers is leading to a drastic reduction in the occupied morphospace, resulting in a homogenization in their trait space, which can directly impact ecosystem functioning and the provision of ecosystem services, such as seed dispersal. Taken together, my dissertation broadens the understanding of how extinction can affect both ecological and evolutionary dynamics of island communities.

List of Figures

List of Tables

Irina Birskis Barros

1 Education

University of California, Merced, Merced, CA USA

- Ph.D. in Quantitative and Systems Biology (2018-2024)
  Thesis: Ecological and Evolutionary Consequences of Extinction Dynamics on Island Communities
  Supervisor: Justin D. Yeakel

Universidade de São Paulo, São Paulo, Brazil

- Master's degree in Ecology (2015-2017)
  Thesis: Evolutionary dynamics of mimetic rings
  Supervisor: Paulo R. Guimarães
- Bachelor's degree in Educational Biology (2012-2015)
- Bachelor's degree in Biology (2009-2013)
  Thesis: Rarity in snakes: a case study with New World Vipers
  Supervisor: Marcio Martins

2 Publications

Peer reviewed

- Camacho, L., Andreazzi, C., Medeiros, L., **Birskis-Barros, I.**, Emer, C., Reigada, C., Guimarães, P.R. Jr. 2022. Cheating interactions favor modularity in mutualistic networks. *Oikos*, e09176.
- **Birskis-Barros, I.**, Freitas, A.V.L. and Guimarães, P.R. Jr. 2021. Habitat generalist species constrain the diversity of mimicry rings in heterogeneous habitats. *Scientific Reports*, 11, 5072.
- **Birskis-Barros, I.**, Alencar, L.R.V., Prado, P.I.K.L., Böhm, M., Martins, M. 2019. Ecological and conservation correlates of rarity in New World pitvipers. *Diversity*, 11(9), 147.

Other types

- Gaiarsa, M.P., Sebastián-González, E., Mortara, S.R., Martins, A.B., Maia, K., Marquitti, F.M.D., Lemos-Costa, P., Castanho, C., **Birskis-Barros, I.**, Astegiano, J., Assis, A.P.A., Andreazzi, C.S., Alencar, L. 2019. The role of sorority in building collective science, *Science*, eLetter.

In preparation

- **Birskis-Barros, I.**, Assis, A.P.A., Kim, S., James, H.F., Yeakel, J. Exploring the relationships between morphological variation, dietary breadth, and patterns of extinction among Hawaiian Honeycreepers (Drepanididae) *Target journal: Am. Nat.*
- **Birskis-Barros, I.** & Yeakel, J. Island Biogeography Theory of Coevolution in pollination networks. *Target journal: Proc. B.*
- **Birskis-Barros, I.**, Freitas, A.V.L., Gaiarsa, M.P., Raimundo, R.L.G, Guimarães, P.R.Jr. A network approach to the evolutionary dynamics of butterflies' color patterns. *Target journal: Ecology*

3 Funding and Awards

- 2024 - QSB Summer Research Fellowship **(U$5000.00)**
- 2024 - Advance Doctoral Candidate Fellowship **(U$23857.30)**
- 2023 - Miguel Velez Scholarship**(U$10000.00)**
- 2023 - Alternate in the American Association of University Women (AAUW) International Doctoral Degree Fellowship
- 2023 - QSB Summer Research Fellowship **(U$4900.00)**
- 2022 - UC Merced Academic Senate Faculty Research Grants Program **(U$5000.00)**
- 2022 - QSB Graduate Research Improvement Award **(U$1500.00)**
- 2021 - QSB Remote Teaching and Research Fellowship **(U$1000.00)**
- 2020 - QSB Summer Research Fellowship **(U$7012.00)**
- 2019 - QSB Travel Award UC Merced **(U$800.00)**
- 2019 - QSB Summer Research Fellowship **(U$5,800.00)**
- 2014 - CAPES: Teaching Initiation Scholarship **(R$ 4,800.00)**
- 2013 - FAPESP: Undergraduate Fellowship - UK Internship **(U$10,284.40)**
- 2012-2013 - FAPESP: Undergraduate Fellowship **(R$5,784.90)**
- 2010-2011 - FAPESP: Undergraduate Fellowship **(R$6,256.80)**.

4 Invited Talks/Lectures

- **2021** - Talk: "Coevolution and assembly of mutualistic systems: from mimetic rings to island biogeography" - Center for Ecology, Evolution and Biogeochemistry, Eawag, Switzerland.
- **2021** - Lecture: "Conservation & Species Interactions" - *Fundamentals of Ecology*, University of California, Merced, CA, USA.
- **2019** - Talk: "Trait convergence and diversity in species-rich interactions: habitat use and heterogeneity affect coevolution of mimetic species" - *Interaction networks and trait evolution - 43rd New Phytologist Symposium*, University of Zürich, Switzerland.

5 Professional Experience

Research Experience

- 2022 - Summer Internship at US Department of Energy (DOE) Joint Genome Institute (JGI);
- 2017-2018, Laboratory manager - Paulo R. Guimarães' lab;
- Feb-Aug 2013, Internship at the Indicators & Assessments Unit in the Institute of Zoology, Zoological Society of London (IoZ-ZSL). Under Monika Böhm and Ben Collen supervision;
- July 2011, Intership at the Centro de Investigaciones Biológicas del Noroeste, S.C., México. Under Gustavo Arnaud supervision;

Field Experiences

- 2009-2011, Atlantic Forest of Southeastern Brazil. Participated in field trips to collect data on habitat use of reptiles and amphibians;
- July 2011, Baja California Desert and islands of Golfo California and Pacific. Worked with natural history of *Crotalus*;
- January 2011, Pantanal. Colected specimens of amphibians and reptiles;

Teaching Experience

- Fall 2023, Sring 2023, Fall 2022, Spring 2022, Fall 2020, Fall 2018 - Teaching assistant, *Fundamentals of Ecology*, University of California, Merced, CA, USA (3 semesters);
- Fall 2021, Spring 2020, Fall 2019, Spring 2019 - Teaching assistant, *Contemporary Biology*, University of California, Merced, CA, USA(4 semesters);
- Spring 2021 - Teaching assistant, *The Natural History of Dinosaurs*, University of California, Merced, CA, USA;
- 2015, Teaching assistant, *Diversity, Natural History and Conservation of South American Vertebrates*. University of São Paulo, Brazil;
- 2011-2012, Teaching assistant, *Community Ecology*. University of São Paulo, Brazil;

6 Complementary Education

- 2024, Transmitting Science - Mapping trait evolution
- 2020, ICTP - The Abdus Salam International Centre for Theoretical Physics, Italy - Winter School on Quantitative Systems Biology: Quantitative Approaches in Ecosystem Ecology;
- 2020, ICTP-SAIFR School on Community Ecology: from patterns to principles. International Center of Theoretical Physics, São Paulo, Brazil;
- 2019, Software Carpentry Workshop - Unix Shell, Version Control with Git, Plotting and Programming in Python. University of California, Merced, CA, USA;
- 2018, Introduction to Dynamical System and Chaos. Santa Fe Institute's Massive Open Online Course;
- 2017, IV Workshop in Ecology and Evolution of species interactions, Tapiraí, SP, Brazil. Professors invited: John N. Thompson, Pedro Jordano, Flávia Marquitti, Mauro Galetti, Mathias Pires, Paulo R. Guimarães Jr.;
- 2016, III Workshop in Ecology and Evolution of species interactions, Cananéia, SP, Brazil. Professors invited: John N. Thompson, Pedro Jordano, Patricia Morellato, Rodrigo Cogni, Paulo R. Guimarães Jr.;
- 2016, Software Carpentry Workshop. Introduction to the use of Shell Programming and Rmarkdown. University of Campinas, São Paulo, Brazil;
- 2015, IV Souther-Summer School on Mathematical Biology, UNESP & International Centre of Theoretical Physics, São Paulo, Brazil;

7 Conference Presentations

- **Birskis-Barros, I**, Assis, APA, James, HF, Kim, S & Yeakel, J.D. 2024. Exploring the relationships between morphological variation, dietary breadth, and patterns of extinction among Hawaiian Honeycreepers (Drepanididae). Poster presentation. 3rd Joint Congress on Evolutionary Biology, Montreal, QC, Canada.
- **Birskis-Barros, I** & Yeakel, J.D. 2022. Coevolution during the assembly process of mutualistic networks on islands. Contributed Talk in an Organized Oral Session (Integrating Empirical and Theoretical Approaches in Mutualistic Networks). ESA Annual Meeting, Montreal, Canada;
- **Birskis-Barros, I**, Freitas, AVL & Guimarães, Jr. PR. 2019. Trait convergence and diversity in species-rich interactions: habitat use and heterogeneity affect coevolution of mimetic species. Poster presentation. 43rd New Phytologist Symposium: "Interaction networks and trait evolution", University of Zürich, Switzerland.
- **Birskis-Barros, I**, Freitas, AVL & Guimarães, Jr. PR. 2017. Habitat heterogeneity and generalism shape the evolution of mimetic rings. Contributed Talk. ESA Annual Meeting, Portland, Oregon, USA;
- **Birskis-Barros, I** & Martins, M. 2011. Rattlesnakes' diet: ecological and evolutionary aspects. Poster presentation. IX Latin-American Herpetological Conference, Curitiba, Brazil;

8 Ad hoc reviewer

- Perspectives in Ecology and Conservation

9 Services

- 2022 - Talaria Summer Institute (TSI) - Mentorship program for female and genderqueer high school students.
- 2020 - 2022 - UC Merced Graduate Student Representative on the Chancellor's Advisory Committee on the Status of Women (CACSW).
- 2021 Girls Who Code Club - James Enochs High School, Modesto, CA - Helping middle schoolers girls to learn how to code. This program aims at reducing the gender gap in STEM.
- 2020 Brazil COVID-19 Observatory - A scientific group formed to help Brazilian government to take better decisions to overcome COVID-19. (*in portuguese*)
- 2011-2013 - Director of the Student Association of the Biological Institute - University of São Paulo
- 2012 - Director of the Students Association of the University of São Paulo
- 2010-2012 - Undergraduate Student Representative on the Department of Ecology at the University of São Paulo
- 2009-2013, Co-Founder and Project Coordinator - "Bio na Rua" ("Biology in the Street"), Biological Institute at University of São Paulo, São Paulo, Brazil

Chapter 1

"We especially need imagination in science. It is not all mathematics, nor all logic, but it is somewhat beauty and poetry"

(Maria Mitchell [1], 1818-1889).

[1]First American scientist to discover a comet ("Miss Mitchell's Comet") and first female astronomy professor. She strongly advocated for science and math education for girls and she became involved in both anti-slavery and suffrage movements.

Chapter 1

Island Biogeography Theory of Coevolution in pollination networks

1 Abstract

Island ecosystems have been pivotal in understanding community assembly and biodiversity, from the competing roles of colonization and extinction, to the influence of spatial structure, species interactions, and evolutionary processes. Network theory has helped our understanding of how ecological interactions shape island biogeography dynamics, using empirical and theoretical studies to explore species-rich island community structures. Mutualistic networks on islands differ from those on the mainland by supporting fewer species and more super-generalists, resulting in a more nested community structure. Coevolution, the reciprocal adaptation between interacting species, can shape traits and interactions within these networks, influencing their assembly. Here we explore how colonization, extinction, and coevolution can intersect to shape species traits and the structure of mutualistic networks. Using a stochastic dynamic model, we integrate Island Biogeography Theory with coevolutionary dynamics, examining pollination networks to understand trait-matching in evolving communities. Our results show that highly nested and connected mainland communities contribute to greater instability on islands, particularly under intermediate extinction rates. While super-generalist species persist longer, their persistence does not greatly exceed those species with fewer interactions beyond a threshold, which itself varies with the extinction rate. Additionally, coevolution leads to greater trait-similarity within communities on islands. Our findings highlight the critical role of coevolution in shaping island communities, especially on small islands where the extinction rate is expected to be elevated.

2 Introduction

Island ecosystems have long played a critical role in our understanding of community assembly, offering insights into the dynamic processes shaping biodiversity. MacArthur & Wilson (1967) proposed the influential Theory of Island Biogeography, describing how colonization and extinction processes can influence island biodiversity over time, leading to species turnover and the eventual attainment of equilibrial community richness. Many empirical studies have demonstrated where these theoretical insights align with observations of island community assembly, as well as inherent limitations. For example, factors such as archipelago structure and history (Whittaker *et al.*, 2008; Aguilée *et al.*, 2021), speciation (Valente *et al.*, 2020), and the structure and dynamics of species interactions (Gravel *et al.*, 2011)

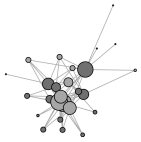

are critical components that also shape island communities, expanding beyond the original scope of the theory.

Species interactions not only constrain the distribution of species, but can also facilitate species coexistence (Vellend, 2008; Palmer *et al.*, 2013). The effects of multiple species interactions and the complex structure of ecological systems can be investigated using tools from network theory (*e.g.* Donatti *et al.*, 2011; Valdovinos & Marsland III, 2021; Birskis-Barros *et al.*, 2021). In this sense, ecological communities can be represented as networks in which species represent nodes of the network and if they interact, are connected by edges, or links. An edge connecting two species can represent many different types of relationships, but is often used to denote energetic or biomass flow transferred between a consumer and resource species engaged in a trophic interaction (Hale *et al.*, 2020; Valdovinos *et al.*, 2023). Advances in network theory have deepened our understanding of how ecological interactions shape island biogeography dynamics, with both empirical and theoretical studies applying these concepts to explore the structure of species-rich island communities (Sugiura, 2010; Castro-Urgal & Traveset, 2014; Massol *et al.*, 2017; Vidal *et al.*, 2020). For example, Gravel *et al.* (2011) demonstrated the importance of integrating food web structure into the classical Island Biogeography Theory model to improve predictions of real community composition on islands. By incorporating the assumption that a consumer species must have at least one prey species present to colonize the island and that losing all prey results in extinction, they showed that the structure of the food web can play a crucial role in determining the species richness of island communities (Gravel *et al.*, 2011).

While trophic interactions describe antagonistic relationships between consumers and their resources, mutualistic interactions account for reproductive services provided to the resource species. Mutualistic interactions often describe an interaction between species where one receives a service (the service receiver) while the other receives a reward for facilitating the service (the service provider). In plant-pollinator interactions, this service is reproductive, where the pollinator delivers pollen to the stigma of female plants, while the reward is energetic, often in the form of nectar. This results in a fitness benefit to both species, and plays a fundamental role in generating and maintaining local biodiversity (Bronstein, 2015). Mutualistic interactions can serve to minimize competition between species (Elias *et al.*, 2008; Bastolla *et al.*, 2009) and in some cases increase the diversity of the community (Valiente-Banuet & Verdú, 2007). The abundance of mutualistic interactions can be substantial in many systems. For example, more than 90% of tropical plants depend on animals for dispersing their seeds, and many plants depends on animals to pollinate their flowers (Bawa, 1990; Jordano, 2000).

Mutualistic systems can be depicted by a bipartite network (Memmott, 1999), consisting of two sets of nodes – here denoting service providers, or pollinators, and service receivers, or plants – and where links between them identify a mutualistic dependence. These networks have been observed to display consistent patterns in their structure, suggesting a common yet enigmatic process governing their assembly (Bascompte *et al.*, 2003; Krishna *et al.*, 2008; Encinas-Viso *et al.*, 2012;

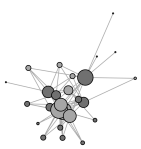

Minoarivelo & Hui, 2016). Specifically, networks of mutualistic species tend to have a highly nested structure, where specialist species interactions tend to be subsets of generalist species interactions (Jordano, 1987; Lewinsohn *et al.*, 2006; Bascompte & Jordano, 2007). Nestedness is an important structural characteristic, as it lowers the intensity of interspecific competition, increasing the number of species that can coexist (Bastolla *et al.*, 2009), promoting diversity. Of particular importance in island systems — where species arrivals and extinctions occur at an accelerated pace — is how these dynamics influence the structure and function of mutualistic communities. Understanding how such dynamics shape the nested architecture of mutualistic networks can shed light on the processes that support ecological resilience in island ecosystems.

Compared to mainland mutualistic systems, those on islands are less diverse, have a lower ratio of pollinator to plant species and a higher number of supergeneralists (*i.e.*species with many interactions)(Olesen *et al.*, 2002; Traveset *et al.*, 2016; Trøjelsgaard & Olesen, 2016). These supergeneralists can play a critical role in shaping the structure of mutualistic networks by increasing the density of interactions (*i.e.*, higher connectance) and promoting network nestedness (Kaiser-Bunbury *et al.*, 2010; González-Castro *et al.*, 2012; Traveset *et al.*, 2016). For example, Trøjelsgaard *et al.* (2013), used island ages as a proxy for the temporal assembly process and showed that recently formed island communities hosted a larger number of generalist pollinators, whereas more established island communities had larger numbers of specialized pollinators and plants.

Remote oceanic islands have provided unique opportunities to integrate ecological and evolutionary dynamics, enhancing our understanding of how diverse ecological communities are formed and maintained (Gillespie, 2016). On islands, speciation plays a crucial role in generating species diversity, with island communities shaped by the interplay of immigration, speciation, and extinction rates (Losos & Ricklefs, 2009; Whittaker *et al.*, 2008). Losos & Schluter (2000) demonstrated that on smaller islands, speciation events are rare, such that immigration is the primary source of new species. However, on larger islands (greater than 3,000 Km^2), speciation surpasses immigration as the dominant driver of species diversity, with the rate of speciation increasing proportionally with island area (Losos & Ricklefs, 2009). Additionally, the number of species generated through speciation only exceeds those arriving through immigration when the speciation rate is greater than half of the extinction rate (Chen & He, 2009). Although very insightful, we still need to scale down to better understand how evolutionary dynamics shape species traits and alter the adaptive landscape, while communities are still being shaped by ecological dynamics, such as immigration and extinction, on islands.

As mutualistic species interact they alter the fitness landscape, influencing the selective forces operating across species (Cosmo *et al.*, 2023). And because species are connected in a network, the coevolutionary changes impacting species that do not interact directly with a particular pollinator or plant (the indirect effects) can often be just as influential as those that do (Guimarães *et al.*, 2017). These pro-

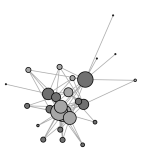

cesses may feed back to alter the forces governing the dynamics of colonization and extinction, introducing a great deal of complexity to coevolving mutualistic island communities. For example, coevolution can favor trait-matching between species, such as the size of the nectar tube in plants and the size of the proboscis among insect pollinators (Ehrlich & Raven, 1964; Thompson, 1994; Pauw *et al.*, 2009). Indeed, this is the subject of Darwin's famous insight into the proboscis length of the then unknown pollinator of the star orchid *Angraecum sesquipedale* (Arditti *et al.*, 2012). However, a key challenge lies in understanding how coevolution influences not only a pair of interacting species, but a diverse and ever-changing community. Coevolution can lead to trait matching between species of different guilds, even when they are components of a larger and more complex mutualistic network (Newman *et al.*, 2014; Biddick & Burns, 2018). Over time, the evolution of traits mediating mutualistic interactions can have profound impact on the eventual structure of the community (Stang *et al.*, 2009; Nuismer *et al.*, 2013; Chamberlain *et al.*, 2014). In fact, trait-matching between plant and pollinating birds has been shown to be directly predictive of island network structure (Biddick & Burns, 2018), while indirect interactions are fundamental to the coevolutionary dynamics of mutualistic networks, especially in nested communities (Guimarães & Deyn, 2016).

Here we aim to understand how mutualistic networks assemble into island communities. We integrate colonization and extinction dynamics into a stochastic model of trait coevolution to uncover how the reciprocal nature of the selective forces driving trait-matching between interacting species influence the assembly process, and vice versa, to alter the composition and stability of evolving communities. Specifically, we aim to address three main questions. First, how do extinction rates influence the structure of mutualistic networks and the mean trait of species on islands? Second, does the structure of the mainland community (source) influence that of assembling island communities? And third, does coevolution, when governing the extinction process, play a significant role in shaping the structure of mutualistic networks of island communities? Our investigation contributes to a deeper understanding of community assembly processes and informs conservation efforts aimed at preserving ecosystem function and biodiversity in island systems.

3 Methods

We begin with an interaction network between two groups of species: those delivering a reproductive service while receiving trophic rewards (*e.g.* pollinators), and those receiving a reproductive service and providing trophic rewards (*e.g.* pollinating plants). This bipartite network is specified by the adjacency matrix $\mathbf{A}$, where the rows i of the matrix represent plant species and the columns j represent animal pollinator species for a given mutualistic system. If two species engage in a mutualistic interaction, the matrix element $a_{ij} = 1$; and is zero otherwise. Throughout we will simulate evolutionary dynamics of species assembling into an island community. While the composition of species in the island community de-

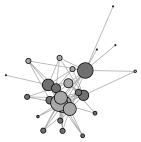

pends on those who have successfully colonized, their interactions with each other are assumed to be as observed in the full empirical community on the mainland. Within each system, we evaluate the dynamic structure of the island community as species colonize and go extinct, and as the mutualistic traits of species coevolve over time, where species' traits are assumed to determine the efficacy of each pairwise mutualistic interaction. Each species' trait is represented by a quantitative character where trait-matching between plant and pollinator is presumed to maximize fitness. In other words, in a simple interaction pair, without the confounding effects of the community, the traits of plant and pollinator species will eventually evolve to match, where, for example, the size of the pollinator's proboscis will evolve to fit the the length of the plant's nectar tube, and vice versa.

3.1 The dynamics of coevolutionary assembly

We investigate the combined effect of trait coevolution in a mutualistic system as it assembles and evolves from an established mainland community. Throughout, we assume that the traits of species in the mainland community have reached a coevolutionary steady state prior to the assembly process (cf. Guimarães *et al.*, 2011), and that the mutualistic structure of species present in the assembling community are invariant with respect to the mainland. So while the presence/absence of interactions between coexisting species are the same as those on the mainland, the existence of an interaction is contingent on the co-occurrence of both species in the assembling community, and the interaction is absent if one of the pair is not present on the island. To establish mainland communities, we used 50 empirical pollinator-plant networks from the Web of Life database (http://www.web-of-life.es/), introducing a wide range of network topologies and localities, ranging from Argentina to Canada (Table S1). We did not include empirical island networks, as we intended the network assemblage to represent mainland systems from which simulated island communities were assembled.

The mainland community represents the pool from which the island community is assembled. After finding the deterministic steady state of the mainland community following Guimarães *et al.* (2011), we allowed a species i to assemble into a novel community, arriving with the mean trait value Z_i, initially obtained from the corresponding steady state mainland value. While the mainland steady state is found deterministically, assembly of the island community follows a stochastic process, where species colonize, coevolve, and suffer extinction with probabilities that change with the richness of the community. Following the MacArthur-Wilson Species Equilibrium Model (MacArthur & Wilson, 1963), colonization rates are assumed to decrease as the number of species on the island increase, whereas extinction rates - as well as coevolutionary rates - increase with the number of colonized species. We next detail how colonization, coevolution, and extinction change with the state of the assembling community, and whether and to what extent they depend on species' mutualistic traits.

Colonization. The assembly process is initiated by colonization, where a mu-

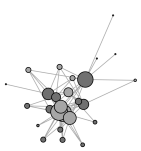

tualist pair, consisting of both a plant and pollinator, is randomly selected from the mainland network to colonize the system. The colonization of subsequent species requires the presence of at least one mutualist partner in the island community. So while the mainland community defines the full suite of potential mutualistic partners for a given species, it is only capable of colonizing the island community if at least one of those potential partners is present on the island. Each colonization event consists of a single species being transported to the island system. Once the species colonizes the island, it realizes the subset of its potential mutualistic interactions allowed by its mutualistic partners in the island community, potentially facilitating additional future colonizations.

Coevolution. The trait coevolutionary process follows that of Guimarães *et al.* (2011), where we track the mean value of a quantitative trait for each species i, Z_i^t, which evolves in one generation t to the next $(t+1)$, and is initialized from the species-specific steady state mainland value. The trait Z_i is assumed to have heritability h^2 and its total additive phenotypic variance in the population is given by σ_f^2, which is assumed to be the same across species. Heritability is defined as $h^2 = \sigma_g^2/\sigma_f^2$, where σ_g^2 is the total additive genetic variance, and we assume throughout that σ_g^2 is constant over time and equal for all species. Trait values for each species change over time due to both mutualistic selection exerted by species j, denoted as M_{ij}, and environmental selection on species i, E_i, such that the trait dynamic can be written in discrete time as

$$Z_i^{t+1} = Z_i^t + h^2\sigma_f^2(M_{ij}^t + E_i^t). \tag{1}$$

We assume that mutualistic selection favors trait-matching, such that

$$M_{ij}^t = \sum_{j=1}^{N} q_{ij}^t \gamma_{ij}^t, \tag{2}$$

where γ_{ij} is the 'trait mismatch' between species i and j, where $\gamma_{ij}^t = \sqrt{(Z_j^t - Z_i^t)^2}$. We note that $\gamma_{ij}^t = 0$ if the trait values of interacting species are equally matched, reaching a fitness maximum, and $\gamma_{ij}^t \gg 0$ if they are mismatched. q_{ij}^t is the impact that each interaction has on the mutualistic selection differential, such that

$$q_{ij}^t = m_i \frac{a_{ij} e^{-\alpha(\gamma_{ij}^t)}}{\sum_{j=1}^{N} a_{ij} e^{-\alpha(\gamma_{ij}^t)}}, \tag{3}$$

where m_i is the strength of mutualistic selection, a_{ij} is the corresponding element of the adjacency matrix, and $\alpha(\gamma_{ij}^t)$ is a scaling parameter controlling the sensitivity of mutualistic selection to trait matching. In other words, q_{ij} is the relative evolutionary effect of species j on species i in relation to all of its interacting partners, ranging from 0 (no interaction) to 1. Because the island community is a subset of that of the mainland, the mutualistic selection (M_{ij}) exerted on species i will differ accordingly, favoring trait-matching of species present in the island community at a given point in time (see Eq. 2), diverging from the mainland steady state where all species are present.

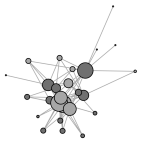

The environmental effect on the mutualistic trait for species i selects towards an environmental optimum θ_i. For simplicity, we assume that species i on the mainland and the island will have the same θ_i value, suggesting that the mainland and on the island environments are similar. Environmental trait optima are randomly chosen from a uniform distribution between 0 and 1 for each species and kept constant over the course of a given simulation. The environmental effect on selection is then defined as

$$E_i^t = (1 - \sum_{j=1}^{N} q_{ij}^t)(\theta_i - Z_i^t), \tag{4}$$

where $1 - \sum_{j=1}^{N} q_{ij}^t$ is the strength of the environmental selection.

Combining equations 1, 2, 4, along with $h^2 = \sigma_g^2/\sigma_f^2$ we obtain the full trait dynamic

$$Z_i^{t+1} = Z_i^t + \sigma_g^2[\sum_{j=1}^{N} q_{ij}^t(\gamma_{ij}^t) + (1 - \sum_{j=1}^{N} q_{ij}^t)(\theta_i - Z_i^t)]. \tag{5}$$

Primary extinction. Local extinctions are introduced as a stochastic process, where species are removed from the island community, but can recolonize at a later point in time. We distinguish primary extinctions from secondary extinctions, the latter of which occurs subsequent to a primary extinction. We examined two primary extinction scenarios: random extinctions, where all species have the same probability of going extinct, and trait-based extinctions, where the probability of extinction increases with the mismatch of plant and pollinator traits (higher γ_i).

Following optimal foraging assumptions (Krebs *et al.*, 1983), we assume that increased mismatch between a mutualistic pair results in lower interaction efficiency. We can formalize this notion by assuming that lower interaction efficiency means a longer average handling times performing mutualistic services, reducing the species' net reward (Pimm & Pimm, 1982; Maglianesi *et al.*, 2014; Klumpers *et al.*, 2019b). While we do not simulate individual interactions in our model, we can use this formalization to derive the probability of extinction as a function of trait mismatch between species i and j, γ_{ij}. If we assume that mutualistic interactions between a pollinator i and its set of mutualistic partners results in some net profitability (measured as either energetic or reproductive reward), its expectation can be written as

$$\mathrm{E}\{P_i\} = \frac{g}{\mathrm{E}\{T_i\}}, \tag{6}$$

where we formalize $\mathrm{E}\{\cdot\}$ as an expectation and denote g as the gain, assumed to be constant, and $\mathrm{E}\{T_i\}$ as the expected time a species spends in a pollination interaction. The time a pollinator i expends visiting N partner species, T_i, is a function of its trait mismatch relative to the plants j it is pollinating, and can be written as

$$T_i = a + \frac{b}{N} \sum_{j=1}^{N} \gamma_{ij}. \tag{7}$$

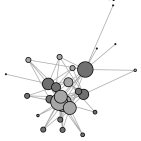

Here, a represents the mean handling time if mutualistic partners are perfectly matched ($\gamma_{ij} = 0$), and b represents the effect of dissimilarity on increases to the temporal cost, where for simplicity we assume a linear relationship. We also assume for simplicity that each potential mutualistic partner has equivalent values of a and b.

As species' traits vary, the dissimilarity of a pollinator's trait with respect to its mutualistic partners can be treated as a random variable. A species i thus has a distribution of dissimiliarity values with its set of mutualistic partners, and because these values are constrained between 0 and 1, we can assume they can be described by a beta distribution with expectation $\mathrm{E}\{\gamma_i\}$ and variance $\mathrm{Var}\{\gamma_i\}$. From this, we first derive the expected interaction time a pollinator spends with its mutualistic partners, $\mathrm{E}\{T_i\}$, and approximate the expected profitability as

$$\mathrm{E}\{P_i\} = \frac{g}{\mathrm{E}\{T_i\}} \approx \frac{g(na^2 + 2nab\mathrm{E}\{\gamma_i\} + b^2(n\mathrm{E}\{\gamma_i\}^2 + \mathrm{Var}\{\gamma_i\})}{n(a + b\mathrm{E}\{\gamma_i\}^3)}, \tag{8}$$

where the expectation and variance of a species' dissimilarity with its interacting partners describes its dissimiliarty distribution at a given point in time (see Supplemental Materials for a detailed derivation). While we have illustrated derivation of the expected profitability for a mutualistic service providers, the profitability for service receivers can be estimated in the same way, though with the appropriate change in units, which may be reproductive rather than energetic. We note that this specification serves two important purposes. First, it provides a mechanistic linkage between a quantity with specific ecological and energetic importance (profitability) to the more abstract notion of trait mismatch. Second, while we do not directly connect energetic parameters to empirical systems here, Eq. 8 provides a means to do so, bridging the theory explored here to potential application to mutualistic communities in nature.

The expected profitability for species i, $\mathrm{E}\{P_i\}$, is the expectation of a profitability distribution that remains unspecified. Regardless, we can assume that as the expected profitability declines (as, for example, mutualistic partners become more mismatched), the probability of extinction will increase. If the the unspecified profitability distribution is Gaussian in nature (where $P_i \sim \mathrm{Gauss}\{\mathrm{E}\{P_i\}, \sigma_{P_i}\}$), the probability that a species' profitability will fall below some critical threshold χ, inducing extinction, can be written

$$p_i^{\mathrm{ext}} = \frac{1}{2}\mathrm{Erf}\left(\frac{E\{P_i\} - \chi}{\sqrt{2}\sigma_{P_i}}\right), \tag{9}$$

where Erf() is the error function. This exercise allows us to directly translate the dissimilarity distribution for a species i to a probability of extinction as a function of trait mismatch, which in this case increases sigmoidally with trait dissimilarity.

Secondary extinction. Following primary extinctions, which could either be determined by randomly selecting species for extinction, or by calculating the probability of extinction based on trait mismatch (Eq. 9), secondary extinctions may result. Secondary extinction occurs when a species loses all of its interacting

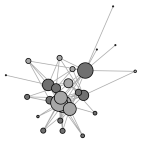

partners, leaving it disconnected from the island community. In the case of a pollinator, this means that its energetic gain is eliminated; in the case of a pollinating plant, this means that its reproductive potential cannot be met. We assume that secondary extinctions follow primary extinctions in the same time step, implicitly assuming plants are annual, rather than perennial species. Moreover, this means that mutualistic interactions are facultative, except in the case where only a single interaction remains. By including both primary and secondary extinctions, we acknowledge the possibility of extinction cascades, where the loss of a single species can ripple through and cause extinctions across many others.

Table 1: Parameters, descriptions, and set values or range.

Parameters	Description	Values
Z_i^t	Mean trait value of species i at time t	var.
h^2	Heritability	0.1
m_i	Strength of mutualistic selection	0.4
α	Scaling factor of trait matching	0.2
θ_i	Environment optima for species i	(0,1)
r_{col}	Colonization rate	1
r_{evol}	Coevolution rate	1
r_{ext}	Extinction rate	0.3, 0.6, 0.9
a	Mean handling time	1
b	Effect of dissimilarity	1
g	Energetic gain of mutualistic interaction	100

3.2 Stochastic assembly algorithm

We implement colonization, coevolution, and extinction processes using a Gillespie Algorithm (see Supplementary Materials for details), where the rates $r_j q_j$ of all possible events j (here, colonization, coevolution, and extinction) are computed in a given step, where r_j are assigned constants to modify the likelihood of event j, and where q_j represents the number of species prone to event j. The time at which the next event happens is calculated by drawing a random number from an exponential distribution with mean $1/\sum_j r_j q_j$. A randomly selected event then occurs from the set of possible events such that the probability of event x is $q_x r_x / \sum_j q_j r_j$, whereas the time interval over which this occurs is given by $\Delta t = 1/\sum_j q_j r_j$. The effect of the event is then implemented and the list of possible events is updated for the next step. This algorithm offers a much better approximation to the true stochastic continuous time process than a simulation in discrete time steps, while providing a much higher numerical efficiency (Gillespie, 1977).

To explore the dynamics of the system, we simulated each network for 5000 time steps (where an event occurs at each step in accordance with the Gillespie algorithm), which we visually confirmed was enough to avoid transient effects. For

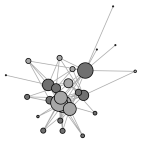

each of the 50 empirical mainland plant-pollinator networks, we implemented 1000 replicates for both random and trait-based extinction scenarios and our results report the mean of these 1000 replicates for each network. Throughout, we set the rate of colonization $r_c = 1$ and the rate of evolution $r_{evol} = 1$. We varied the effect of increasing primary extinction rates relative to those set for colonization and coevolution, from low ($r_{ext} = 0.3$), to medium ($r_{ext} = 0.6$), to high ($r_{ext} = 0.9$). For the summary of model parameters see Table 1.

4 Results

4.1 The structure of island communities

Our theoretical framework generally reveals fast initial assembly of the community, where species richness S sharply increases to oscillate around a steady state value S^*, the value of which varies across mainland networks (Figure 1A and S1). Because different mainland communities range widely in species richness, we compare the effects of assembly across networks by assessing relative richness S/P, or the richness attained on the island S relative to that of the mainland P. While island communities assemble to, and oscillate around, a steady state in species richness relatively quickly, the amplitude of fluctuations also varies from network to network. While temporal fluctuations (*i.e. oscillations*) in relative island community richness may be expected to be larger for less diverse networks, the coefficient of variation (CV_S), defined as $CV_S = \text{SD}\{S\}/S^*$ presents a more comparable depiction of relative fluctuation size.

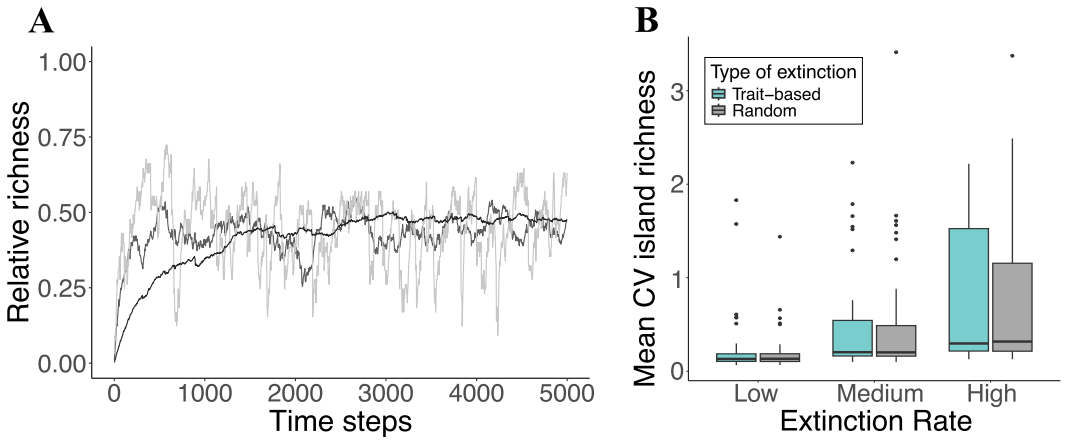

Figure 1: **A)** Example of island species richness dynamics over time for three different networks under medium extinction rate. Richness values of each network is relative to the source (mainland) networks **B)** A boxplot depicting the distribution of the coefficient of variation (CV) of species richness across networks, where each data point in the distribution represents the mean CV calculated from 1000 simulations, evaluated assuming low, medium, and high extinction rates

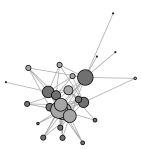

We assessed the CV_S for each assembled network, discarding the first 3000 event steps to avoid the effects of initial conditions. A higher CV_S implies greater community instability (larger fluctuations relative to the mean richness), whereas a lower CV_S indicates a more stable community. Our results show that a higher extinction rate leads to more unstable communities, as expected, for both the random and trait-based extinction scenario (Figure 1B and S2). For each extinction rate, we conducted Mann-Whitney U-test to determine whether there were significant differences in the CV_S values between the two extinction scenarios. Although both extinction scenarios have an elevated CV_S with increased extinction rates, we found no significant differences between the two conditions (Low: $W = 1222$, $p = 0.88$; Medium: $W = 1137$, $p = 0.80$; High: $W = 818$, $p = 0.86$). For example, when extinction rates are high, the mean CV_S for the trait-based extinction scenario is 0.74, whereas that of the random scenario is 0.73. Although the effects of the two different extinction scenarios are roughly similar on average, we observe slightly more variability for the trait-based extinction scenario, particularly when extinction rates are high (Figure 1B and S3).

Since the source that nourishes the island community is the mainland community, we next explore whether fluctuations in island community richness, measured as CV_S, correlate with the structure of different mainland networks. We characterized the structure of both island and mainland communities by calculating three common measures of network structure: modularity, nestedness (NODF), and connectance (Almeida-Neto *et al.*, 2008; Blondel *et al.*, 2008). We used the function *networklevel* in bipartite package in R (Dormann *et al.*, 2008). Connectance is defined by the relative link density (L/S^2, where L is the realized number of links in the island system and S the number of species), whereas nestedness and modularity capture larger-scale patterns of organization in the system, and are often anti-correlated with each other. Nestedness measures to what extent more specialized species are subsets of more generalized species, where a high value indicates that such a pattern predominates. Modularity captures to what extent smaller groups of interacting species are more tightly connected to each other than to other groups, providing insight into how compartmentalized the community is. Typically, nested communities have lower modularity, and modular communities have lower nestedness. Our results show that the effect of mainland network structure on island stability, measured as CV_S, is generally weak but is the strongest at intermediate extinction rates (Figure 2). Higher values of NODF and connectance result in greater fluctuations on the islands, while modularity has a negative relationship only at medium extinction rates ($F_{low} = 2.95$, $p_{low} = 0.08$; $F_{med} = 63.12$, $p_{med} < 0.05$; $F_{high} = 13.82$, $p_{high} = 0.41$). For NODF, a significant relationship is observed across all extinction rates, with the strongest effect at medium extinction ($F_{low} = 10.33$, $F_{med} = 38.52$, $F_{high} = 8.17$, $p < 0.05$). Similarly, connectance significantly influences stability at all rates, with the strongest correlation at medium extinction ($F_{low} = 36.04$, $F_{med} = 63.12$, $F_{high} = 13.82$, $p < 0.05$).

As extinctions rates transition from medium to high, many communities experience complete collapse. We counted how often island communities crashed

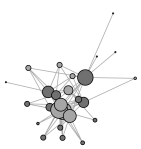

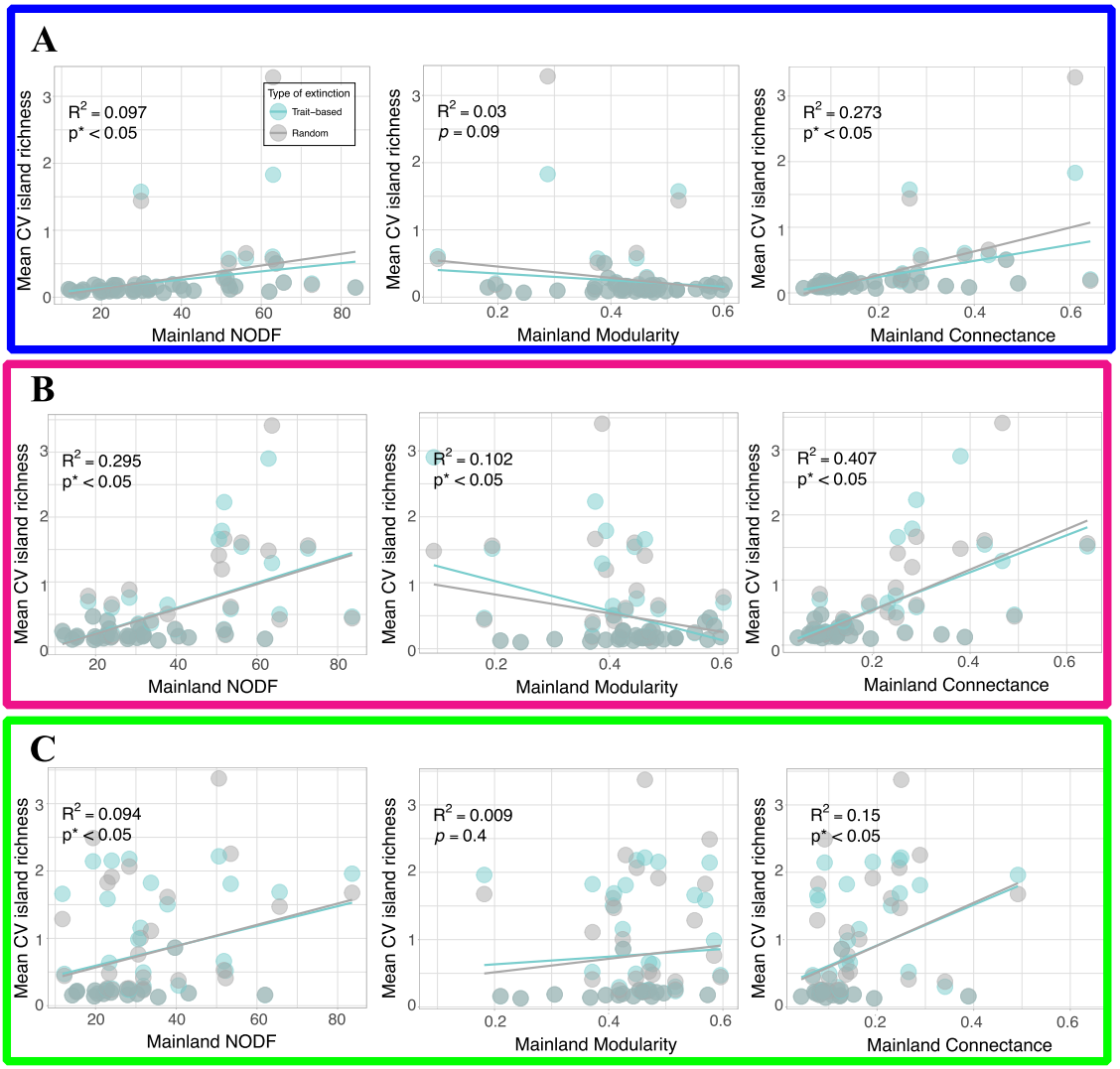

Figure 2: Exploring how mainland network structure affects island community instability (CV_S) at three different extinction rates: **A)** Low (blue), **B)** Medium (pink), and **C)** High (green).

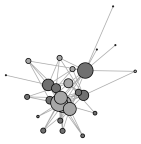

(*i.e.*all species went extinct) across 1,000 simulations for each network. As expected, increasing extinction rates led to more collapses in the system (Figure S4). We then investigated whether the structural features of mainland community networks measured above correlated with a higher likelihood of collapse for the island community. Our results show that the structure of the mainland does not play a great role in the number of island collapses for either extinction scenarios (Figure S5).

We next assess how the dynamic structure of islands corresponds to their dynamics. Island network structure was assessed for the last 1000 time steps of each simulation, at intervals of 100 time steps, and averaged across 1000 replicates, which we repeated for each network. The assembling island communities assemble and evolve structures that diverge from their mainland progenitors, with a relative species richness that declines with increasing extinction rate (Figure 3A). We also observe that island communities have lower modularity and a correspondingly elevated nestedness and connectedness than mainland networks (Figure 3B-D). The degree of nestedness and connectance increases with higher extinction rates, while our metric of modularity appears not to vary much across extinction rates. It is also clear that at higher extinction rates, island communities reveal lower variability in modularity ($SD_{\text{main}} = 0.11$; $SD_{\text{isle}} = 0.07$ and 0.07, trait-based and random extinction, respectively), nestedness ($SD_{\text{main}} = 17.85$; $SD_{\text{isle}} = 11.06$ and 11.12, trait-based and random extinction, respectively) and connectance ($SD_{\text{main}} = 0.14$; $SD_{\text{isle}} = 0.09$ and 0.09, trait-based and random extinction, respectively) than their mainland progenitors (see Figure 3 B-D). We performed a Kruskal-Wallis test to test the difference between the three groups, fallowed by a pairwise comparisons. We found significant difference between mainland and island structure, but the different extinction scenarios do not reveal large structural differences (Table S2).

4.2 Species Persistence on islands

The assessment of mainland (source) and island (realized) structure illustrates how larger-scale patterns of interactions may influence the dynamics of the island community. As a next step, we assessed the role of species-specific characteristics, such as the number of interacting mutualistic partners, on these dynamics.

Since community trajectories fluctuate around different steady states S^*, we calculate persistence as the percentage of each species' occurrence on the island over the temporal span of the simulation. We examine the persistence of species within each mutualistic community relative to the number of its potential mutualistic partners in the mainland community, which we denote as the 'potential degree'. The potential degree of each species describes its inherent ability to specialize or generalize across mutualistic partners, which may or may not be realized as colonizations and extinctions change the composition of species in island communities. We observe that a species' persistence on the island increases sharply with its potential degree, saturating to a fixed persistence value for species with very high potential degree (Figure 4A and S6). This pattern indicates that spe-

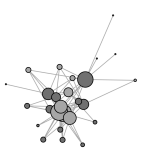

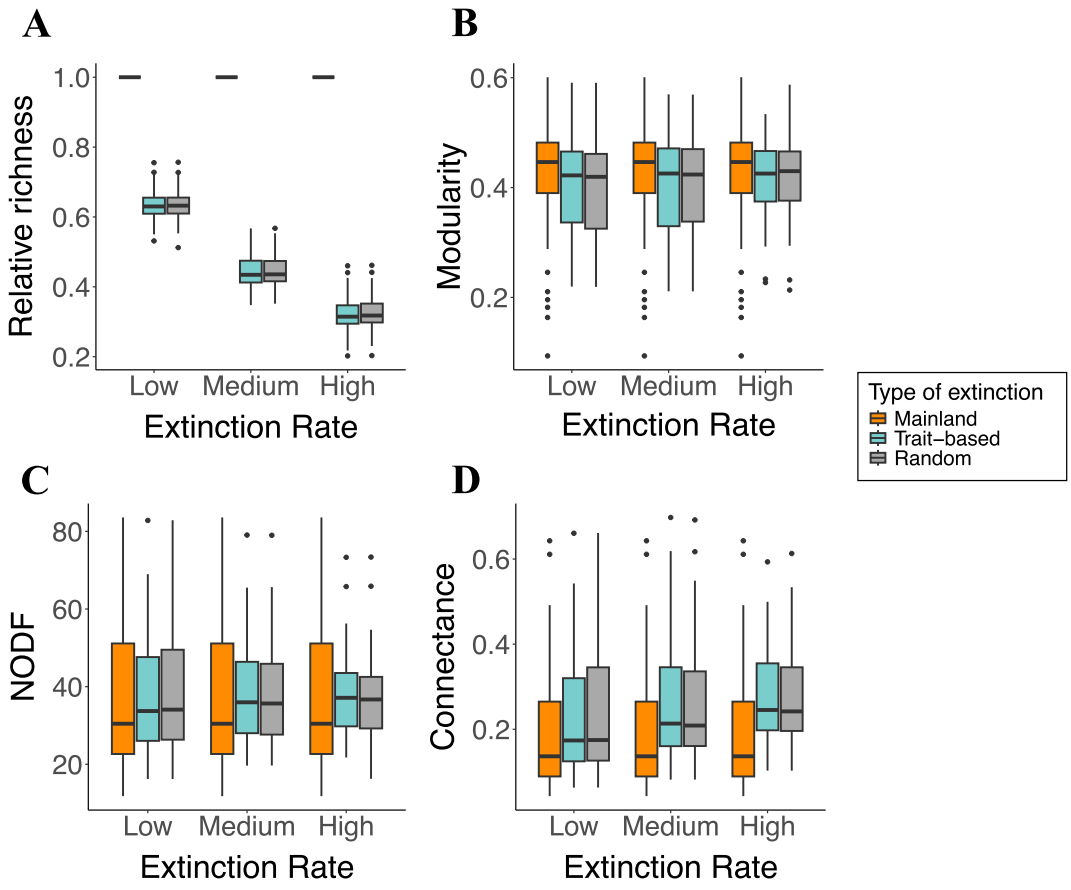

Figure 3: Structure of assembled networks on the island compared to the mainland for different extinction rates. Each point represents the mean from 1,000 simulations for each of the fifty pollination networks. **A)** Relative richness; **B)** Modularity; **C)** Nestedness (NODF); **D)** Connectance.

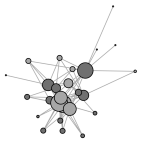

cialist species with low degree have low persistence, as their few interactions limit their ability to weather changes in community composition across the assembly dynamic. Vitally, these low-degree species are prone to both primary and secondary extinctions, as they are more frequently losing their few partners. The steep increase in persistence with each additional interaction means that the observed 'generalization advantage' saturates at a relatively low interaction degree.

We can determine the number of interactions corresponding to 50% of the maximum persistence across low, medium, and high extinction rates by identifying the half-saturation point of a saturating function fitted to the persistence data (lines in Figure 4A). We observe the mean of the approximated half saturation points in units of degree is ca. 0.8 assuming a low extinction rate, with effectively no difference between trait-based and random extinction scenarios (Fig. 4B). A low half-saturation degree means that a relatively small number of interactions promote a substantial increase in persistence. In this case, because the half-saturation degree is < 1, a single interaction enables, on average, persistence in the system for $> 50\%$ of the evaluated simulation time. As the rate of extinction increases, the potential for even generalists to persist is eroded, and the half-saturation degree increases to ca. 2.51 (Fig. 4B). Accordingly, increasing extinction rates increases the number of interactions needed to maximize species' persistence on islands. Lastly, our results indicate that as extinction rates increase, the variability in the half-saturation degree also increases, demonstrating that certain networks require more interactions than others to reach the 50% threshold of maximum persistence.

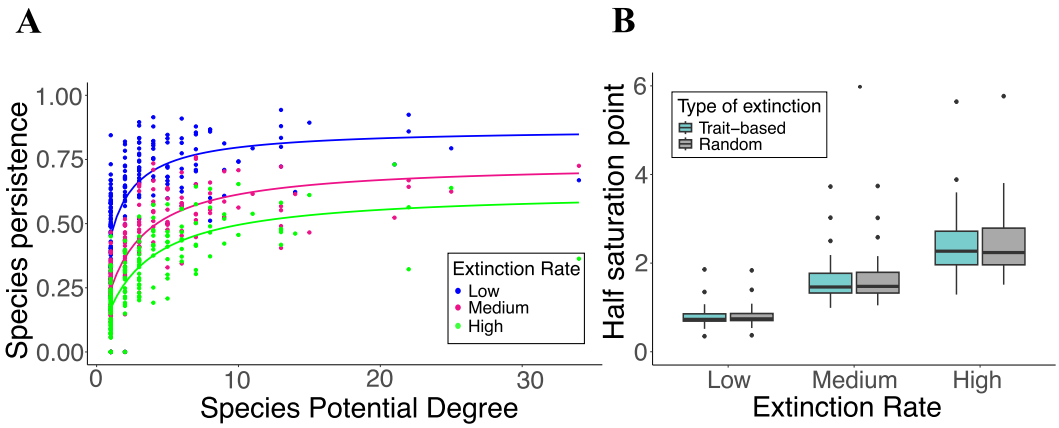

Figure 4: **A)** Species persistence relative to the potential species degree for a single island community under low, medium, and high extinctions rates. Each point is a species and we used the same mainland network as the source. **B)** A boxplot depicting the distribution of the approximated half saturation across networks, where each data point in the distribution represents the mean calculated from 1000 simulations, evaluated assuming low, medium, and high extinction rates.

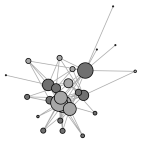

4.3 Coevolutionary assembly dynamics of island communities

To better understand the effect of coevolution on assembled island communities, we calculated average trait dissimilarity taken across the community ($\bar{\gamma}$). We computed the average species trait dissimilarity $\bar{\gamma}$ at the last time step of our simulation across 1000 replicates for all mainland networks under both extinction scenarios, and across increasing extinction rates. At the community level, a low mean trait dissimilarity value means that species on the island community have traits that are, on average, more similar. While the random extinction scenario removes species randomly, regardless of trait dissimilarity, the trait-based extinction scenario assumes species more dissimilar than their mutualistic partners are more prone to primary extinctions.

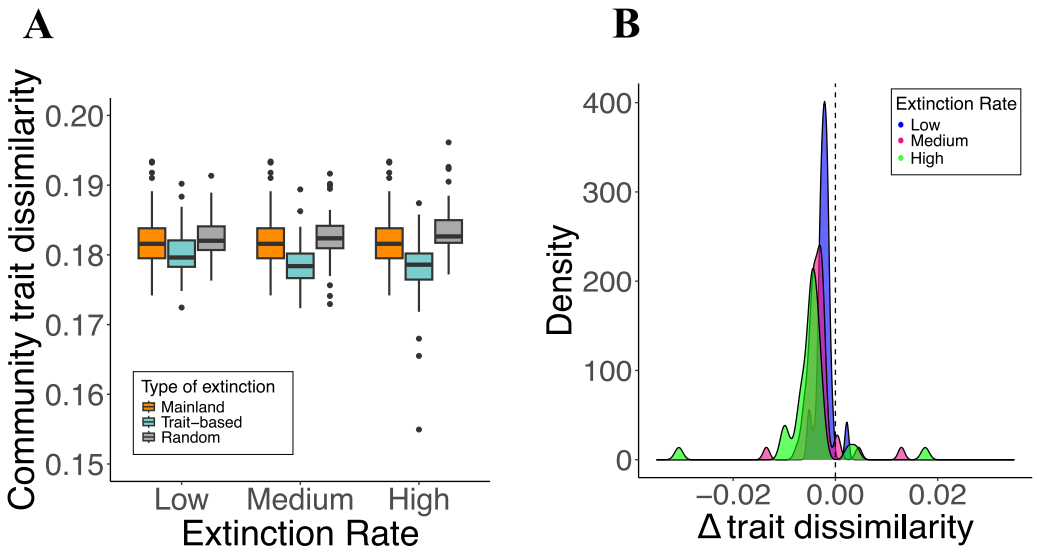

Figure 5: **A)**Higher extinction rates decreases trait mismatching among species on the island community. Trait dissimilarity is the mean trait mismatch of the island community of 1000 simulations across 50 networks. **B)** Δ is the paired difference of trait dissimilarity of the same networks in a trait-based minus the random extinction scenario for the 50 pollination networks. Low, medium, and high extinction rates represent $r_{\text{ext}} = (0.3, 0.6, 0.9)$, respectively.

First, we observe that the interplay between coevolutionary dynamics and the assembly process results in island communities that have average trait dissimilarity values that differ greatly from their mainland counterparts, and this difference grows as the extinction rates increase (Figure 5A). Second, there is a clear difference in $\bar{\gamma}$ between trait-based and random extinction scenarios. The ANOVA test showed that mainland, island with trait-based, and random extinction differed significantly across all three extinction rates ($F_{low} = 5.31$, $F_{med} = 1.82$, $F_{high} = 9.51$, $p < 0.05$)and the post-hoc test further revealed significant differences between the three groups. As the extinction rate increases, the mean dissimiliarty of mainland

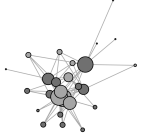

and island communities under the random extinction scenario also increases (Figure 5A). When extinctions are a function of trait dissimilarity, we observe that the mean dissimilarity values are much lower in island systems compared to mainland communities (Figure 5A). Over the course of the assembly process, species that are dissimilar are more likely to suffer extinction, with communities becoming increasingly similar. Because both the trait-based and random extinction scenarios employ the same coevolutionary process, which favors trait matching, the decrease in dissimilarity in trait-based extinction communities can be interpreted as the result of the assembly, rather than the coevolutionary dynamic.

Second, we note that the assessment of community dissimilarity across networks may mask to what extent individual networks increase or decrease in dissimilarity as extinctions move from random to trait-based. Comparing the difference between community dissimilarity values for the random and trait-based extinction scenarios on a per-network basis, where $\Delta\bar{\gamma} = \bar{\gamma}_{\text{trait}} - \bar{\gamma}_{\text{rand}}$, negative values indicate that networks assembling under the trait-based extinction scenario result in lower community dissimilarity, while positive $\Delta\bar{\gamma}$ indicates that the trait-based extinction scenario results in higher community dissimilarity values. We observe a clear shift to lower negative values for $\Delta\bar{\gamma}$ from low to high extinction rates (Fig. 5B). This result demonstrates that on a per-community basis, the effect of trait-based extinctions serves to lower the trait dissimilarity of interacting species, an effect that grows with increasing extinction rates.

5 Discussion

We investigate the assembly and coevolution of island communities from a mainland source pool by integrating a coevolutionary model premised on trait-matching with a stochastic assembly dynamic. By combining these approaches we aim to disentangle the potential influence of both ecological and evolutionary dynamics in shaping the structure and function of assembling island communities.

Beyond capturing the expectation that island richness is inversely related to the rate of extinction, we also observed that the relative size of fluctuations in richness (measured as CV_S) over the course of assembly increased with extinction rate, while differing widely among island communities (Figure 1 and S3). When the extinction rate is low, the island can assemble a larger range of species, however the assembly dynamics and resulting fluctuations may be relatively insensitive to both structure (interactions) and function (trait matching between mutualistic partners). As the extinction rate increases, the community reaches a steady state composed of fewer species, though the dynamics may increasingly reflect the selective process being imposed. When extinction rates are too high, the island is in a constant state of flux – from both the primary extinctions but perhaps even more-so the secondary extinction cascades. Higher extinction rates also led to networks that were more nested and connected, but less modular, providing insight into the roles of structure in determining dynamics. The idea that the structural properties of ecological networks — such as connectance, modularity,

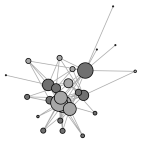

and nestedness — play a crucial role in determining the robustness of ecological communities, *i.e.* how the community respond to a extinction cascade affect, have been explored for different type of ecological interactions, with mixed results. For instance, connectance has been shown to either increase or decrease robustness depending on specific model assumptions (Dunne *et al.*, 2002; Thebault & Fontaine, 2010; Lever *et al.*, 2014), while modularity can enhance robustness by confining cascading effects to specific modules or, conversely, increase vulnerability within those modules (Tylianakis *et al.*, 2010). Nestedness, however, is often considered a proxy for robustness (Memmott *et al.*, 2004), though the positive relationship between nestedness and robustness has only been clearly demonstrated when specialists have a higher probability of extinction than generalists (Burgos *et al.*, 2007). The observation that increased extinction rates contribute to a wide range of CV_S across networks suggests that inherent differences in network structure play a key role in generating destabilizing fluctuations. Notably, when species extinctions are influenced by trait dissimilarity, this variability in the relative size of fluctuations is amplified compared to when extinctions are random (Figure 1B). This indicates that while coevolutionary processes within our framework help reduce trait dissimilarity, extinction events based on trait differences can heighten fluctuations in certain island communities, resulting in less stable systems.

Because island systems pull from the species and associated structures of mainland communities, the notion that multiple spatial scales contribute to the regional processes shaping community assembly (Freckleton & Watkinson, 2002; Leibold *et al.*, 2004; Fukami, 2004) is inherently captured within our assembly framework. Here, the structure of the mainland communities giving rise to assembled islands provides insight into the potential interactions available to species, the realization of which depends on the state of the island community at a given point in time. Our result shows that when extinction rates are intermediate – not so low that they have little effect, and not so high the community is constantly crashing – the influence of mainland structure on island communities is strongest. Mainland communities that are more nested, more connected, and less modular tend to generate island communities that are more unstable (Figure 2B). That both increased connectance and nestedness correlate with larger fluctuations, while increased modularity has the opposite effect, and that there is effectively no difference between trait-based and random extinction scenarios, suggests three potentially intertwined effects. First, mainland structure does not appear to determine observable differences between systems with and without trait-dependent extinctions, suggesting the relationships are instead primarily driven by the assembly process rather than coevolution-mediated changes in traits. Second, small-world type interaction structures, where the indirect paths connecting species are short, may more effectively drive larger extinction cascades, as the influence of one species' extinction can directly impact more species in the network (Watts & Strogatz, 1998; Guimaraes Jr, 2020). Third, and the converse of the second effect, such cascades are likely dampened by more modular networks, where the impact of a cascade may be severe within a module, but be less likely to expand outside

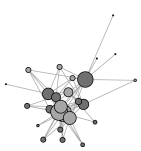

of it (Stouffer & Bascompte, 2010; Dáttilo, 2012).

We also demonstrate that the persistence of supergeneralists is not incredibly higher than that of generalists with fewer interactions, and this is reflected by the saturating function that best fits persistence as a function of species' degree (Figure 4A). Specialists, on the hand, have a higher turnover rate. Because specialists can more readily evolve to match their partner's trait value, this suggests that it is the ecological processes – a combination of both the ability to colonize and a resistance to secondary extinction cascades – that instead shapes the generalist advantage. Moreover, our model prediction that benefits saturate with increasing numbers of interactions is a pattern that is also observed in natural systems. Olesen *et al.* (2011) explored the temporal dynamics of mutualistic networks over a span of 12 years and uncovered a similar pattern: species with fewer interactions had higher turnover rates, and while those with more interactions persisted longer, the gains followed a saturating relationship, such that larger numbers of interactions delivered diminishing returns. A common assembly process proposed by Barabási & Albert (1999), known as "preferential attachment", describes the assembly of nodes in a network that tend to attach to those with many connections, where the 'rich get richer'. Processes that are analogous to preferential attachment can also govern network disassembly, where less-connected species are more prone to local extinction, and this has been shown to give rise to more nested networks (Tylianakis *et al.*, 2018). While our assembly process does not follow a preferential attachment algorithm as potential interactions are predetermined by a mainland source, less connected species are more prone to secondary extinction cascades, potentially contributing to the increased nestedness we observed in our assembling island communities (Figure 3). Intriguingly, this tendency for less-connected species to be lost during network disassembly has also been observed in empirical mutualistic networks (Aizen *et al.*, 2012; Burkle *et al.*, 2013).

Our work advances upon previous findings by integrating the ecological processes of colonization and extinction with the dynamics of coevolution into a unified framework, where the emergence of island structure and dynamics from a mainland progenitor can be evaluated with respect to the influence of both. Empirical observations of mainland versus oceanic island mutualistic systems have not revealed clear structural differences between them, as oceanic islands are less diverse, but do not show significant differences in the connectance, nestedness, or modularity of their interactions compared to mainland systems. (Traveset *et al.*, 2016). Importantly, they compared many island networks to mainland networks, without taking into account pairwise comparisons (mainland/source–island) or characteristics such as island size and distance from the mainland, both of which are known to impact the balance between colonization and extinction (MacArthur & Wilson, 1967). Along these lines, our framework shows that structural differences between mainland and island systems can be sensitive to extinction rate, where structural divergence between mainland and island systems increase with the rate of extinctions (Figure 3). When extinction rates are low, the similarity between island and mainland community structure increases (Figure 3B-D).

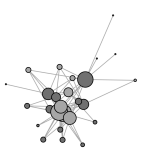

Lastly, our results show that coevolution leads to greater trait-similarity in island communities experiencing trait-based extinctions, particularly when extinction rates are high (Figure 5). Despite high species turnover, we observe that the coevolutionary dynamic serves to promote the persistence of species with similar traits, resulting in communities with greater trait-matching. However we do not find this trait-matching dynamic to leave a clear imprint on the assembled structure of island communities, as is demonstrated by the similarity of assembled islands with random versus trait-based extinctions (Figure 3). We note that coevolutionary effects in our framework may be lessened by the fact that each simulation consists of only a single mainland source and island community. As such, following a given species extinction, its recolonization effectively resets its trait value to that of the mainland, erasing any memory of previous evolutionary change. In natural systems where the island is part of a larger archipelago, there may be a greater likelihood of an ecological rescue by other island populations, connected by dispersal, that have retained this coevolutionary memory. By preserving the memory of coevolutionary processes, such dynamics could magnify the effects of coevolution and its influence in the assembly process, and this would be an obvious next step for future work.

Although studies directly linking coevolution to community assembly are limited (but see Leibold *et al.*, 2022), there have been substantial efforts demonstrating how coevolution operates across varying spatial scales. Because local communities experience different selection pressures, coevolutionary dynamics at larger spatial scales can generate a geographic mosaic (Benkman, 1999; Gomulkiewicz *et al.*, 2000; Thompson *et al.*, 2017; Thompson, 2019). Geographic mosaics can function to maintain a larger diversity of phenotypes in a given region, directly impacting how the structure of mutualistic interactions varies across time and space (Thompson & Cunningham, 2002; Anderson & Johnson, 2008; Thompson, 2019). Because spatial mosaics are connected via dispersal, each serves to provide a flow of new species or phenotypes to the other. For example, Medeiros *et al.* (2018) used a mathematical model to show that increasing gene flow between mutualistic communities leads to higher trait-matching and trait convergence between interacting species. In other cases, when two populations evolve in response to very different environmental optima, gene flow can serve to flood populations with suboptimal phenotypes, resulting in migrational meltdown (Ronce & Kirkpatrick, 2001; Yeakel *et al.*, 2018)

The traits of plants and pollinators involved in pollen delivery and sequestration directly impact both the time and energy invested in each interaction, such that lower dissimilarity promotes pollination efficiency (Klumpers *et al.*, 2019a), and this is expected to increase fitness (Anderson & Johnson, 2008). That island networks with random extinctions are more dissimilar, and those with trait-based extinctions are less, clearly demonstrates that coevolutionary forces are shaping the nature of species interactions (Figure 5B). Yet, as we have stated, this coevolutionary process does not leave a clear signature in the structure of island communities. Because only primary extinctions are a function of trait dissimi-

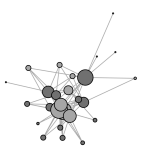

larity between interacting partners, we suggest that it is not primary extinctions but secondary extinction cascades that drive the structural differences we observe between islands and their mainland source communities (Figure 3B-D). So while coevolutionary dynamics shape the trait landscape within the community, on average pushing the system towards trait-matching, whatever structural imprint such a process might leave is erased by the large footprint of cascading extinctions following an initial extinction event.

By combining both the ecological processes of assembly with coevolution, we show that island communities, characterized by smaller size, and higher instability and turnover, can provide important insights into the drivers of structure and dynamics. Importantly, we show that the effects of coevolutionary trait-matching in complex mutualistic systems can be subtle, yet persistent, when communities are undergoing continuous reorganization and shuffling. Island communities contain an important source of biodiversity, and understanding the interplay between the ecological and evolutionary processes at work is crucial for elucidating the factors driving species diversity, assembly, and dynamics in relatively isolated habitats. This knowledge not only enhances our comprehension of biodiversity patterns but also informs conservation efforts by providing insights into how to preserve and manage these unique ecosystems in the face of environmental challenges and human impacts.

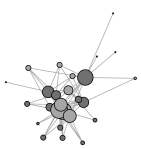

References

Aguilée, R., Pellerin, F., Soubeyrand, M., Choin, J. & Thébaud, C. (2021). Biogeographic drivers of community assembly on oceanic islands: The importance of archipelago structure and history. *Journal of Biogeography*, 48, 2616–2628.

Aizen, M.A., Sabatino, M. & Tylianakis, J.M. (2012). Specialization and rarity predict nonrandom loss of interactions from mutualist networks. *Science*, 335, 1486–1489.

Almeida-Neto, M., Guimaraes, P., Guimaraes Jr, P.R., Loyola, R.D. & Ulrich, W. (2008). A consistent metric for nestedness analysis in ecological systems: reconciling concept and measurement. *Oikos*, 117, 1227–1239.

Anderson, B. & Johnson, S.D. (2008). The geographical mosaic of coevolution in a plant–pollinator mutualism. *Evolution*, 62, 220–225.

Arditti, J., Elliott, J., Kitching, I.J. & Wasserthal, L.T. (2012). 'good heavens what insect can suck it'–charles darwin, angraecum sesquipedale and xanthopan morganii praedicta. *Botanical Journal of the Linnean Society*, 169, 403–432.

Barabási, A.L. & Albert, R. (1999). Emergence of scaling in random networks. *science*, 286, 509–512.

Bascompte, J. & Jordano, P. (2007). Plant-Animal Mutualistic Networks: The Architecture of Biodiversity. *Annual Review of Ecology, Evolution, and Systematics*, 38, 567–593.

Bascompte, J., Jordano, P., Melián, C.J. & Olesen, J.M. (2003). The nested assembly of plant–animal mutualistic networks. *Proceedings of the National Academy of Sciences*, 100, 9383–9387.

Bastolla, U., Fortuna, M.A., Pascual-García, A., Ferrera, A., Luque, B. & Bascompte, J. (2009). The architecture of mutualistic networks minimizes competition and increases biodiversity. *Nature*, 458, 1018–1020.

Bawa, K.S. (1990). Plant-pollinator interactions in tropical rain forests. *Annual review of Ecology and Systematics*, 21, 399–422.

Benkman, C.W. (1999). The selection mosaic and diversifying coevolution between crossbills and lodgepole pine. *The American Naturalist*, 153, S75–S91.

Biddick, M. & Burns, K.C. (2018). Phenotypic trait matching predicts the topology of an insular plant–bird pollination network. *Integrative Zoology*, 13, 339–347.

Birskis-Barros, I., Freitas, A.V. & Guimarães Jr, P.R. (2021). Habitat generalist species constrain the diversity of mimicry rings in heterogeneous habitats. *Scientific Reports*, 11, 5072.

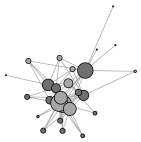

Blondel, V.D., Guillaume, J.L., Lambiotte, R. & Lefebvre, E. (2008). Fast unfolding of communities in large networks. *Journal of statistical mechanics: theory and experiment*, 2008, P10008.

Bronstein, J.L. (2015). *Mutualism*. Oxford University Press.

Burgos, E., Ceva, H., Perazzo, R., Devoto, M., Medan, D., Zimmermann, M. & Delbue, A.M. (2007). Why Nestedness in Mutualistic Networks? *Journal of Theoretical Biology*, 249, 307–313.

Burkle, L.A., Marlin, J.C. & Knight, T.M. (2013). Plant-pollinator interactions over 120 years: loss of species, co-occurrence, and function. *Science*, 339, 1611–1615.

Castro-Urgal, R. & Traveset, A. (2014). Differences in flower visitation networks between an oceanic and a continental island. *Botanical Journal of the Linnean Society*, 174, 478–488.

Chamberlain, S.A., Cartar, R.V., Worley, A.C., Semmler, S.J., Gielens, G., Elwell, S., Evans, M.E., Vamosi, J.C. & Elle, E. (2014). Traits and phylogenetic history contribute to network structure across Canadian plant–pollinator communities. *Oecologia*, 176, 545–556.

Chen, X.Y. & He, F. (2009). Speciation and endemism under the model of island biogeography. *Ecology*, 90, 39–45.

Cosmo, L.G., Assis, A.P.A., de Aguiar, M.A.M., Pires, M.M., Valido, A., Jordano, P., Thompson, J.N., Bascompte, J. & Guimarães, P.R. (2023). Indirect effects shape species fitness in coevolved mutualistic networks. *Nature*, 619, 788–792.

Dáttilo, W. (2012). Different tolerances of symbiotic and nonsymbiotic ant-plant networks to species extinctions. *Network Biology*, 2, 127.

Donatti, C.I., Guimarães, P.R., Galetti, M., Pizo, M.A., Marquitti, F.M. & Dirzo, R. (2011). Analysis of a hyper-diverse seed dispersal network: modularity and underlying mechanisms. *Ecology letters*, 14, 773–781.

Dormann, C.F., Gruber, B. & Fründ, J. (2008). Introducing the bipartite package: analysing ecological networks. *interaction*, 1, 8–11.

Dunne, J.A., Williams, R.J. & Martinez, N.D. (2002). Network structure and biodiversity loss in food webs: Robustness increases with connectance. *Ecology Letters*, 5, 558–567.

Ehrlich, P.R. & Raven, P.H. (1964). Butterflies and Plants: A Study in Coevolution. *Evolution*, 18, 586–608.

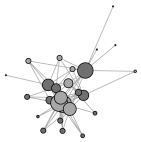

Elias, M., Gompert, Z., Jiggins, C. & Willmott, K. (2008). Mutualistic Interactions Drive Ecological Niche Convergence in a Diverse Butterfly Community. *PLOS Biology*, 6, e300.

Encinas-Viso, F., Revilla, T.A. & Etienne, R.S. (2012). Phenology drives mutualistic network structure and diversity. *Ecology Letters*, 15, 198–208.

Freckleton, R. & Watkinson, A. (2002). Large-scale spatial dynamics of plants: metapopulations, regional ensembles and patchy populations. *Journal of Ecology*, 90, 419–434.

Fukami, T. (2004). Assembly History Interacts with Ecosystem Size to Influence Species Diversity. *Ecology*, 85, 3234–3242.

Gillespie, D.T. (1977). Exact stochastic simulation of coupled chemical reactions. *The journal of physical chemistry*, 81, 2340–2361.

Gillespie, R.G. (2016). Island time and the interplay between ecology and evolution in species diversification. *Evolutionary Applications*, 9, 53–73.

Gomulkiewicz, R., Thompson, J.N., Holt, R.D., Nuismer, S.L. & Hochberg, M.E. (2000). Hot Spots, Cold Spots, and the Geographic Mosaic Theory of Coevolution. *The American Naturalist*, 156, 156–174.

González-Castro, A., Traveset, A. & Nogales, M. (2012). Seed dispersal interactions in the Mediterranean Region: Contrasting patterns between islands and mainland. *Journal of Biogeography*, 39, 1938–1947.

Gravel, D., Massol, F., Canard, E., Mouillot, D. & Mouquet, N. (2011). Trophic theory of island biogeography. *Ecology Letters*, 14, 1010–1016.

Guimarães, P.R. & Deyn, G.B.D. (2016). Ecological networks: Assembly and consequences. *Oikos*, 125, 443–445.

Guimarães, P.R., Pires, M.M., Jordano, P., Bascompte, J. & Thompson, J.N. (2017). Indirect effects drive coevolution in mutualistic networks. *Nature*, 550, 511–514.

Guimarães, P.R.J., Jordano, P. & Thompson, J.N. (2011). Evolution and coevolution in mutualistic networks. *Ecology Letters*, 14, 877–885.

Guimaraes Jr, P.R. (2020). The structure of ecological networks across levels of organization. *Annual Review of Ecology, Evolution, and Systematics*, 51, 433–460.

Hale, K.R., Valdovinos, F.S. & Martinez, N.D. (2020). Mutualism increases diversity, stability, and function of multiplex networks that integrate pollinators into food webs. *Nature Communications*, 11, 2182.

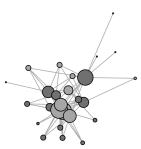

Jordano, P. (1987). Patterns of Mutualistic Interactions in Pollination and Seed Dispersal: Connectance, Dependence Asymmetries, and Coevolution. *The American Naturalist*, 129, 657–677.

Jordano, P. (2000). Fruits and frugivory.

Kaiser-Bunbury, C.N., Traveset, A. & Hansen, D.M. (2010). Conservation and restoration of plant–animal mutualisms on oceanic islands. *Perspectives in Plant Ecology, Evolution and Systematics*, 12, 131–143.

Klumpers, S.G., Stang, M. & Klinkhamer, P.G. (2019a). Foraging efficiency and size matching in a plant–pollinator community: the importance of sugar content and tongue length. *Ecology letters*, 22, 469–479.

Klumpers, S.G.T., Stang, M. & Klinkhamer, P.G.L. (2019b). Foraging efficiency and size matching in a plant–pollinator community: The importance of sugar content and tongue length. *Ecology Letters*, 22, 469–479.

Krebs, J.R., Stephens, D.W., Sutherland, W.J. *et al.* (1983). Perspectives in optimal foraging.

Krishna, A., Jr, P.R.G., Jordano, P. & Bascompte, J. (2008). A neutral-niche theory of nestedness in mutualistic networks. *Oikos*, 117, 1609–1618.

Leibold, M.A., Govaert, L., Loeuille, N., De Meester, L. & Urban, M.C. (2022). Evolution and Community Assembly Across Spatial Scales. *Annual Review of Ecology, Evolution, and Systematics*, 53, 299–326.

Leibold, M.A., Holyoak, M., Mouquet, N., Amarasekare, P., Chase, J.M., Hoopes, M.F., Holt, R.D., Shurin, J.B., Law, R., Tilman, D. *et al.* (2004). The metacommunity concept: a framework for multi-scale community ecology. *Ecology letters*, 7, 601–613.

Lever, J.J., van Nes, E.H., Scheffer, M. & Bascompte, J. (2014). The sudden collapse of pollinator communities. *Ecology letters*, 17, 350–359.

Lewinsohn, T.M., Inácio Prado, P., Jordano, P., Bascompte, J. & M. Olesen, J. (2006). Structure in plant–animal interaction assemblages. *Oikos*, 113, 174–184.

Losos, J.B. & Ricklefs, R.E. (2009). Adaptation and diversification on islands. *Nature*, 457, 830–836.

Losos, J.B. & Schluter, D. (2000). Analysis of an evolutionary species–area relationship. *Nature*, 408, 847–850.

MacArthur, R.H. & Wilson, E.O. (1963). An Equilibrium Theory of Insular Zoogeography. *Evolution*, 17, 373–387.

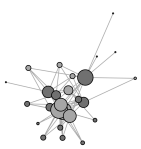

MacArthur, R.H. & Wilson, E.O. (1967). *The Theory of Island Biogeography*. Princeton University Pree, Princeton, NJ.

Maglianesi, M.A., Blüthgen, N., Böhning-Gaese, K. & Schleuning, M. (2014). Morphological traits determine specialization and resource use in plant–hummingbird networks in the neotropics. *Ecology*, 95, 3325–3334.

Massol, F., Dubart, M., Calcagno, V., Cazelles, K., Jacquet, C., Kéfi, S. & Gravel, D. (2017). Chapter Four - Island Biogeography of Food Webs. In: *Advances in Ecological Research* (eds. Bohan, D.A., Dumbrell, A.J. & Massol, F.). Academic Press, vol. 56 of *Networks of Invasion: A Synthesis of Concepts*, pp. 183–262.

Medeiros, L.P., Garcia, G., Thompson, J.N. & Guimarães, P.R. (2018). The geographic mosaic of coevolution in mutualistic networks. *Proceedings of the National Academy of Sciences*, 115, 12017–12022.

Memmott, J. (1999). The structure of a plant-pollinator food web. *Ecology letters*, 2, 276–280.

Memmott, J., Waser, N.M. & Price, M.V. (2004). Tolerance of pollination networks to species extinctions. *Proceedings of the Royal Society B: Biological Sciences*, 271, 2605–2611.

Minoarivelo, H.O. & Hui, C. (2016). Trait-mediated interaction leads to structural emergence in mutualistic networks. *Evolutionary Ecology*, 30, 105–121.

Newman, E., Manning, J. & Anderson, B. (2014). Matching floral and pollinator traits through guild convergence and pollinator ecotype formation. *Annals of Botany*, 113, 373–384.

Nuismer, S.L., Jordano, P. & Bascompte, J. (2013). Coevolution and the Architecture of Mutualistic Networks. *Evolution*, 67, 338–354.

Olesen, J.M., Eskildsen, L.I. & Venkatasamy, S. (2002). Invasion of pollination networks on oceanic islands: Importance of invader complexes and endemic super generalists. *Diversity and Distributions*, 8, 181–192.

Olesen, J.M., Stefanescu, C. & Traveset, A. (2011). Strong, Long-Term Temporal Dynamics of an Ecological Network. *PLoS ONE*, 6, e26455.

Palmer, T.M., Stanton, M.L., Young, T.P., Lemboi, J.S., Goheen, J.R. & Pringle, R.M. (2013). A role for indirect facilitation in maintaining diversity in a guild of African acacia ants. *Ecology*, 94, 1531–1539.

Pauw, A., Stofberg, J. & Waterman, R.J. (2009). Flies and Flowers in Darwin's Race. *Evolution*, 63, 268–279.

Pimm, S.L. & Pimm, J.W. (1982). Resource Use, Competition, and Resource Availability in Hawaiian Honeycreepers. *Ecology*, 63, 1468–1480.

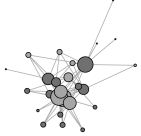

Ronce, O. & Kirkpatrick, M. (2001). When sources become sinks: migrational meltdown in heterogeneous habitats. *Evolution*, 55, 1520–1531.

Stang, M., Klinkhamer, P.G., Waser, N.M., Stang, I. & Van der Meijden, E. (2009). Size-specific interaction patterns and size matching in a plant–pollinator interaction web. *Annals of botany*, 103, 1459–1469.

Stouffer, D.B. & Bascompte, J. (2010). Understanding food-web persistence from local to global scales. *Ecology letters*, 13, 154–161.

Sugiura, S. (2010). Species interactions–area relationships: Biological invasions and network structure in relation to island area. *Proceedings of the Royal Society B: Biological Sciences*, 277, 1807–1815.

Thebault, E. & Fontaine, C. (2010). Stability of Ecological Communities and the Architecture of Mutualistic and Trophic Networks. *Science*, 329, 853–856.

Thompson, J.N. (1994). *The Coevolutionary Process*. University of Chicago Press, USA.

Thompson, J.N. (2019). *The geographic mosaic of coevolution*. University of Chicago Press.

Thompson, J.N. & Cunningham, B.M. (2002). Geographic structure and dynamics of coevolutionary selection. *Nature*, 417, 735–738.

Thompson, J.N., Schwind, C. & Friberg, M. (2017). Diversification of trait combinations in coevolving plant and insect lineages. *The American Naturalist*, 190, 171–184.

Traveset, A., Tur, C., Trøjelsgaard, K., Heleno, R., Castro-Urgal, R. & Olesen, J.M. (2016). Global patterns of mainland and insular pollination networks. *Global Ecology and Biogeography*, 25, 880–890.

Trøjelsgaard, K., Báez, M., Espadaler, X., Nogales, M., Oromí, P., Roche, F.L. & Olesen, J.M. (2013). Island biogeography of mutualistic interaction networks. *Journal of Biogeography*, 40, 2020–2031.

Trøjelsgaard, K. & Olesen, J.M. (2016). Ecological networks in motion: Micro- and macroscopic variability across scales. *Functional Ecology*, 30, 1926–1935.

Tylianakis, J.M., Laliberté, E., Nielsen, A. & Bascompte, J. (2010). Conservation of species interaction networks. *Biological conservation*, 143, 2270–2279.

Tylianakis, J.M., Martínez-García, L.B., Richardson, S.J., Peltzer, D.A. & Dickie, I.A. (2018). Symmetric assembly and disassembly processes in an ecological network. *Ecology Letters*, 21, 896–904.

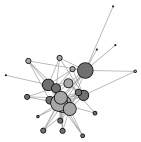

Valdovinos, F.S., Dritz, S. & Marsland, R. (2023). Transient dynamics in plant–pollinator networks: fewer but higher quality of pollinator visits determines plant invasion success. *Oikos*, 2023, e09634.

Valdovinos, F.S. & Marsland III, R. (2021). Niche theory for mutualism: A graphical approach to plant-pollinator network dynamics. *The American Naturalist*, 197, 393–404.

Valente, L., Phillimore, A.B., Melo, M., Warren, B.H., Clegg, S.M., Havenstein, K., Tiedemann, R., Illera, J.C., Thébaud, C., Aschenbach, T. & Etienne, R.S. (2020). A simple dynamic model explains the diversity of island birds worldwide. *Nature*, pp. 1–5.

Valiente-Banuet, A. & Verdú, M. (2007). Facilitation can increase the phylogenetic diversity of plant communities. *Ecology Letters*, 10, 1029–1036.

Vellend, M. (2008). Effects of diversity on diversity: Consequences of competition and facilitation. *Oikos*, 117, 1075–1085.

Vidal, M.C., Wang, S.P., Rivers, D.M., Althoff, D.M. & Segraves, K.A. (2020). Species richness and redundancy promote persistence of exploited mutualisms in yeast. *Science*, 370, 346–350.

Watts, D.J. & Strogatz, S.H. (1998). Collective dynamics of 'small-world'networks. *nature*, 393, 440–442.

Whittaker, R.J., Triantis, K.A. & Ladle, R.J. (2008). A general dynamic theory of oceanic island biogeography. *Journal of Biogeography*, 35, 977–994.

Yeakel, J.D., Gibert, J.P., Gross, T., Westley, P.A. & Moore, J.W. (2018). Eco-evolutionary dynamics, density-dependent dispersal and collective behaviour: implications for salmon metapopulation robustness. *Philosophical Transactions of the Royal Society B: Biological Sciences*, 373, 20170018.

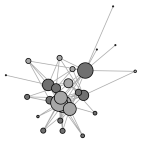

S1 Supplementary Material

S1.1 Analytical approximation

We performed an analytical approximation to better understand how trait mismatch related with the probability of extinction (p). In our model, t is the time a species j spend interacting with species i. We define t as:

$$t_{ij} = a + b\sqrt{(Z_j - Z_i)^2} \tag{S1}$$

where a is the time if perfectly match and b is the effect of dissimilarity on time. We assume these are the same for all species.

We can then calculate T, which is the total time a species spend in a mutualistic interactions with other species.

$$T_i = a + \frac{b}{n}\sum_{j=1}^{n}\sqrt{(Z_j - Z_i)^2} \tag{S2}$$

where n is the total number of species who species i interacts with.

Let define $\gamma_i = \sqrt{(Z_j - Z_i)^2}$. We will treat γ_i as a random variable and it will be drawn from a *Beta Distribution* with shape parameter α and β.

From the *Beta Distribution* we have:

$$E(\gamma) = \frac{\alpha}{\alpha + \beta} \tag{S3}$$

$$Var(\gamma) = \frac{\alpha\beta}{(\alpha + \beta)^2(\alpha + \beta + 1)} \tag{S4}$$

From S3 and S4 we can calculate the $E(T_i)$:

$$E(T_i) = \int_0^1 P(\gamma_i/\alpha\beta)(a + b\gamma)\, dx = a + \frac{b\alpha}{\alpha + \beta} \tag{S5}$$

Because $Var(T) = E(T^2) - E(T)^2$, we then find:

$$Var(T_i) = \frac{b^2\alpha\beta}{n(\alpha + \beta)^2(1 + \alpha + \beta)} \tag{S6}$$

Now we define our profitability (P) as $P = \frac{g}{T}$, where g is the energetic gain of a mutualistic interaction and we assume to be constant among species. Thus, to calculate the expected profitability (E(P)) we we use the *Delta Method* approximation. Where:

$$EP(T) \approx P(E(T)) + \frac{1}{2}P\text{“}(E(T))Var(T) \tag{S7}$$

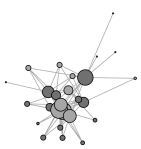

$$\approx \frac{g}{E(T)} + \frac{1}{2}\frac{2g}{E(T)^3}Var(T) \tag{S8}$$

Combining S5 and S6 in S8, we have:

$$EP(T) = \frac{g(na^2 + 2nabE(\gamma) + b^2(nE(\gamma)^2 + Var(\gamma))}{n(a + bE(\gamma)^3)} \tag{S9}$$

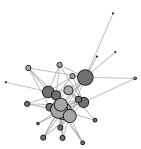

S1.2 Tables

Table S1: Empirical networks used as mainland sources.

Network	Richness	NODF	Modularity	Connectance
1	184	14.23873549	0.475424383	0.042944053
2	64	37.81390987	0.407417048	0.229166667
3	204	22.58099947	0.458793211	0.090114943
4	103	43.05299921	0.305314438	0.151371308
5	143	19.68300426	0.367755818	0.093370445
6	124	20.49405685	0.573327974	0.080362727
7	65	18.16607981	0.600920447	0.088636364
8	94	22.97842332	0.569003642	0.078282828
9	56	52.24284773	0.371166334	0.265151515
10	80	11.78630001	0.55047619	0.076252723
11	106	15.29377094	0.496383958	0.072544643
12	96	12.26008706	0.595800304	0.066869301
13	39	51.31313131	0.395124717	0.28
14	46	40.53764617	0.516776554	0.340686275
15	49	24.01294151	0.486968144	0.190883191
16	49	28.3718074	0.449011446	0.246031746
17	109	22.00459636	0.394785981	0.10791038
18	59	62.00698363	0.210409359	0.389147287
19	204	30.29379718	0.417036302	0.124039133
20	60	19.36751796	0.57671875	0.091428571
21	103	23.38299422	0.476938056	0.135817308
22	53	31.15384615	0.424567605	0.163003663
23	112	27.94153197	0.443159279	0.122660295
24	25	83.58751609	0.181923222	0.491666667
25	63	65.61027603	0.409322792	0.24691358
26	21	51.88679245	0.37633218	0.288461538
27	25	56.18849206	0.445331484	0.43
28	35	63.72412774	0.388352222	0.466666667
29	35	62.86346612	0.093526577	0.38
30	113	30.59627041	0.584480227	0.139146568
31	39	53.49656713	0.429576574	0.288888889
32	23	29.88410596	0.519705718	0.264705882
33	13	11.9047619	0.163518008	0.388888889
34	10	62.96296296	0.288101962	0.611111111
35	15	72.65306122	0.195834711	0.642857143
36	51	50.56889673	0.463412698	0.25
37	105	19.8495749	0.459036859	0.070306363
38	95	22.84928435	0.470859341	0.08234127
39	116	23.80843113	0.424446998	0.081774082

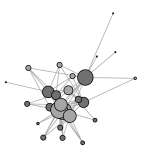

Table S1: (continued)

Network	Richness	NODF	Modularity	Connectance
40	93	24.14551257	0.46889382	0.098484848
41	83	39.67637728	0.425227076	0.126865672
42	93	27.86605248	0.453690007	0.085714286
43	81	31.85541898	0.418353686	0.117691154
44	93	31.74693878	0.461230487	0.088900862
45	75	31.82727497	0.447642911	0.101080247
46	71	28.37614854	0.516888722	0.124794745
47	77	51.81188441	0.470538313	0.143442623
48	51	33.71946622	0.371613243	0.137254902
49	141	15.39290372	0.483599322	0.087693441
50	106	35.51303715	0.245710571	0.193859649

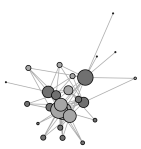

Table S2: Pairwise comparisons of NODF, modularity, and connectance values among mainland, trait-based (TB), and random (R) extinction scenarios using the Wilcoxon rank sum test with Bonferroni correction. Significant p-values ($<$ 0.05) are in bold.

Metric	**Category**	**Comparison**	**p-value**
NODF	Low	M-TB	**<0.05**
		M-R	**<0.05**
		TB-R	1
	Medium	M-TB	**<0.05**
		M-R	**<0.05**
		TB-R	1
	High	M-TB	**<0.05**
		M-R	**<0.05**
		TB-R	1
MOD	Low	M-TB	**<0.05**
		M-R	**<0.05**
		TB-R	1
	Medium	M-TB	**<0.05**
		M-R	**<0.05**
		TB-R	1
	High	M-TB	**<0.05**
		M-R	**<0.05**
		TB-R	1
Connectance	Low	M-TB	**<0.05**
		M-R	**0.05**
		TB-R	1
	Medium	M-TB	**<0.05**
		M-R	**<0.05**
		TB-R	1
	High	M-TB	**<0.05**
		M-R	**<0.05**
		TB-R	1

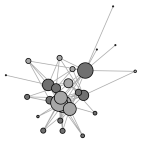

S1.3 Figures

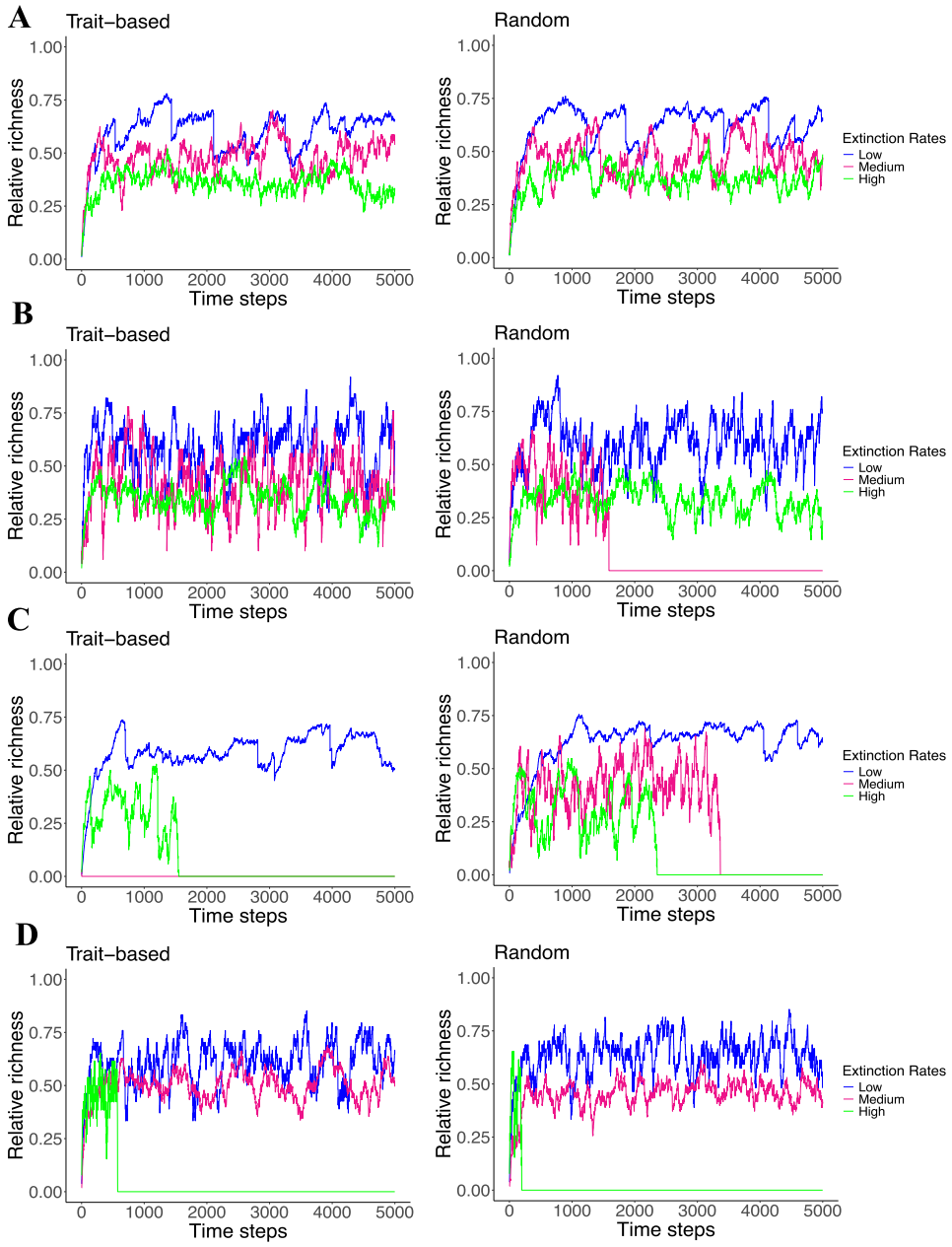

Figure S1: Richness of the island relative to total richness in the mainland for four different networks (**A-D**) in trait-based and random extinctions scenarios.

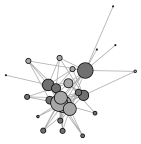

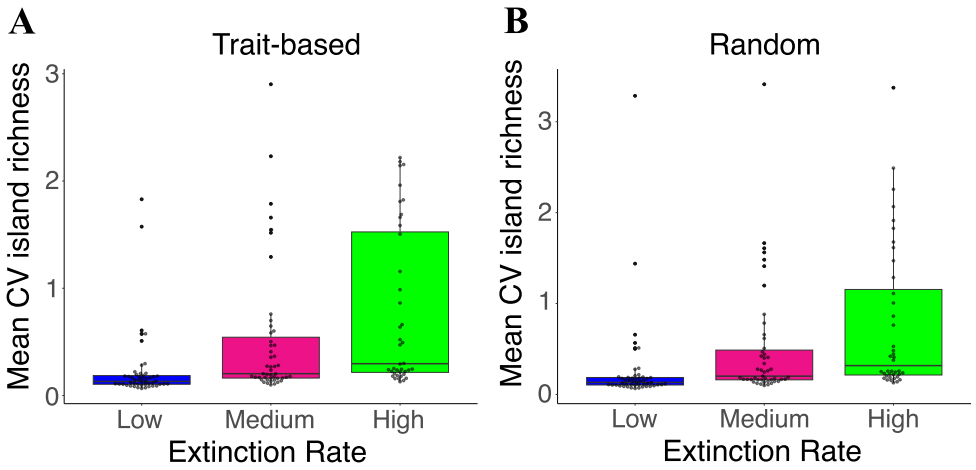

Figure S2: Mean CV of island richness communities across 1000 simulations at different extinction rates. Each point represents a network. **A)** Trait-based extinction scenario and **B)** random extinction scenario.

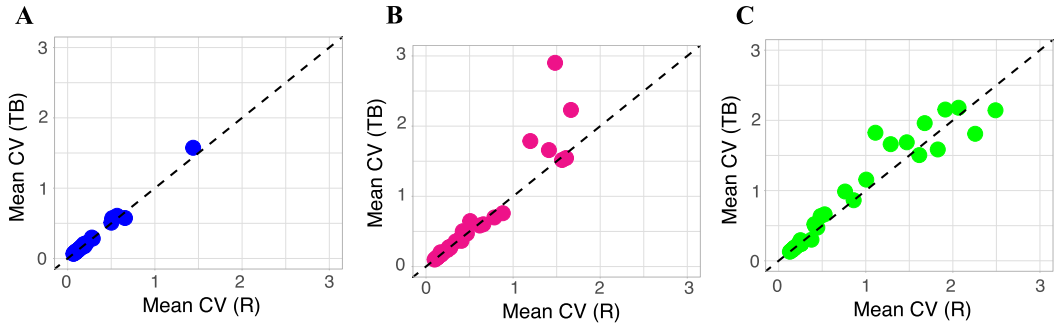

Figure S3: Correlation between the mean CV values of island richness in trait-based (TB) and random (R) scenarios under **A)** low, **B)** medium, and **C)** high extinction rates. Each data point represents the mean CV of a network calculated from 1000 simulations.

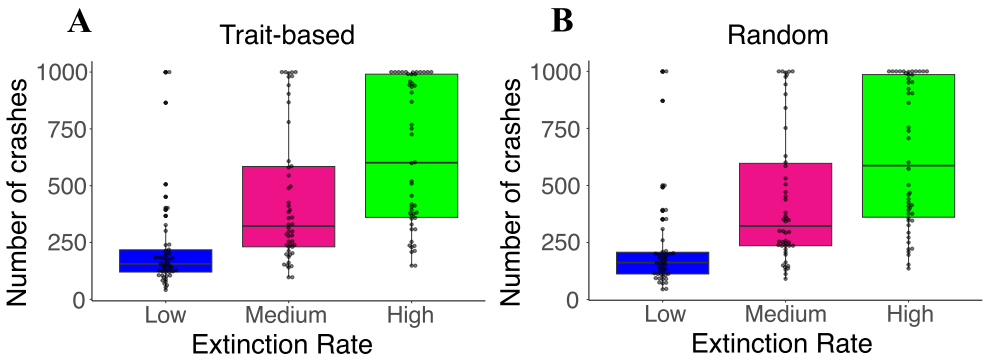

Figure S4: Number of crashes in island communities across 1000 simulations at different extinction rates. Each point represents a network. **A)** Trait-based extinction scenario and **B)** Random extinction scenario.

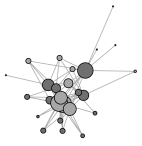

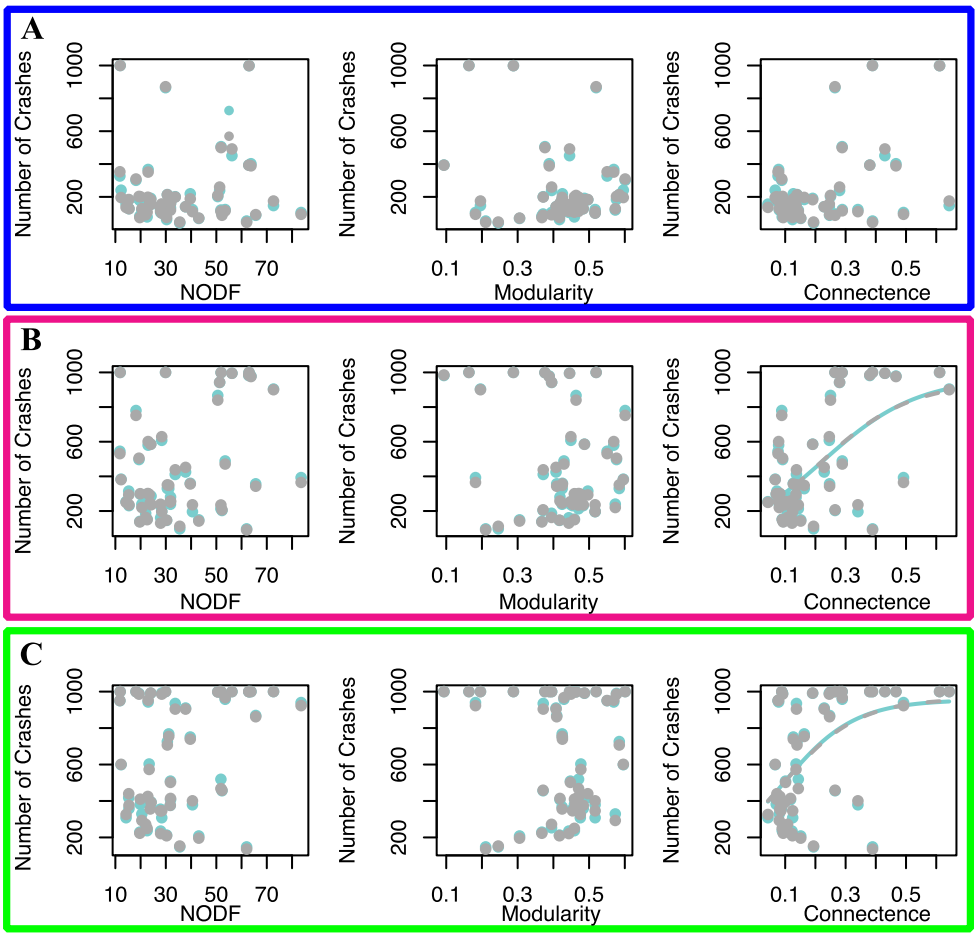

Figure S5: We fitted a logistic regression model to assess how the structure of mainland networks impacts the number of island community collapses across three extinction rates: **A)** Low (blue), **B)** Medium (pink), and **C)** High (green).

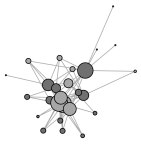

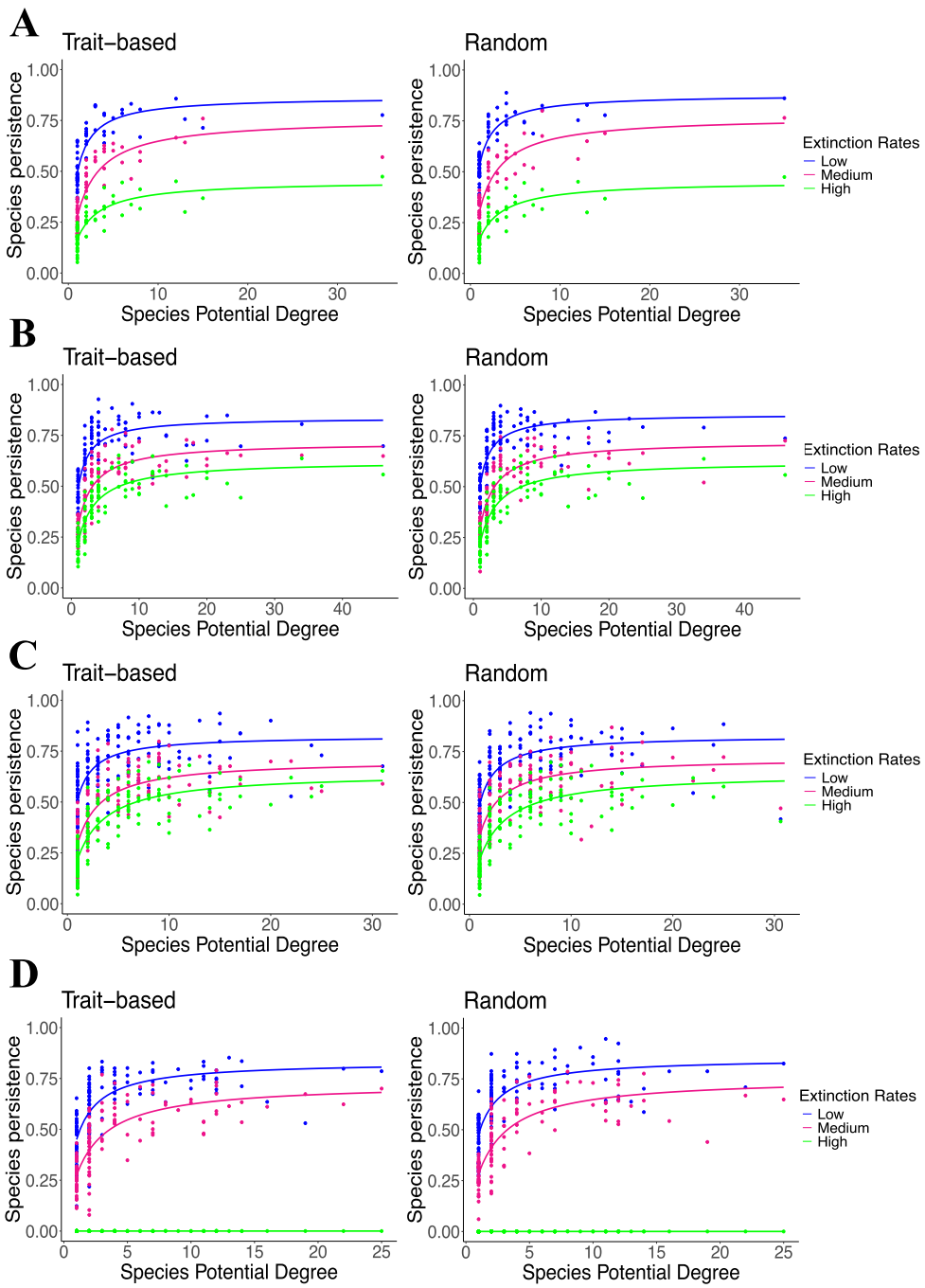

Figure S6: Species persistence on the island is related to the number of interactions species have on the mainland for four different networks (**A-D**) in trait-based and random extinction scenarios. Maximum persistence (= 1) means that the species was present on the island throughout all 5000 time steps in our simulation.

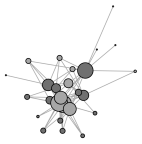

Chapter 2

"Now, when I see a landscape or learn about a new animal, I think, 'How would stable isotopes help figure how these things work?' It might be surprising to anyone else that someone could spend such a long time devoted to things I can't see, smell, taste or hear. But, to others, not surprising at all. We're isotope nerds!"

(Marilyn Fogel - The Isotope Queen [1], 1952-2022)

[1] Pioneered the field of biogeochemistry. Known for revolutionizing the use of stable isotopes not only in geochemistry but also in ecology and cosmochemistry, she was elected to the National Academy of Sciences in 2019.

Chapter 2

Exploring the relationships between morphological variation, dietary breadth, and patterns of extinction among Hawaiian Honeycreepers (Drepanididae)

1 Abstract

Trait variation is essential for population-level responses to novel selective pressures, potentially promoting resilience. As such, specialization is linked to a higher intrinsic vulnerability to extinction, while more generalist species tend to demonstrate increased persistence in disturbed environments. Among birds, beak morphology is a complex trait crucial for many tasks directly influencing fitness, such as the acquisition of resources, and is often predictive of dietary guild. We hypothesize that species with increased morphological variation in their beaks may access a greater range of food resources, resulting in a larger dietary niche, which in turn might lead to more resilience to extinction. Hawaiian honeycreepers, a diverse group of Fringillid birds isolated to the Hawaiian archipelago, once comprised ca. 50 species occupying a wide range of eco-morphological niches, with less than 40% species persisting today. To investigate to what extent intraspecific morphological variation is predictive of dietary breath and consequently extinction risk across species, we quantified beak morphological variation of extinct and extant Hawaiian honeycreepers collected between 1880 and 1914. We also estimated species' niche breadth from stable isotope ratios of feather keratin. Our result shows that frugivorous and granivorous species present the highest intraspecific beak morphological variation, even though granivorous species reveal the smallest isotopic breadth. While a direct link between morphology and diet variation was not evident at the community level, our analysis revealed that species within a guild with lower morphological variation tended to have a narrower dietary niche. Additionally, species that have gone extinct exhibited lower morphological variation, suggesting a possible link between evolutionary potential and extinction vulnerability. While the historical onset of extinction pressure in Hawaiian honeycreepers is well known and unrelated to beak morphological variation, our study reinforces the notion that at least for some guilds, having great beak morphological variation could have helped species to persist in fast-changing environments.

2 Introduction

The potential for a species to adapt to new environments generally increases the odds of persistence in the face of environmental change (Bürger & Lynch, 1995;

Lande & Shannon, 1996; Milot *et al.*, 2020a). The variability of certain traits within a species impact its evolutionary response to new selective pressures, where increased trait variability often translates to increased resilience (Bürger & Lynch, 1995). This is because the response to selection depends not only on the magnitude of the selective pressure but also on the amount of variation within the population (Assis *et al.*, 2017). However, the significance of the amount of variation to selection depends on the type of trait, with traits that are critical for essential functions, such as feeding, being more influential in determining an individual's fitness. Therefore, greater variation in functional traits can be especially important for a species' persistence in a changing environment.

In birds, beak morphology comprises a complex trait important for many tasks directly related to fitness, such as thermoregulation (Tattersall *et al.*, 2017), nest construction (Sheard *et al.*, 2023), sexual display (Derryberry *et al.*, 2012), and the acquisition and processing of resources (Levey, 1987; Wheelwright, 1985; Dehling *et al.*, 2016). Among these diverse functions, cranial and beak morphology in birds can also strongly predict dietary guild membership (Pigot *et al.*, 2016; Felice *et al.*, 2019). For example, pollinating birds often have beak shapes that match the floral morphology of the plants they pollinate, suggesting a strong constraint on pollinators' traits related to food acquisition (Abrahamczyk & Kessler, 2015), whereas granivorous birds have beak shapes that correlate with the seeds they must crack (Benkman, 1999). However, the relationship between beak morphology and diet is usually explored only at the species level with little information on the role of intraspecific beak morphological variation and individual diet.

Ecological studies typically treat species as groups of homogeneous individuals, focusing on the mean trait of each species and not accounting for variation or its impact on ecological dynamics. However, within-species trait variation can significantly influence these dynamics, affecting factors such as species persistence and coexistence (Gibert & Brassil, 2014), population dynamics (Pelletier *et al.*, 2007), and the strength of ecological interactions (Bolnick *et al.*, 2011). When considering species diet or resource use, studies also treat individuals as ecologically equivalent. For example, by describing the network structure of an ecological community, the links usually show the interactions at the species level. However, a species classified as a generalist (with many interactions) may consist either of individuals that are all generalists or of individuals that are specialized on different resources, collectively accounting for the species' overall dietary variation (Bolnick *et al.*, 2003). Southern sea otter (*Enhydra lutris nereis*), for instance, is generally considered a dietary generalist at the species level. However, individual otters vary significantly in their diets, with some specializing in snails, others in crabs and abalone, while others maintain a more generalist diet (Estes *et al.*, 2003).

Since beak morphology in birds is closely related to diet, the among-individual variation observed within a species' beak structure may influence the species' dietary niche breadth measured across individuals, as different beak shapes can facilitate the exploration of different types of resources within a guild. Consequently, greater morphological variation within a species could lead to a broader

dietary niche. Conversely, limited variation in beak shape within a species might restrict its diet, resulting in a narrower dietary niche. Because a species' niche breadth can also affect its ability to persist in a changing environment (Lavergne *et al.*, 2013; Soto-Saravia *et al.*, 2021), it is plausible to expect that species with less beak variation would have a narrower dietary niche breadth and, consequently, a higher risk of extinction. This is because, although specialists species are very efficient at exploiting specific resources, they are vulnerable when those resources become limited (Terraube *et al.*, 2011). On the other hand, when environmental conditions change, generalist species—whether composed of generalist individuals or a set of specialist individuals—have a subset of individuals that can still thrive, reducing the overall impact on the species. Moreover, a broader niche breadth can provide a buffer against environmental instability, increasing species persistence, whereas specialists may suffer more severely and have a higher chance of extinction.

Hawaiian honeycreepers (Aves: Fringillidae: Carduelinae) radiated across the Hawaiian archipelago approximately 5.7 million years ago (Lerner *et al.*, 2011), evolving to occupy a wide range of eco-morphological niches. These species-specific dietary niches include specializations on seeds, nectar, fruits, insects, and snails, accompanied by a diversity of beak shapes (Tokita *et al.*, 2017). In fact, this group has one of the greatest variation in beak morphology among birds, even when compared to other lineages that have also undergone adaptive radiations (Lovette *et al.*, 2002; Tokita *et al.*, 2017; Miles *et al.*, 2023). Historically, nearly 50 honeycreeper species were distributed across Hawaii islands, today less than 40% of species persist, having been heavily impacted by recent anthropogenic and environmental change (Pratt & Conant, 2005). Though the factors contributing to these extinctions are varied, avian malaria was likely a significant driver, with surviving species now limited to higher elevations where mosquito presence is limited (Atkinson *et al.*, 2000; Boyer, 2008; Paxton *et al.*, 2016).

Although originally occupying very different dietary guilds, most extant honeycreeper species consume primarily nectar and/or invertebrates (Pratt & Conant, 2005). At a macroevolutionary scale, different guilds are subject to different rates of evolutionary adaptation (Felice *et al.*, 2019). Similarly, other guilds act as macroevolutionary sink, such as omnivorous birds that have higher extinction rates when compared to other guilds (Burin *et al.*, 2016). However, from a microevolutionary perspective, we still lack an understanding of whether different guilds have varying resilience in response to large disturbances. Because microevolutionary rates of evolution are driven in large part by intraspecific trait variation (Houle, 1992), beak shape variability and/or dietary flexibility of different dietary guilds may have contributed to which species survived and which did not. Thus, from a microevolutionary perspective, we could expect not only variability within a species, but we might expect that different guilds have different variability, which could either help or hinder their capacity to persist in a changing environment. As the pattern of extinctions observed among honeycreeper species is known, it is possible to assess whether and to what extent the intraspecific variability of beak

morphology and diet correlates with persistence.

Here we measure intraspecific variation in beak morphology and niche breadth from stable isotope ratios for both extinct and extant Hawaiian honeycreeper species. Our study is, to our knowledge, the first to reveal the isotope composition of historical honeycreepers. We aim to determine 1) whether there exists a correlation between morphological variation and niche breadth across species, and 2) whether a greater within-species morphological variation and/or niche breadth may have increased the likelihood of persistence. We first use geometric morphometrics to examine both across-species differences in beak morphology, as well as within-species variability in beak morphology, and to what extent known or assumed diets correlate with these changes in beak shape. Using feather tissues sampled from historical museum collections, we next analyze carbon and nitrogen isotopic ratios of honeycreeper species, thereby estimating the isotope niche of each, from which we obtain relative measures of dietary differentiation and variability across species (Bearhop *et al.*, 2004; Newsome *et al.*, 2007, 2012; Yeakel *et al.*, 2016). Together, we examine whether and to what extent differences in beak morphology correlates with differences and/or variability in isotopic niche.

Hawaiian honeycreepers offer particular advantages for exploring the relationship between form, function, and extinction risk, given the wealth of information documenting species' extinctions and their morphological and functional diversity. While the historical onset of extinction pressure in this group has been well-studied (van Riper III *et al.*, 1986; Pratt & Conant, 2005; Ricklefs, 2017), it is not known how potential differences in morphological or dietary niches may have influenced the pattern of extinction. Understanding this relationship is important because it directs the potential and pace of a species' evolutionary response, which is crucial for our understanding of the pressures on extant birds facing a future fraught with risk.

3 Methods

3.1 Specimens used and categorization

For both isotopic and morphometric analyses, we sampled individuals of Hawaiian honeycreepers housed in the Museum of Comparative Zoology at Harvard University (MCZ), the Museum of Vertebrate Zoology at the University of California, Berkeley (MVZ), and the Royal Ontario Museum (ROM). We measured both beak morphology and sampled feathers to obtain stable carbon and nitrogen isotopic ratios for 165 specimens representing 24 honeycreeper species (16 extant and 8 extinct). We measured only beak morphology for an additional 202 individuals, representing an additional four species (2 extant and 2 extinct). All specimens were originally collected between 1880 and 1913, and only adult individuals were included in our analysis to avoid potential ontogenetic signals in both diet and morphology. Due to the rarity of specimens, both females and males were measured and sampled. We note that there is no significant sexual dimorphism in

the size and shape of skull and beak morphology within this group (Tokita *et al.*, 2017), such that we do not separate samples by sex in our analyses.

Historical information on species' guilds was obtained from Pratt & Conant (2005). Among the 28 species included in this study, two are classified as frugivorous, three as graminivorous, four as nectarivorous, six eat both invertebrates and nectar, and ten eat exclusively invertebrates (Table 1). We used IUCN Red List classifications of 'extinct in the wild', and both 'critically endangered' and 'not been observed in nature in the last 30 years', to classify species as 'extinct'.

Table 1: Historical information on species' guilds. IUCN categories: EX (extinct); CR (critically endangered), EN (endangered), and VU (vulnerable) are threatened species; and NT (near threatened) and LC (least concern) are non-threatened species.

Diet	**ID**	**Species**	**IUCN**	**Last Obs.**
Fruits	1	*Psittirostra psittacea*	CR	1989
	2	*Rhodacanthis palmeri*	EX	1896
Seeds	3	*Chloridops kona*	EX	1894
	4	*Loxioides bailleui*	CR	–
	5	*Telespiza cantans*	VU	–
Nectar	6	*Himatione fraithii*	EX	1923
	7	*Himatione sanguinea*	LC	–
	8	*Palmeria dolei*	CR	–
	9	*Vestiaria coccinea*	VU	–
Invertebrates/ Nectar	10	*Akialoa obscura*	EX	1903
	11	*Akialoa stejnegeri*	EX	1967
	12	*Chlorodrepanis flava*	NT	–
	13	*Chlorodrepanis stejnegeri*	EN	–
	14	*Chlorodrepanis virens virens*	LC	–
	15	*Chlorodrepanis virens wilsoni*	LC	–
	16	*Magumma parva*	EN	–
Invertebrates	17	*Hemignathus affinis*	EX	1996
	18	*Hemignathus hanapepe*	EX	1889
	19	*Hemignathus wilsoni*	EN	–
	20	*Loxops caeruleirostris*	CR	–
	21	*Loxops coccineus*	EN	–
	22	*Loxops mana*	EN	–
	23	*Oreomystis bairdi*	CR	–
	24	*Paroreomyza flammea*	EX	1963
	25	*Paroreomyza maculata*	CR	1985
	26	*Paroreomyza montana*	EN	–

3.2 Morphological data

To measure beak morphology, we captured lateral photos of each individual's beak and digitized the complete outline using five landmarks and six semi-landmarks with the 'geomorph' package (R programming environment) (Adams & Otárola-Castillo, 2013) (Figure S1). We used the entire avian bill (both upper and lower beaks) because this group appears to have lower integration between the upper and lower beaks. We took measurements from the right side of the specimens, though in cases where the right side exhibited any type of damage, we used the left side. To standardize the shape data, we conducted a Generalized Procrustes Analysis using also *geomorph* package (Adams & Otárola-Castillo, 2013), where beaks were rotated, scaled, and aligned. All specimens underwent digitization twice, and repeatability was estimated following the methodology outlined by Lessells & Boag (1987). Repeatabilities of landmarks were high on average across all species (mean = 0.82; SD = 0.07).

3.2.1 Beak Size

We measured species' beak size using centroid size (CS), where

$$CS = \sqrt{\sum_{i=1}^{n} ((x_i - \bar{x})^2 + (y_i - \bar{y})^2)} \quad (1)$$

in which (X_i,Y_i) are the coordinates of each landmark, and ($\bar{x}$, $\bar{y}$) are the coordinates of the centroid. To capture the variation in centroid size within species, we used the coefficient of variation (CV) of centroid size among individuals, where a lower CV indicates that individuals of that species have very similar beak sizes, while a higher CV indicates greater variation in beak size among individuals of that species.

3.2.2 Beak Shape

We used the scaled landmark coordinates following the Generalized Procrustes Superimposition (GPS) to generate a covariance matrix of species' beak shape. This matrix is a square matrix where the principal diagonal describes the variance in the landmark coordinates, and the off-diagonal elements represent the covariance among them. This covariance matrix, also known as the **P**-matrix (*i.e.*, phenotypic variance/covariance matrix), is used as a proxy for the **G**-matrix (*i.e.*, additive genetic covariance matrix). The **G**-matrix would be the ideal tool for studying a population's potential to respond to selection, as the response depends on the amount of available genetic variation, but it is often difficult to calculate because it requires pedigree data.

To estimate the variation in beak shape within a species, i.e. morphospace occupancy, we used the Coefficient of Variation of Eigenvalues (ICV) of the phenotypic covariance matrix. The ICV of the covariance matrix describes the dis-

tribution of total variation in the morphospace, high values of ICV indicates that most variation is concentrated in the first few eigenvalues, while low values of ICV indicate that morphological variation is well distributed in more dimensions of morphospace. ICV for species i, given by

$$ICV_i = \frac{\sigma_i}{\lambda_i}, \tag{2}$$

where σ_i is the standard deviation of the eigenvalues of the covariance matrix and λ_i is the mean of the eigenvalues for species i. We then calculated the relative value of ICV (ICV_r) as

$$ICV_r = 1 - \frac{ICV_{\max} - ICV_i}{ICV_{\max} - ICV_{\min}}, \tag{3}$$

where $ICV_{\max}$ and $ICV_{\min}$ are the maximum and minimum values of ICV among species in our dataset, scaling this relative measure between 0 and 1. In this sense, low values (closer to 0) of ICV_r represents a higher integration among traits in which most of the variation is on the first and second PCs, such that trait variability is low. Whereas higher values of ICV_r (close to 1) means that trait variation is more distributed in different directions of the morphospace and, consequently, that trait variability is high.

3.3 Isotope data

To calculate the isotopic niche breadth of the Hawaiian honeycreepers, we measured ratios of stable carbon and nitrogen isotopes from feather tissue collected from museum specimens. All stable isotope compositions are expressed in delta (δ) notation, where

$$\delta = 1000 * (\frac{R_{\text{sample}}}{R_{\text{standard}}} - 1), \tag{4}$$

and where R represents either $^{13}C/^{12}C$ or $^{15}N/^{14}N$, and is expressed in units of per mil (‰). We collected three contour feathers from the ventral feather tracts of each individual. Given that individuals were collected in different seasons, contour feathers are expected to provide a dietary average that integrates across potential seasonal variation.

To prepare feathers for isotopic analysis, we cleaned each sample using a 2:1 chloroform methanol solution to remove lipids, subsequently air-drying each sample for a minimum of 24 hours. We measured ca. 0.5 mg of each sample, each of which were placed in a tin capsule and combusted in a Costech 4010 Elemental Analyzer coupled with a Delta V Plus Continuous Flow Isotope Ratio Mass Spectrometer. Carbon and nitrogen isotope values were corrected for instrument drift, mass linearity and standardized to the international VPDB ($\delta^{13}C$) and AIR ($\delta^{15}N$) scales using the USGS 41a and USGS 40 standard reference materials. Reference material $\delta^{13}C$ values (mean ± standard deviation) were USGS 40: -26.38 ± 0.14‰ ($n = 67$) and USGS 41a: 36.54 ± 0.23‰ ($n = 34$). Reference material $\delta^{15}N$ values were USGS 40: -4.52 ± 0.11‰ ($n = 67$) and USGS 41a: 47.54 ± 0.15‰ ($n = 34$).

Elemental carbon and nitrogen contents were determined via linear regression of CO_2 and N_2. We also analyzed 26 aliquiots of an internal squid tissue for quality control, which was identical to its long term average isotopic composition ($\delta^{13}C = -18.59 \pm 0.19‰$; $\delta^{15}N = 11.90 \pm 0.16‰$). We adjusted the $\delta^{13}C$ values of historical specimens to account for changes in industrial CO_2 concentrations in the atmosphere, known as the Suess effect (Keeling, 1979). To calculate the isotopic niche breadth of honeycreeper species we used the 'SIBER' package (R programming environment) to estimate the standard ellipse area (SEAc) which implements a Bayesian approach to account for the effects of sample size (Jackson *et al.*, 2019). The SEAc provides a measure of the bivariate isotopic niche space established by $\delta^{13}C$ and $\delta^{15}N$ values for collected individuals within each species, with units of ‰^{2}.

4 Results

4.1 Intraspecific morphological variation

To ensure large enough sample sizes to capture an accurate measures of morphological variation, we excluded all species with fewer than seven individuals in our sample. Although seven is an arbitrary number, our rarefaction analysis showed that this number is sufficient to capture the mean variability within a species (Figure S2). Additionally, to determine if our morphological variation was correlated with sample size, we ran a linear model and found no significant correlation between sample size and morphological variation in our data based on the results (Figure S3).

We examined species-specific differences in 1) intraspecific beak size variation, by using the CV of the centroid size and, 2) intraspecific beak shape variation, by using the relative values of coefficient of variation of eigenvalues (ICV_r) of the covariance matrix.

4.1.1 Beak Size

We found great variation in beak size ranging from 0.048 to 0.140. Beak size CV varied greatly between ecological guilds, with great overlap in beak size CV between different guilds (Figure 1A-B). The species with the greatest within-species variation in beak size was *Akialoa stejnegeri*, which has a mixed nectarivorous/insectivorous diet, followed by *Hemignathus wilsoni* and *Oreomystis bairdi*, both insectivorous birds (Figure 1A). The species with the lowest beak size variation were *Himatione fraithii* and *Paroreomyza flammea*, which are nectarivorous and insectivorous birds, respectively. Birds that have a diet based on invertebrates have the greatest range of within-species beak size variation, with some species where individuals varied little in beak size, whereas for other species, there is a great variation in beak size among individuals (Figure 1A-B). To examine guild-level differences in beak size within-species, we conducted a Kruskal-Wallis rank

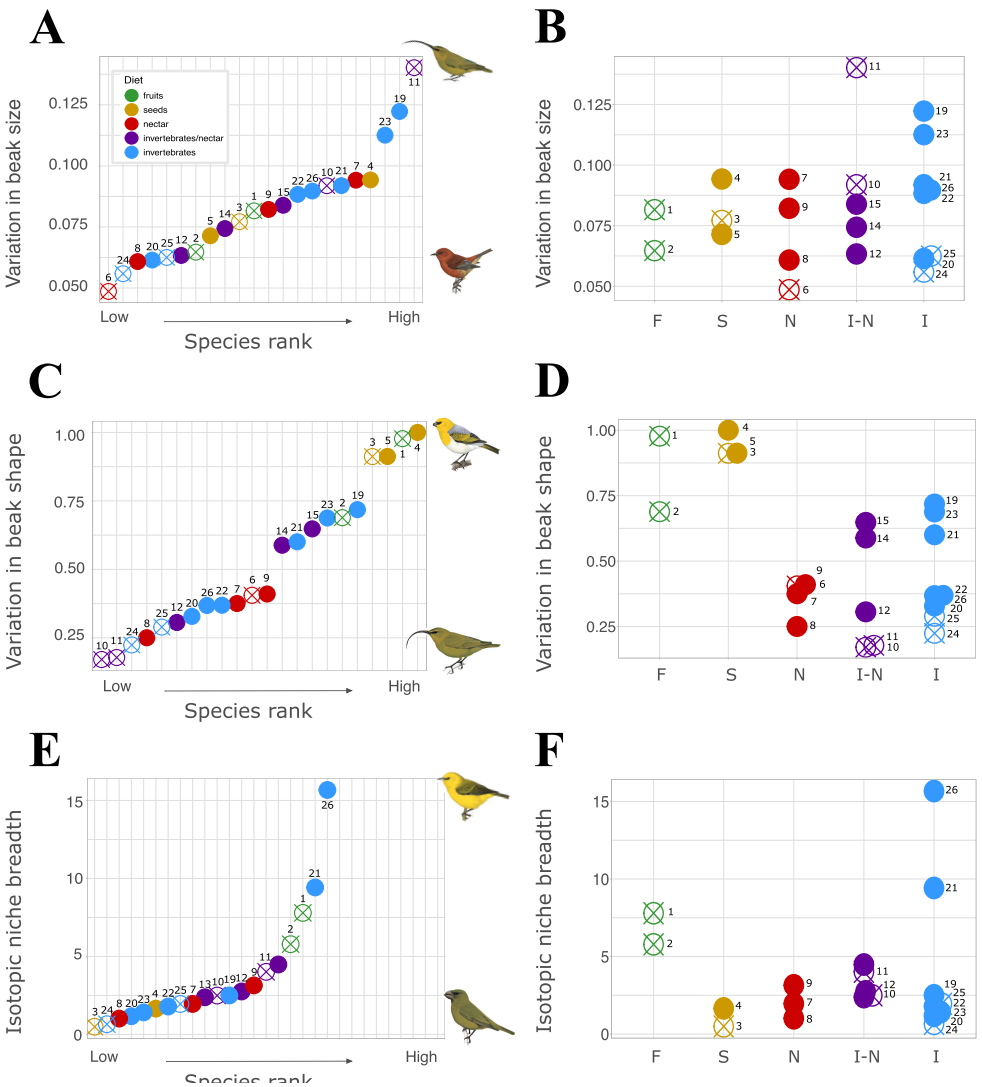

Figure 1: Species in ascending order of variation of **A)** variation in beak size (CV centroid size); **C)** variation in beak shape (ICV_r); **E)** dietary niche breadth ($SEAc$). Differences within guilds of **B)** Within-species variability in beak size (CV centroid size), **D)** Within-species variability in beak shape (ICV_r),**F)** isotopic niche breadth (SEAc). Solid and open-crossed points denote extant and extinct species. On the top right and bottom right are illustrations of the species with the highest and lowest values, respectively. 1, *Psittirostra psittacea*; 2, *Rhodacanthis palmeri*; 3, *Chloridops kona*; 4, *Loxioides bailleui*; 5, *Telespiza cantans*; 6, *Himatione fraithii*; 7, *Himatione sanguinea*; 8, *Palmeria dolei*; 9, *Vestiaria coccinea*; 10, *Akialoa obscura*; 11, *Akialoa stejnegeri*; 12, *Chlorodrepanis flava*; 13, *Chlorodrepanis stejnegeri*; 14, *Chlorodrepanis virens virens*; 15, *Chlorodrepanis virens wilsoni*; 16, *Magumma parva*; 17, *Hemignathus affinis*; 18, *Hemignathus hanapepe*; 19, *Hemignathus wilsoni*; 20, *Loxops caeruleirostris*; 21, *Loxops coccineus*; 22, *Loxops mana*; 23, *Oreomystis bairdi*; 24, *Paroreomyza flammea*; 25, *Paroreomyza maculata*; 26, *Paroreomyza montana*. F, fruits; S, seeds; N, nectar, I-N, mixed invertebrates and nectar; I, invertebrates. (Illustrations from Billerman *et al.* (2022))

sum test. Because the number of species is very low for frugivorous and granivorous, we exclude these two guilds of our test. We observe no significant difference in beak size variation among nectarivorous, mixed nectarivorous/insectivorous, and insectivorous guilds ($\chi^2 = 1.34$, $df = 2$, $p = 0.51$) (Figure 1B).

4.1.2 Beak Shape

We observe three distinct groupings of species – denoted as high, intermediate, and low – as a function of intraspecific beak shape variation (Figures 1C). All granivorous species are found in the grouping with the highest beak shape variation, with *Loxioides bailleui* exhibiting the greatest variation among all species. One of the two extinct frugivorous species, *Psittirostra psittacea*, is also found in this high shape-variability group, with the remaining species (*Rhodacanthis palmeri*) at the high-end of the intermediate group. Across species, all nectarivores occur in the low shape-variability group, while mixed nectarivore/insectivore and insectivores are distributed across the intermediate and low groups.

Within guilds, extinct species presented the lowest measures of intra-specific shape variation, with the exception of nectarivorous and excluding frugivorous (all extinct species)(Figure 1D). Then, to explore if there was any difference across guilds in the intraspecific amount of beak variation we performed a Kruskal-Wallis rank sum test. Again, we excluded frugivorous and granivorous due to small sample sizes. Our result revealed no significant difference among the nectarivorous, mixed nectarivorous/insectivorous, and insectivorous guilds ($\chi^2 = 0.75$, $df = 2$, $p = 0.68$) (Figure 1D).

4.2 Carbon and nitrogen isotopic signatures

Because we are using dietary guilds constructed from observational data, we first evaluate whether those observational guilds correlate with isotopic differences (Figure 2A). Honeycreepers occupy a great area in isotope space with a range of ca. 14.5 and 27.8 of δ^{13}C and δ^{15}N values, respectively. However, there is a great overlap across guilds for most species, with δ^{13}C values spanning ca. -24.0 to -18.0‰, and δ^{15}N values spanning ca. 0.8 to 12.1‰ (Figure 2A and Figure S4). In contrast, *Himatione fraithii* and *Telespiza cantans* reveal highly distinctive δ^{13}C and δ^{15}N values, together ranging from -21.2 to -9.4‰ and 18.8 to 28.6‰, respectively.

We then examined differences in δ^{13}C and δ^{15}N among species within the same guilds (Figure 2B-F). The two frugivores species have distinct isotopic signatures, with *Psittirostra psittacea* showcasing a great deal of variability in δ^{15}N values (Figure 2B), while *Rhodacanthis palmeri* varies more along the δ^{13}C values. Granivore species diverge greatly in their wide range of δ^{13}C and δ^{15}N values (Figure 2C), though this is primarily driven by *Telespiza cantans*, which has much higher δ^{15}N values than other granivores, and has δ^{13}C values ranging from -20.2 to -9.4. The other two granivorous honeycreepers (*Loxioides bailleui*, and *Chloridops kona*) have comparatively low δ^{13}C and δ^{15}N values and ranges, and overlap,

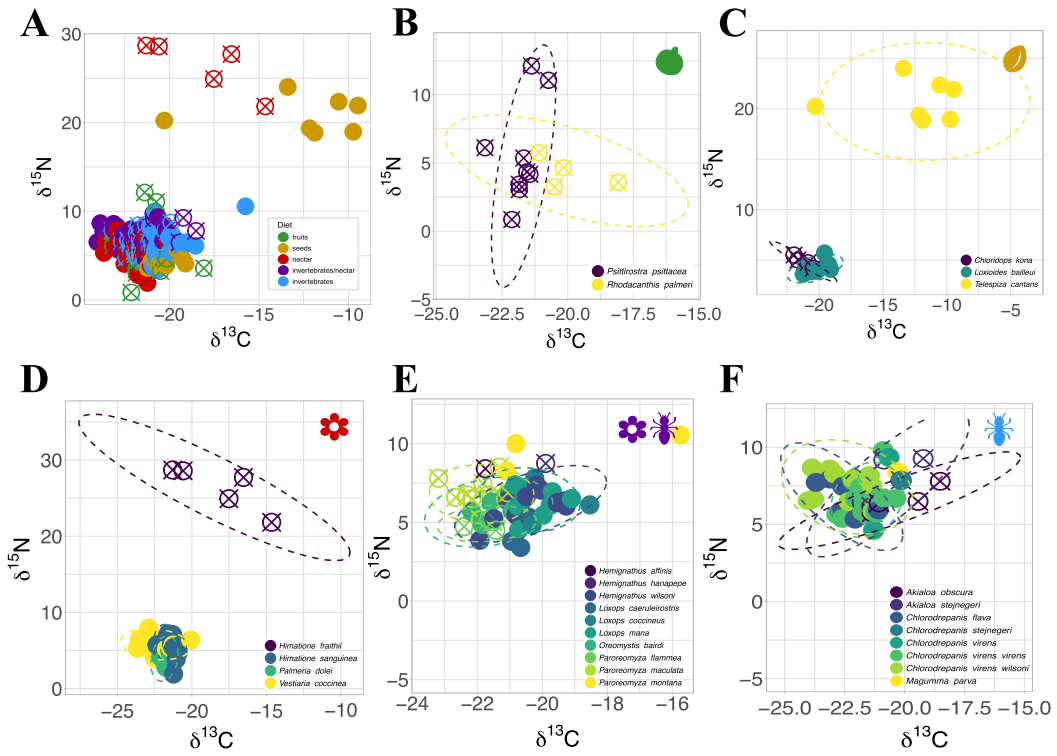

Figure 2: Stable isotope values ($\delta^{13}C$ and $\delta^{15}N$) of Hawaian Honeycreepers. Each point is a an individual, open crossed points represent extinct species, and ellipse areas of species are shown. **A)** All species in their guilds. **B)** Frugivorous species; **C)** Gramnivorous species; **D)** Nectarivorous species; **E** Mixed invertebrate and nectar-feeder; **F** Invertebrate-feeder. Note the change in scale across panels.

although the extinct *Chloridops kona* has a much narrowed dietary niche breadth (Figure 2C). Nectarivorous species reveal isotopic groupings similar to those of granivores, with one species, *Himatione fraithii*, showcasing high δ^{15}N values and variable δ^{13}C values (Figure 2D), whereas the others have low δ^{13}C and δ^{15}N values and ranges. Mixed nectarivorous and insectivorous honeycreepers have a large isotopic ranges, with δ^{13}C values spanning -24.02 to -18.51‰ and δ^{15}N values spanning 4.56 to 9.78‰ (Figure 2E). Most insectivorous honeycreepers have overlapping δ^{13}C and δ^{15}N values (Figure 2F), with the extinct *Paroreomyza flammea* and *Peroreomyza maculata* falling lower along the δ^{13}C axis, and more distinct than the rest.

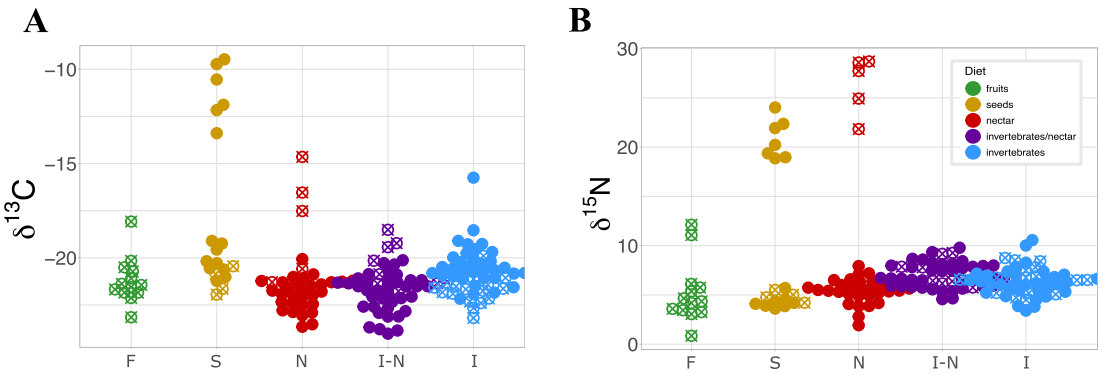

Figure 3: Isotopic differences across species categorized by dietary guild. Each point is an individual and solid and open-crossed points denote extant and extinct species, respectively. **A)** δ^{13}C (‰) and **B)** δ^{15}N (‰) values. F, fruits; S, seeds; N, nectar, I-N, mixed invertebrates and nectar; I, invertebrates.

To determine if there were significant differences in δ^{13}C values among foraging guilds, we performed a Kruskal-Wallis rank sum test excluding *Himatione fraithii* and *Telespiza cantans* species, which account for those with extremely divergent δ^{13}C and δ^{15}N values. We used Kruskal–Wallis rank sum test since our data violated the assumptions of homogeneity of variances for a parametric statistical analysis. We observe significant differences between guilds for δ^{13}C values ($\chi^2 = 25.30$, df $= 4$, $p < 0.05$) and δ^{15}N values ($\chi^2 = 45.35$, df $= 4$, $p < 0.05$) (Figure 3A,B). To explore which guilds differ in δ^{13}C values, we then conducted *post-hoc* pairwise comparisons using the Wilcoxon rank sum test with Bonferroni correction. The results reveal significant differences in δ^{13}C values between: gramnivores vs. nectarivores, nectarivore/invertivores vs. granivores, and between invertivores vs. nectarivores (Table S1). No significant differences were found between other guild pairs (see Table S1 for pairwise scores). We also observe significant differences between the δ^{15}N values of mixed nectarivore/invertivores vs. frugivores, nectarivores vs. gramnivores, mixed nectarivore/invertivores vs. granivores, invertivores vs. gramnivores, mixed nectarivore/invertivores vs. nectarivores, and between invertivores vs. nectarivores (Table S2).

We measured the isotopic niche breadth of both extinct and extant species by

calculating the standard ellipse area corrected for sample size (SEAc) (Jackson *et al.*, 2019). Isotopic niche breadth varied widely across species (Figure 1E and Figure 1F), with *Paroreomyza montana* and *Loxops coccineus*, both insectivorous species, exhibiting the broadest isotopic breadth. Frugivorous honeycreepers also displayed very broad dietary niches (Figure 1F). In contrast, gramnivores had the narrowest dietary niches, with *Chloridops kona* showing the narrowest dietary niche among all species (Figure 1E and Figure 1F).

4.3 Is there a correlation?

We next aim to assess if higher morphological variation translates to a broader isotopic niche breadth, so we used a linear regression analysis accounting for phylogeny with the *phylolm* package in R (Ho *et al.*, 2016). For this, we used the phylogeny available in McTavish *et al.* (2024) and applied the λ phylogenetic model of trait evolution (Pagel, 1999). The results are shown for all species with the imputed phylogenetic tree (Figure S5). Our analysis indicated that there is no significant relationship between either variation in beak shape and dietary niche breadth ($R^2 = 0.01$, $p = 0.72$), or variation in beak size and dietary niche breadth ($R^2 = 0.02$, $p = 0.6$) at the community level (Figure S5). However, when we looked within guilds, our result showed that lower morphological variation tends to be related to lower niche breadth (Figure S6).

4.4 Patterns of extinction

We also explored if differences in within-species variation in beak size, beak shape, and isotopic niche breadth, were related to extinction status (Figure 4). To assess for statistical significance, we used the Mann-Whitney U test, a non-parametric test comparing the central tendency between two independent groups. We observe no significant difference in beak size ($U = 2$, $n_{extinct} = 8$, $n_{extant} = 14$, $p = 0.23$)(Figure 4A), beak shape ($U = 7$, $n_{extinct} = 8$, $n_{extant} = 14$, $p = 0.40$) (Figure 4B), or isotopic niche breadth ($U = 8$, $n_{extinct} = 8$, $n_{extant} = 14$,$p = 0.93$) (Figure 4C) Due to the effects that frugivores and gramnivores are responding to different drivers of selection since fruit and nut size variation select for very different beak shape and size morphologies (see discussion below), we also examine extinct vs. extant honeycreepers with those groups excluded. This results in a significant difference between extinct and extant species, with extinct species having much lower beak shape variation than those alive today ($U = 6$, $p* = 0.01$)(Figure 4D). Lastly, we tested whether, within guilds, variation in beak morphology and isotopic niche breadth were related to extinction status. Specifically, we examined species variability relative to the mean variability of their dietary guild. We excluded frugivorous species since the only two representatives of this guild are extinct. Our analysis shows that, relative to the guild's variability, extinct species tend to have lower variability in beak shape ($U = 13$, $n_{extinct} = 6$, $n_{extant} = 14$, $p* = 0.01$) (Figure S7).

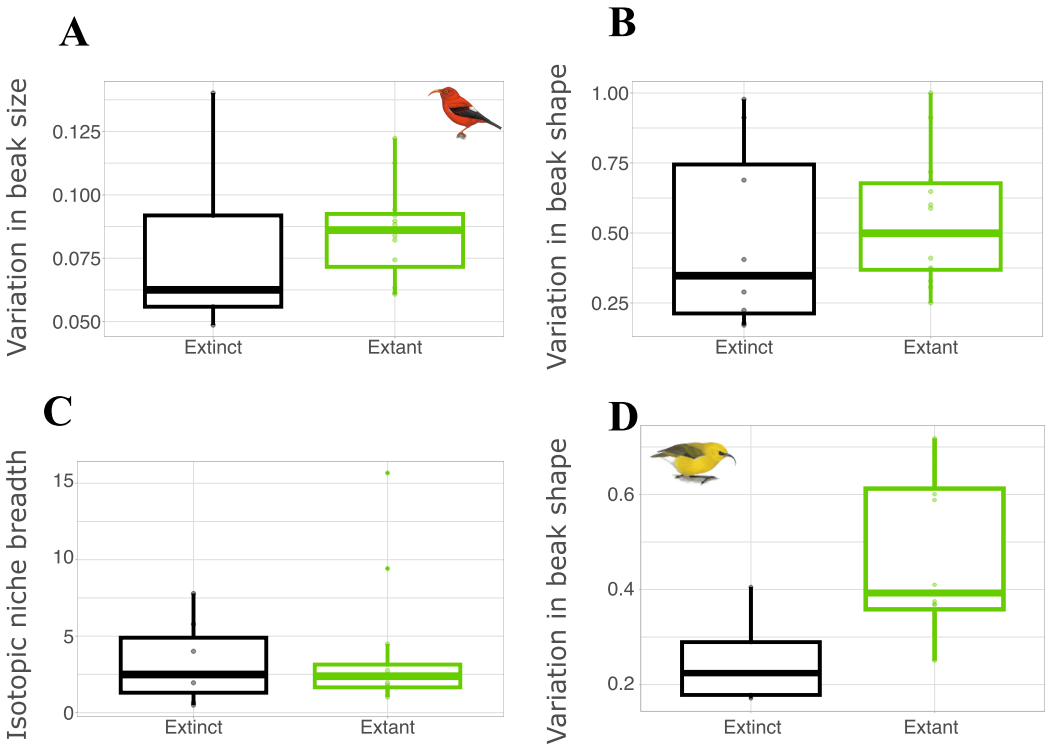

Figure 4: Boxplot depicting traits distribution for extinct (black) and extant (green) species. **A)** Variability in beak size ($CVcentroidsize$). Illustration of *Vestiaria coccinea*, an extant species; **B)** Variability in beak shape (ICV_r); **C)** Isotopic niche breadth ($SEAc$); **D)** Variability in beak shape (ICV_r) excluding frugivore and granivore species. Illustration of *Hemignathus hanapepe*, an extinct species. (Illustrations from *Birds of the World*)

5 Discussion

Variation is the raw fuel of evolution, as it is essential in guaranteeing that a population can respond to novel selective pressures (Lande & Shannon, 1996; Assis *et al.*, 2016). Therefore, estimating intraspecific variation in particular phenotypes can be a useful proxy for estimating a species' evolutionary potential (Hansen & Houle, 2008), particularly for those closely associated with energy acquisition and reproduction, both of which have profound and direct effects on organismal fitness. Increased variation in these phenotypes may indicate that the species has a greater potential to adapt to rapidly changing selective pressures, buffering birth and survival rates among individuals with favorable traits, ultimately reducing the risk of extinction for the population (Forester *et al.*, 2022). Indeed, this 'evolutionary resilience' is an important element considered when developing conservation management approaches for endangered or at-risk species (Sgrò *et al.*, 2011).

Here we examine the notion that intraspecific morphological variation can be linked to intraspecific niche breadth, as estimated from carbon and nitrogen stable isotope ratios, and to what extent these characteristics are at all related to extinction. Such an analysis requires that we examine a large number of species occupying a diversity of ecological niches, and, critically, that we have foreknowledge of each species' potential for extinction. To do so, we examine museum collections of Hawaiian honeycreepers across a known series of extinctions spanning late 19^{th} to early 20^{th} century.

After an initial series of extinctions following the arrival of Polynesian populations ca. 1219–1266, a second wave occurred after European colonization in the 18^{th} century (Boyer, 2008), driven by the combined effects of deforestation, invasive species such as rabbits and rats, and diseases like avian malaria (Boyer, 2008). This latter driver was perhaps the leading direct cause of many honeycreeper extinctions, restricting survivors to high altitudes where mosquitoes are absent due to cooler temperatures (van Riper III *et al.*, 1986; Atkinson *et al.*, 2000). Our sampling of honeycreeper species from museum collections spans a temporal period from 1880 to 1913 during which species, occupying multiple Hawaiian islands, became extinct. Importantly, these species have associated dietary guilds based on observational accounts (*e.g.* Munro, 1944), allowing us to assess variability in beak morphology and isotopic niche breadth across both species and expected diet. Because Hawaiian honeycreepers demonstrate large differences in both beak morphology and diet, and have known extinction outcomes, they are well-suited to facilitating a direct comparison of species attributes against known extinction and/or current conservation status.

The large diversity of ecological niches occupied by honeycreeper species corresponds with a similarly large diversity of beak shapes and sizes, each meeting different dietary demands. While the relationship between dietary categories and beak shape and size among birds is a classic system used to probe form-to-function in ecology, the role of intraspecific variation in form, and how that may relate to ecological function, is less well understood. Along these lines, Van Valen (1965)

proposed the niche variation hypothesis, where greater morphological variation among individuals in a population would correlates with increased population niche width, which emerges as a product of individual specialization. Van Valen specifically formalized this notion around island populations, where species could attain greater morphological variation due to the initially reduced interspecific competition (i.e., less niche packing). The idea that morphological variation is mirrored in diet variation among populations has been tested empirically, with mixed results (Díaz, 1994; Bolnick *et al.*, 2007; Costa *et al.*, 2008; Maldonado *et al.*, 2017; Costa-Pereira *et al.*, 2019). Using isotopic area from carbon and nitrogen isotope ratios as a proxy for dietary niche breadth, we found no statistical support for a direct correlation between morphological and dietary variability across honeycreeper species (Figure S5). This lack of correlation exists with respect to variability in both beak size and shape. With the community, the small number of samples making up some established dietary guilds precluded a guild-by-guild statistical evaluations. It is worth noting, however, that when comparing dietary and size/shape variation within guilds (Figure S6) we find that increased morphological variation relates to increased niche breadth, with the exception of nectarivorous/invertebrate and invertebrate guilds.

Frugivores and granivores present a striking pattern of beak shape morphological variation when compared to other honeycreeper species. Their substantially elevated beak shape variability may emerge from several different evolutionary processes. First, frugivorous and granivorous honeycreepers may be under more relaxed stabilizing selection for beak shape, or even be subjected to higher diversifying selection. Both processes would lead to a higher population-level beak shape variation. Second, fluctuating selection may also promote increased beak shape variability, following the dynamics outlined by Stroud *et al.* (2023), which demonstrates that the cumulative effect of fluctuations in form, strength, direction, or existence of selective forces over time can maintain variation around a particular adaptive peak. Because the morphologically diverse fruits and seeds available to honeycreepers across the Hawaiian archipelago are likely to have varied responses to divergent environmental conditions (Hulme & Benkman, 2002), which themselves vary over time, the cumulative effect of such shifting selective landscapes may promote variability in frugivorous and granivorous honeycreeper beak shape. For example, Price (1987) showed that among Darwin's finches,food scarcity can drive both dietary generalization on remaining seeds, as well as specialization on either large or small seeds, which could explaining the high level of intra-specific variation in beak morphology in these species. This is because despite individuals specializing in small or large seeds during food shortages, few possess the optimal morphology for either. Thus, breeding between small and large individuals can result in intermediate phenotype, driving high morphological variation in the population. Finally, introgressive hybridization – the transfer of genetic material between species through repeated backcrossing – may also contribute to beak shape variability. Though hybridization is frequently observed in other bird groups, particularly those radiating across island habitats (Grant & Grant, 1997,

2016), there is only one reported hybridization event among two nectarivorus honeycreepers (*Vestiaria coccinea* and *Himatione sanguinea*; Knowlton *et al.*, 2014), suggesting otherwise strong pre- and/or post-zygotic reproductive barriers.

Most frugivorous and granivorous honeycreepers evince a more generalist diet (Munro, 1944; Pratt & Conant, 2005). However, we observe that *Loxioides bailleui*, with the highest intraspecific variation in beak shape, is also a known specialist on the seeds from Māmane trees (*Sophora chrysophylla*) (Hess *et al.*, 2014). We note that Māmane trees (*Sophora chrysophylla*) are known to be highly polymorphic, growing either as shrubs or trees, which may influence the size and shape of their seeds and drive opposing selective forces on beak shape, promoting variability. Additionally, when Māmane seeds are scarce, *L. bailleui* is known to fall back on other plant parts, including foliage, flowers, and flower buds (Hess *et al.*, 2014), sometimes supplementing its diet with the seeds and fruits of other plants (Munro, 1944). Another frugivore with high beak shape variation, *Psittirostra psittacea*, while described as feeding primarily on the fruits of the ʻieʻie plant (*Freycinetia arborea*), has in practice a more generalist diet, and has been reported to feed on introduced plants such as guavas and mulberries (Munro, 1944; Pratt & Conant, 2005).

The documented diets of frugivorous and granivorous honeycreepers translate differently with respect to their isotopic niches. While the isotopic niches of granivores are relatively narrow, those of frugivores are comparatively broad, suggesting that: *i*) there may be strong environmental signals captured by either or both carbon and nitrogen isotopic ratios (such as elevational effects, canopy effects, and/or differences in aridity), or *ii*) the resources from which the dietary guilds are composed are not isotopically distinct. So while granivores exhibit the smallest isotopic niche breadth, such that their food sources appear isotopically similar, this may not reflect the true diversity of their realized diets. That frugivores generally have broad isotopic niches may reflect their generalist dietary preferences, but could also arise from those species occupying a diversity of habitats. For example, *Psittirostra psittacea* has high variability in δ^{15}N values (Figure 2B), but this species was also common and abundant, occurring across most of the Hawaiian Islands from low to high altitudes before it went extinct (Munro, 1944). So while we did not capture significant differences in mean isotopic values across islands (Figure S8, but see Kennedy *et al.* (2018)), we cannot discount the role of habitat variability in contributing to the measured variability in δ^{13}C and δ^{15}N within and across species.

We found that within granivorous and invertebrate-feeder dietary guilds, species with lower morphological and isotopic variability – relative to other species in those guilds – tend to be those more likely to suffer extinction (Figure 1). Extinct species categorized as invertivore/nectarivorous reveal a mixed pattern, with very low beak shape variability, intermediate isotopic variability, yet very high beak size variability. Extinct nectarivores show an opposing, but still mixed, pattern, where the single representative species has high beak shape variability but low beak size variability. This species, *Himatione fraithii*, was endemic to Laysan Island, a low

atoll approximately $4, \mathrm{km}^2$ in size, and was last seen in 1923. The main causes of its extinction are thought to be the combined effects of habitat destruction and the introduction of invasive species such as rabbits, all of which culminated in a severe storm in 1923 (Pimm, 2003). Interestingly, both *H. fraithii* as well as *Telespiza cantans*, an extant granivore, reveal a distinctive isotope composition with exceptionally high δ^{15}N values. Alongisde *H. fraithii*, *T. cantans* is also endemic to Laysan Island, which was used for mining guano until the early twentieth century (Homer, 1952). We suspect that the elevated δ^{15}N values of both species is likely due to the influence of seabird guano, which is extremely enriched in 15^{N} relative to terrestrial sources (Szpak *et al.*, 2012a,b; Vizzini *et al.*, 2016).

If we examine patterns of extinction across guilds (Figure 4), the various patterns between morphology and isotopic variability observed within dietary guilds and extinction outcome contributes to a suggestive but unclear relationship. While there are no clear differences in isotopic niche breadth, lower variation in beak size and shape may appear to align with those species that are now extinct, however these relationships are not statistically significant. If we exclude frugivorous and granivorous species, such that our comparison is restricted to nectivorous, insectivorous/nectarivorous, and insectivorous species, we observe a statistically significant difference in beak shape variability between extinct and extant species, where those that are extinct exhibited less variability in beak shape than those that are extant. Additionally, within guilds, species with lower variation in beak shape are those that are extinct (Figure S7). This would appear to support Van Valen's niche variation hypothesis (Van Valen, 1965), and perhaps compellingly, link extinction as a possible outcome of limited beak shape variability.

It is then important to consider the justification for removing frugivorous and granivorous species, and whether a comparison without these species is ecologically meaningful. As described above, frugivorous and granivorous honeycreepers (both extant and extinct) have highly elevated beak shape variability, which is likely due to the large variety of fruit and seed shapes contributing to their diets. As such, a single category for each of these food types is likely too broad, integrating a larger diversity of dietary morphotypes than do the other guilds, and where subdividing fruits and seeds to account for hardness, toughness, and/or geometry, may be more appropriate for understanding connections to beak shape. Because there are only two species in this combined group currently extant (both granivores; Figure 1D), both of which have measures of beak shape variability equal to or higher than those that are extinct, the qualitative trend would remain in alignment with the notion that lower beak shape variability may increase the likelihood of extinction.

The ability of a species to persist in response to disturbances, or its adaptive capacity (Sgrò *et al.*, 2011), is crucial for survival in environments facing large-scale disruptions (Bürger & Lynch, 1995; Milot *et al.*, 2020b; Forester *et al.*, 2022). For example, little brown bats (*Myotis lucifugus*) declined more than 90% following the introduction of a fungal pathogen causing the white-nose syndrome (Hoyt *et al.*, 2021), but rebounded, it is thought, primarily due to its maintenance of substantial genetic variation despite such population bottlenecks (Auteri & Knowles, 2020).

Along these lines Ørsted *et al.* (2019) showed experimentally that fruit fly lineages with lower genetic diversity are more prone to extinction.

Because so many honeycreeper species suffered extinction during the first half of the 20th century, most of what we know about their ecology comes from observations from natural historians in the early 1900's (Perkins, 1903; Munro, 1944). These observations, as well as the collections of specimens for museums, offer the only window into this once highly diverse group, and the potential to unravel why some went extinct, while others did not. By leveraging stable isotope analysis to reconstruct the likely ecological roles and dietary habits of these species, alongside morphological measures of beak size and shape, we aim to shed light on how these characteristics may have interacted with the pressures being exerted on this diverse community. Our findings not only enhance our knowledge of the ecological diversity within this group but reveal the different roles of dietary and morphological variability within different dietary guilds, and their potential for contributing to the most recent wave of Hawaiian honeycreeper extinctions.

References

Abrahamczyk, S. & Kessler, M. (2015). Morphological and behavioural adaptations to feed on nectar: how feeding ecology determines the diversity and composition of hummingbird assemblages. *Journal of Ornithology*, 156, 333–347.

Adams, D.C. & Otárola-Castillo, E. (2013). geomorph: an r package for the collection and analysis of geometric morphometric shape data. *Methods in ecology and evolution*, 4, 393–399.

Assis, A., Patton, J., Hubbe, A. & Marroig, G. (2016). Directional selection effects on patterns of phenotypic (co) variation in wild populations. *Proceedings of the Royal Society B: Biological Sciences*, 283, 20161615.

Assis, A.P.A., Rossoni, D.M., Patton, J.L. & Marroig, G. (2017). Evolutionary processes and its environmental correlates in the cranial morphology of western chipmunks (Tamias). *Evolution*, 71, 595–609.

Atkinson, C.T., Dusek, R.J., Woods, K.L. & Iko, W.M. (2000). Pathogenicity of avian malaria in experimentally-infected hawaii amakihi. *Journal of Wildlife Diseases*, 36, 197–201.

Auteri, G.G. & Knowles, L.L. (2020). Decimated little brown bats show potential for adaptive change. *Scientific Reports*, 10, 3023.

Bearhop, S., Adams, C.E., Waldron, S., Fuller, R.A. & MacLeod, H. (2004). Determining Trophic Niche Width: A Novel Approach Using Stable Isotope Analysis. *Journal of Animal Ecology*, 73, 1007–1012.

Benkman, C.W. (1999). The selection mosaic and diversifying coevolution between crossbills and lodgepole pine. *The American Naturalist*, 153, S75–S91.

Billerman, S.M., Keeney, B.K., Rodewald, P.G. & Schulenberg, T.S. (2022). Birds of the world.

Bolnick, D.I., Amarasekare, P., Araújo, M.S., Bürger, R., Levine, J.M., Novak, M., Rudolf, V.H.W., Schreiber, S.J., Urban, M.C. & Vasseur, D.A. (2011). Why intraspecific trait variation matters in community ecology. *Trends in Ecology & Evolution*, 26, 183–192.

Bolnick, D.I., Svanbäck, R., Araújo, M.S. & Persson, L. (2007). Comparative support for the niche variation hypothesis that more generalized populations also are more heterogeneous. *Proceedings of the National Academy of Sciences*, 104, 10075–10079.

Bolnick, D.I., Svanbäck, R., Fordyce, J.A., Yang, L.H., Davis, J.M., Hulsey, C.D. & Forister, M.L. (2003). The ecology of individuals: incidence and implications of individual specialization. *The American Naturalist*, 161, 1–28.

Boyer, A.G. (2008). Extinction patterns in the avifauna of the Hawaiian islands. *Diversity and Distributions*, 14, 509–517.

Bürger, R. & Lynch, M. (1995). Evolution and extinction in a changing environment: A quantitative-genetic analysis. *Evolution; International Journal of Organic Evolution*, 49, 151–163.

Burin, G., Kissling, W.D., Guimaraes Jr, P.R., Şekercioğlu, Ç.H. & Quental, T.B. (2016). Omnivory in birds is a macroevolutionary sink. *Nature Communications*, 7, 11250.

Costa, G.C., Mesquita, D.O., Colli, G.R. & Vitt, L.J. (2008). Niche expansion and the niche variation hypothesis: does the degree of individual variation increase in depauperate assemblages? *The American Naturalist*, 172, 868–877.

Costa-Pereira, R., Araújo, M.S., Souza, F.L. & Ingram, T. (2019). Competition and resource breadth shape niche variation and overlap in multiple trophic dimensions. *Proceedings of the Royal Society B*, 286, 20190369.

Dehling, D.M., Jordano, P., Schaefer, H.M., Böhning-Gaese, K. & Schleuning, M. (2016). Morphology predicts species' functional roles and their degree of specialization in plant–frugivore interactions. *Proceedings of the Royal Society B: Biological Sciences*, 283, 20152444.

Derryberry, E.P., Seddon, N., Claramunt, S., Tobias, J.A., Baker, A., Aleixo, A. & Brumfield, R.T. (2012). Correlated evolution of beak morphology and song in the neotropical woodcreeper radiation. *Evolution*, 66, 2784–2797.

Díaz, M. (1994). Variability in seed size selection by granivorous passerines: effects of bird size, bird size variability, and ecological plasticity. *Oecologia*, 99, 1–6.

Estes, J., Riedman, M., Staedler, M., Tinker, M. & Lyon, B. (2003). Individual variation in prey selection by sea otters: patterns, causes and implications. *Journal of Animal Ecology*, pp. 144–155.

Felice, R.N., Tobias, J.A., Pigot, A.L. & Goswami, A. (2019). Dietary niche and the evolution of cranial morphology in birds. *Proceedings of the Royal Society B*, 286, 20182677.

Forester, B.R., Beever, E.A., Darst, C., Szymanski, J. & Funk, W.C. (2022). Linking evolutionary potential to extinction risk: Applications and future directions. *Frontiers in Ecology and the Environment*, 20, 507–515.

Gibert, J.P. & Brassil, C.E. (2014). Individual phenotypic variation reduces interaction strengths in a consumer–resource system. *Ecology and Evolution*, 4, 3703–3713.

Grant, P.R. & Grant, B.R. (1997). Hybridization, sexual imprinting, and mate choice. *The American Naturalist*, 149, 1–28.

Grant, P.R. & Grant, B.R. (2016). Introgressive hybridization and natural selection in darwin's finches. *Biological Journal of the Linnean Society*, 117, 812–822.

Hansen, T.F. & Houle, D. (2008). Measuring and comparing evolvability and constraint in multivariate characters. *Journal of Evolutionary Biology*, 21, 1201–1219.

Hess, S.C., Banko, P.C., Miller, L.J. & Laniawe, L.P. (2014). Habitat and food preferences of the endangered palila (loxioides bailleui) on mauna kea, hawai 'i. *The Wilson Journal of Ornithology*, 126, 728–738.

Ho, L.S.T., Ane, C., Lachlan, R., Tarpinian, K., Feldman, R., Yu, Q., van der Bijl, W., Maspons, J., Vos, R. & Ho, M.L.S.T. (2016). Package 'phylolm'. *See http://cran. r-project. org/web/packages/phylolm/index. html (accessed February 2018)*.

Homer, R. (1952). Expedition to laysan island. *The Palimpsest*, 33.

Houle, D. (1992). Comparing evolvability and variability of quantitative traits. *Genetics*, 130, 195–204.

Hoyt, J.R., Kilpatrick, A.M. & Langwig, K.E. (2021). Ecology and impacts of white-nose syndrome on bats. *Nature Reviews Microbiology*, 19, 196–210.

Hulme, P.E. & Benkman, C.W. (2002). Granivory. *Plant–animal interactions: an evolutionary approach*, pp. 185–208.

Jackson, A., Parnell, A. & Jackson, M.A. (2019). Package 'siber'. *R package version*, 2.

Keeling, C.D. (1979). The suess effect: 13carbon-14carbon interrelations. *Environment International*, 2, 229–300.

Kennedy, S.R., Dawson, T.E. & Gillespie, R.G. (2018). Stable isotopes of Hawaiian spiders reflect substrate properties along a chronosequence. *PeerJ*, 6, e4527.

Knowlton, J.L., Flaspohler, D.J., Mcinerney, N.C.R. & Fleischer, R.C. (2014). First Record of Hybridization in the Hawaiian Honeycreepers: 'I'iwi (Vestiaria coccinea) × 'Apapane (Himatione sanguinea). *The Wilson Journal of Ornithology*, 126, 562–568.

Lande, R. & Shannon, S. (1996). The Role of Genetic Variation in Adaptation and Population Persistence in a Changing Environment. *Evolution*, 50, 434–437.

Lavergne, S., Evans, M.E., Burfield, I.J., Jiguet, F. & Thuiller, W. (2013). Are species' responses to global change predicted by past niche evolution? *Philosophical Transactions of the Royal Society B: Biological Sciences*, 368, 20120091.

Lerner, H.R.L., Meyer, M., James, H.F., Hofreiter, M. & Fleischer, R.C. (2011). Multilocus Resolution of Phylogeny and Timescale in the Extant Adaptive Radiation of Hawaiian Honeycreepers. *Current Biology*, 21, 1838–1844.

Lessells, C. & Boag, P.T. (1987). Unrepeatable repeatabilities: a common mistake. *The Auk*, 104, 116–121.

Levey, D.J. (1987). Seed Size and Fruit-Handling Techniques of Avian Frugivores. *The American Naturalist*, 129, 471–485.

Lovette, I.J., Bermingham, E. & Ricklefs, R.E. (2002). Clade-specific morphological diversification and adaptive radiation in Hawaiian songbirds. *Proceedings of the Royal Society B: Biological Sciences*, 269, 37–42.

Maldonado, K., Bozinovic, F., Newsome, S.D. & Sabat, P. (2017). Testing the niche variation hypothesis in a community of passerine birds.

McTavish, E.J., Gerbracht, J.A., Holder, M.T., Iliff, M.J., Lepage, D., Rasmussen, P.C., Redelings, B., Sanchez-Reyes, L.L. & Miller, E.T. (2024). A complete and dynamic tree of birds. *bioRxiv*, pp. 2024–05.

Miles, D.B., Ricklefs, R.E. & Losos, J.B. (2023). How exceptional are the classic adaptive radiations of passerine birds? *Proceedings of the National Academy of Sciences*, 120, e1813976120.

Milot, E., Béchet, A. & Maris, V. (2020a). The dimensions of evolutionary potential in biological conservation. *Evolutionary Applications*, 13, 1363–1379.

Milot, E., Béchet, A. & Maris, V. (2020b). The dimensions of evolutionary potential in biological conservation. *Evolutionary Applications*, 13, 1363–1379.

Munro, G.C. (1944). *Birds of Hawaii.* Tongg Publishing Company. Honolulu, HI.

Newsome, S.D., Martinez del Rio, C., Bearhop, S. & Phillips, D.L. (2007). A niche for isotopic ecology. *Frontiers in Ecology and the Environment*, 5, 429–436.

Newsome, S.D., Yeakel, J.D., Wheatley, P.V. & Tinker, M.T. (2012). Tools for quantifying isotopic niche space and dietary variation at the individual and population level. *Journal of Mammalogy*, 93, 329–341.

Ørsted, M., Hoffmann, A.A., Sverrisdóttir, E., Nielsen, K.L. & Kristensen, T.N. (2019). Genomic variation predicts adaptive evolutionary responses better than population bottleneck history. *PLoS Genetics*, 15, e1008205.

Pagel, M. (1999). Inferring the historical patterns of biological evolution. *Nature*, 401, 877–884.

Paxton, E.H., Camp, R.J., Gorresen, P.M., Crampton, L.H., Leonard, D.L. & VanderWerf, E.A. (2016). Collapsing avian community on a Hawaiian island. *Science Advances*, 2, e1600029.

Pelletier, F., Clutton-Brock, T., Pemberton, J., Tuljapurkar, S. & Coulson, T. (2007). The evolutionary demography of ecological change: linking trait variation and population growth. *Science*, 315, 1571–1574.

Perkins, R. (1903). Vertebrata. fauna hawaiiensis, vol. 1, pt 4.

Pigot, A.L., Trisos, C.H. & Tobias, J.A. (2016). Functional traits reveal the expansion and packing of ecological niche space underlying an elevational diversity gradient in passerine birds. *Proceedings of the Royal Society B: Biological Sciences*, 283, 20152013.

Pimm, S. (2003). Expiry dates. *Nature*, 426, 235–236.

Pratt, H.D. & Conant, S. (2005). *The Hawaiian Honeycreepers: Drepanidinae*. OUP Oxford.

Price, T. (1987). Diet variation in a population of darwin's finches. *Ecology*, 68, 1015–1028.

Ricklefs, R.E. (2017). Historical Biogeography and Extinction in the Hawaiian Honeycreepers. *The American Naturalist*, 190, E106–E111.

Sgrò, C.M., Lowe, A.J. & Hoffmann, A.A. (2011). Building evolutionary resilience for conserving biodiversity under climate change. *Evolutionary applications*, 4, 326–337.

Sheard, C., Street, S.E., Evans, C., Lala, K.N., Healy, S.D. & Sugasawa, S. (2023). Beak shape and nest material use in birds. *Philosophical Transactions of the Royal Society B*, 378, 20220147.

Soto-Saravia, R.A., Garrido-Cayul, C.M., Avaria-Llautureo, J., Benítez-Mora, A., Hernández, C.E. & Gonzalez-Suarez, M. (2021). Threatened neotropical birds are big, ecologically specialized, and found in less humanized refuge areas. *Avian Conservation and Ecology*, 16.

Stroud, J.T., Moore, M.P., Langerhans, R.B. & Losos, J.B. (2023). Fluctuating selection maintains distinct species phenotypes in an ecological community in the wild. *Proceedings of the National Academy of Sciences*, 120, e2222071120.

Szpak, P., Longstaffe, F.J., Millaire, J.F. & White, C.D. (2012a). Stable isotope biogeochemistry of seabird guano fertilization: results from growth chamber studies with maize (zea mays). *PloS one*, 7, e33741.

Szpak, P., Millaire, J.F., White, C.D. & Longstaffe, F.J. (2012b). Influence of seabird guano and camelid dung fertilization on the nitrogen isotopic composition of field-grown maize (zea mays). *Journal of Archaeological Science*, 39, 3721–3740.

Tattersall, G.J., Arnaout, B. & Symonds, M.R. (2017). The evolution of the avian bill as a thermoregulatory organ. *Biological Reviews*, 92, 1630–1656.

Terraube, J., Arroyo, B., Madders, M. & Mougeot, F. (2011). Diet specialisation and foraging efficiency under fluctuating vole abundance: a comparison between generalist and specialist avian predators. *Oikos*, 120, 234–244.

Tokita, M., Yano, W., James, H.F. & Abzhanov, A. (2017). Cranial shape evolution in adaptive radiations of birds: Comparative morphometrics of Darwin's finches and Hawaiian honeycreepers. *Philosophical Transactions of the Royal Society B: Biological Sciences*, 372, 20150481.

van Riper III, C., van Riper, S.G., Goff, M.L. & Laird, M. (1986). The Epizootiology and Ecological Significance of Malaria in Hawaiian Land Birds. *Ecological Monographs*, 56, 327–344.

Van Valen, L. (1965). Morphological variation and width of ecological niche. *The American Naturalist*, 99, 377–390.

Vizzini, S., Signa, G. & Mazzola, A. (2016). Guano-derived nutrient subsidies drive food web structure in coastal ponds. *PLoS One*, 11, e0151018.

Wheelwright, N.T. (1985). Fruit-Size, Gape Width, and the Diets of Fruit-Eating Birds. *Ecology*, 66, 808–818.

Yeakel, J.D., Bhat, U., Elliott Smith, E.A. & Newsome, S.D. (2016). Exploring the Isotopic Niche: Isotopic Variance, Physiological Incorporation, and the Temporal Dynamics of Foraging. *Frontiers in Ecology and Evolution*, 4, 1.

S1 Supplementary Information

S1.1 Tables

Table S1: Pairwise comparisons of δ^{13}C values among bird guilds using the Wilcoxon rank sum test with Bonferroni correction. Significant p-values (< 0.05) are in bold.

Comparison	**p-value**
Fruits vs. Invertebrates	1.0
Fruits vs. Invertebrates/Nectar	1.0
Fruits vs. Nectar	1.0
Fruits vs. Seeds	0.76
Invertebrates vs. Invertebrates/Nectar	**<0.05**
Invertebrates vs. Nectar	**<0.05**
Invertebrates vs. Seeds	1.0
Invertebrates/Nectar vs. Nectar	1.00
Invertebrates/Nectar vs. Seeds	**<0.05**
Nectar vs. Seeds	**<0.05**

Table S2: Pairwise comparisons of δ^{15}N values among bird guilds using the Wilcoxon rank sum test with Bonferroni correction. Significant p-values (< 0.05) are in bold.

Comparison	**p-value**
Fruits vs. Invertebrates	0.05
Fruits vs. Invertebrates/Nectar	**<0.05**
Fruits vs. Nectar	1.0
Fruits vs. Seeds	1.0
Invertebrates vs. Invertebrates/Nectar	0.02
Invertebrates vs. Nectar	**<0.05**
Invertebrates vs. Seeds	**<0.05**
Invertebrates/Nectar vs. Nectar	**<0.05**
Invertebrates/Nectar vs. Seeds	**<0.05**
Nectar vs. Seeds	0.06

S1.2 Figures

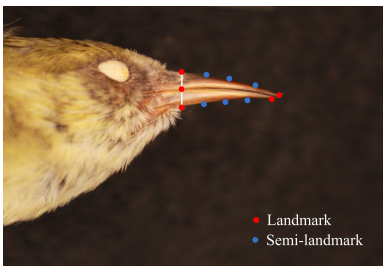

Figure S1: Landmarks (red) and semi-landmarks (blue) digitized on the beak of a specimen of *Loxops mana*.

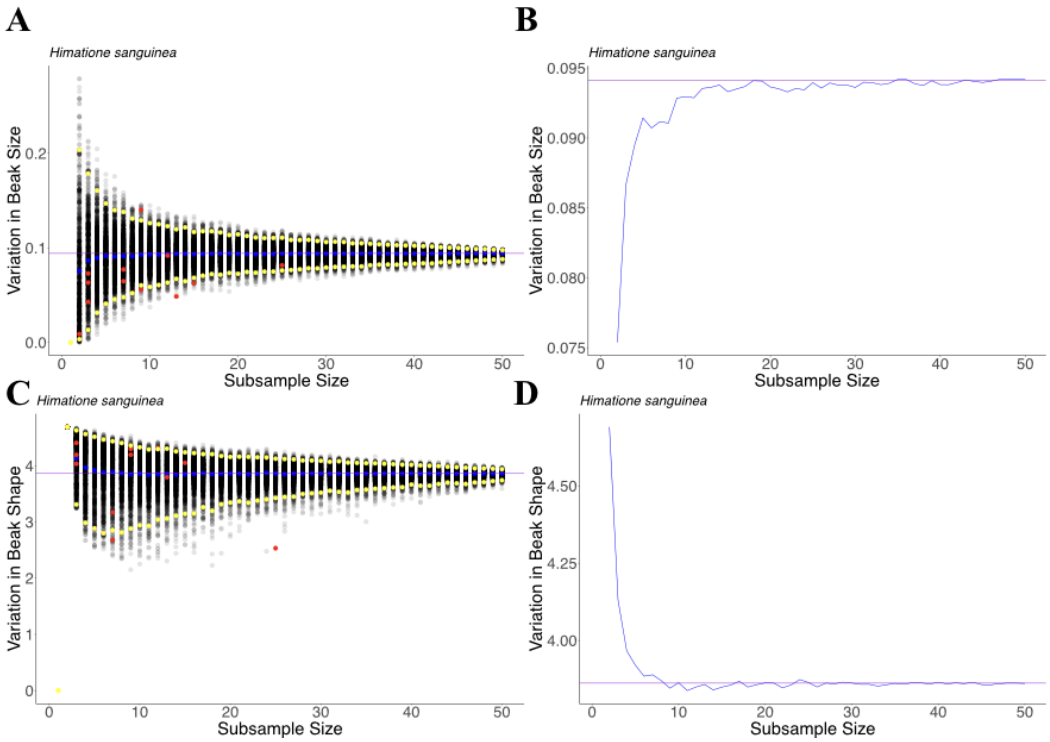

Figure S2: Rarefaction analysis comparing the mean value of within-species variation in **A-B** beak size (CV centroid size) and **C-D** beak shape (ICV). For each sample size (range from 1 to 50) we calculated the mean for 1000 simulation, which represents a black point in our graph **A** and **C**. Purple lines are our empirical data for *Himatione sanguinea*. Blue points is the mean value of our simulations, yellow points show the 95% confidence interval of our simulations and red points are the empirical values of extinct species in our dataset. **A)** within-species variation in beak size. **B)** The curve of the mean value in our simulation (blue line) for CV centroid size. **C)** within-species variation in beak shape (ICV) **D)** The curve of the mean value in our simulation (blue line) for (ICV).

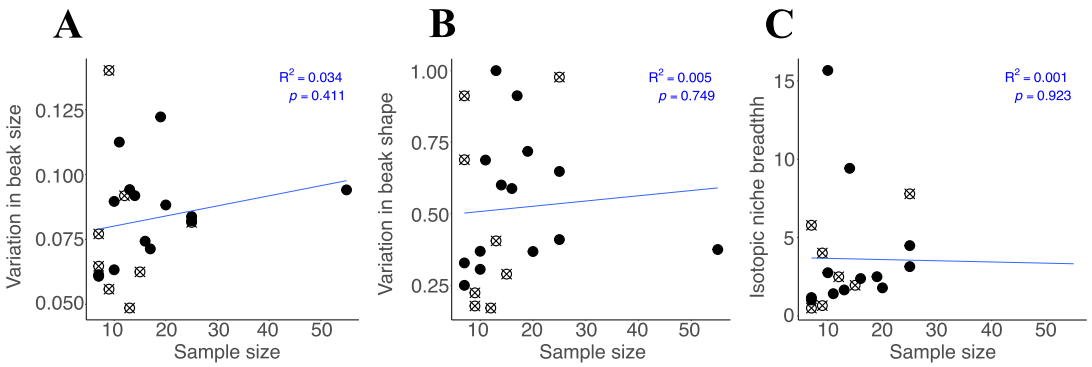

Figure S3: Linear regression between sample size and **A)** Variation in beak size (CV Centroid Size); **B)** Variation in beak shape (ICV_r); and **C)** Isotopic niche breadth (SEAc). Each point is a species and open crossed points represent extinct species.

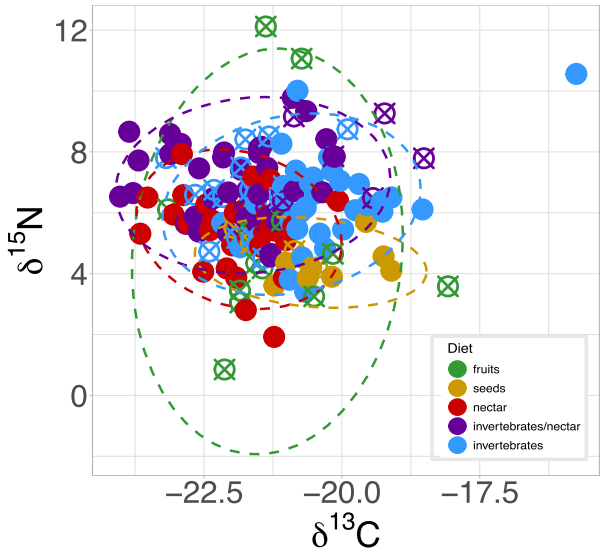

Figure S4: Stable isotope values (δ^{13}C and δ^{15}N) of Hawaiian honeycreepers, excluding species from Laysan Island. Each point represents an individual, with open crossed points indicating extinct or possibly extinct species. The ellipse area for each guild is shown.

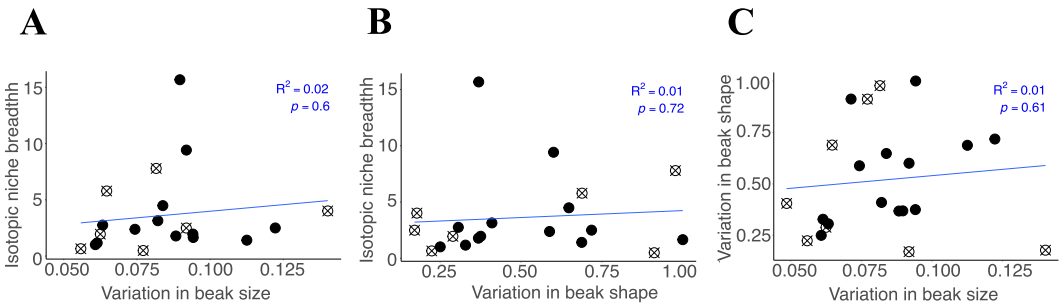

Figure S5: Phylogenetic linear regression between **A)** within-species variation in beak shape (ICV_r) and dietary niche breadth ($SEAc$); **B)** within-species variation in beak size ($CVCentroidsize$) and dietary niche breadth ($SEAc$); **C)** within-species variation in beak size ($CVCentroidsize$) and within-species variation in beak shape (ICV_r). Each point is a species and open crossed points represent extinct species.

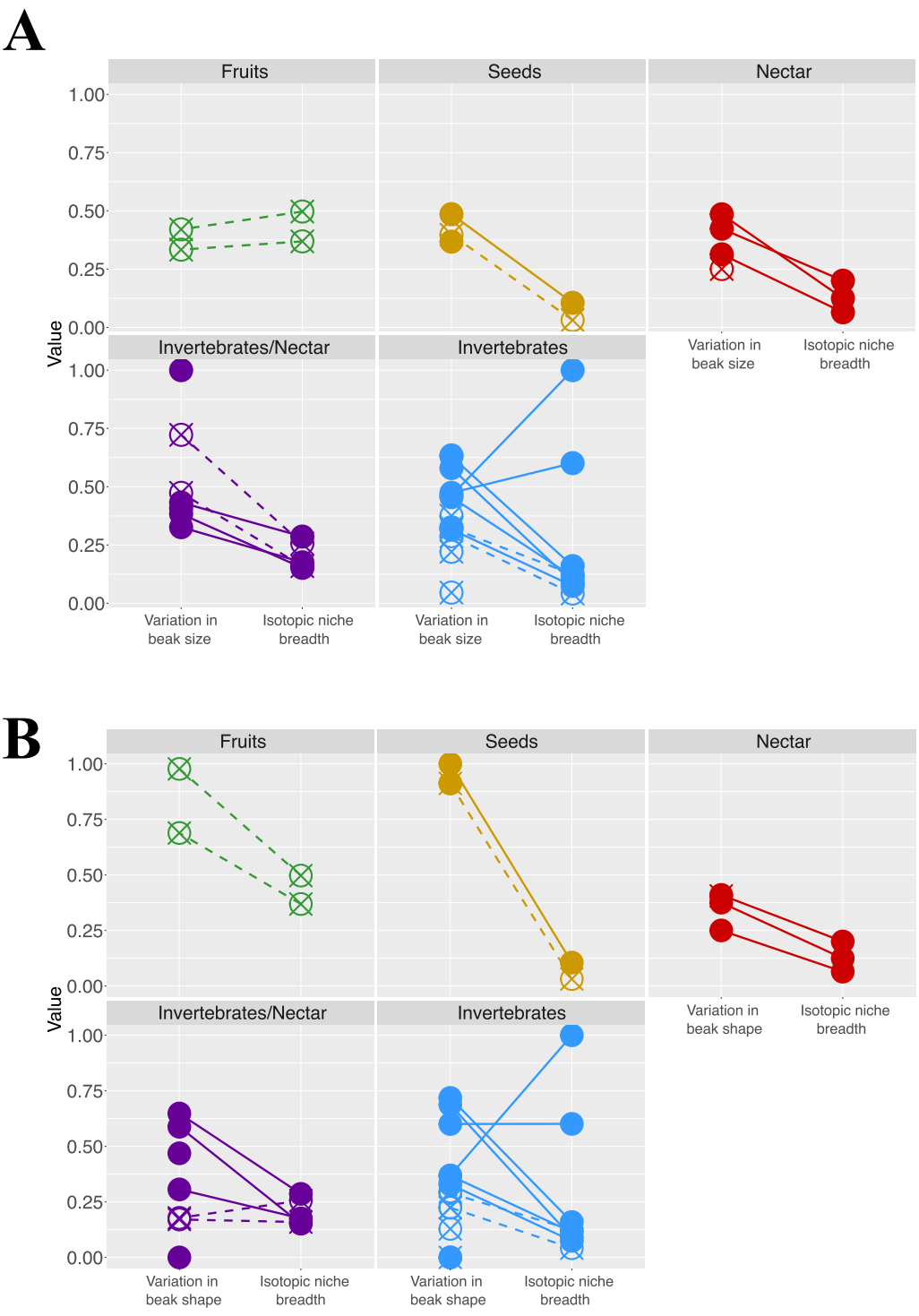

Figure S6: Within a guild, species with low variation in beak morphology tend to have low isotopic niche breadth. **A)** Comparison of relative values of intra-specific variation in beak shape with relative values of isotopic niche breadth; **B)** relative values of beak size and isotopic niche breadth. Lines connect values from the same species (points). Open crossed points and dashed lines indicate extinct species.

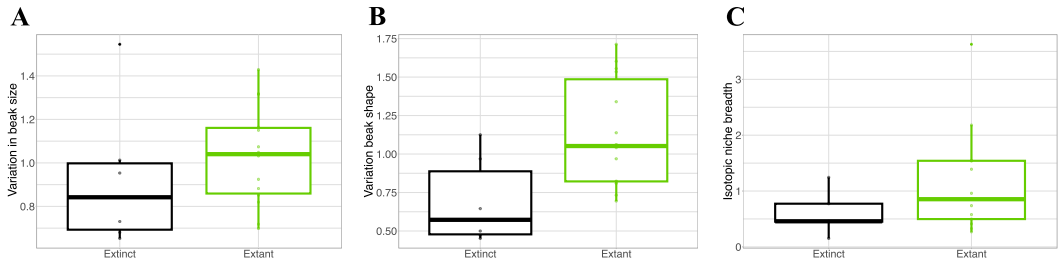

Figure S7: Boxplot depicting species variability for extinct (black) and extant (green) relative to the mean dietary guild variability. **A)** Variability in beak size ($CV centroidsize$); **B** Variability in beak shape (ICV_r); **C** Isotopic niche breadth ($SEAc$);

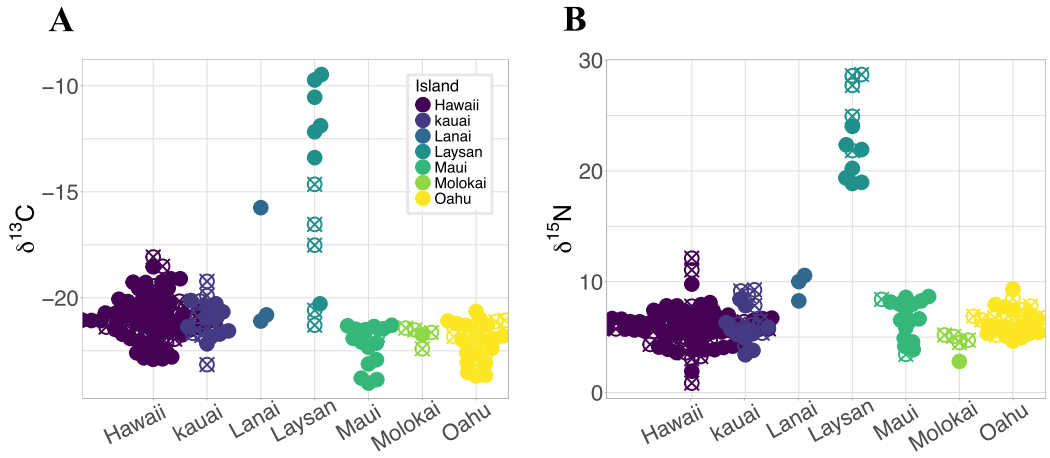

Figure S8: Beeswarm plots showing the difference among islands. Each point is an individual and open crossed points represent individuals of extinct species. **A)** $\delta^{13}C$ expressed in units of per mil (‰); **B)** $\delta^{15}N$ expressed in units of per mil (‰).

Chapter 3

"I am gratified that the Museum has its contribution to make to the solution of the great problems of evolution. That is the ultimate, if not the only goal, is it not, of our special kind of scientific work?"

(Annie Montague Alexander [1], 1867-1950)

[1]Born in Honolulu, Hawaii, she was a naturalist who preserved more than 22,000 mammals, 17,000 plants, and 1,500 fossil specimens, including many previously undescribed species. She was the founder and patron of both the Museum of Paleontology and the Museum of Vertebrate Zoology at the University of California, Berkeley (MVZ).

Chapter 3

Signatures of adaptive peaks shifts in beak morphology in Hawaiian Honeycreepers

1 Abstract

Bird beaks exhibit remarkable morphological diversity and are integral to foraging, thermoregulation, and song production. The evolution of beak morphology is influenced by multiple distinct and potentially conflicting selective pressures, though diet and feeding behaviors are often the primary forces shaping selection among passerines. Hawaiian honeycreepers originally consisted of more than 50 species, and showcased a striking diversity of beak shapes and foraging behaviors, though two-thirds of these species are now extinct. Here we use geometric morphometrics and phylogenetic comparative methods to explore the adaptive landscapes of extinct and extant Hawaiian honeycreepers and identify where adaptive peak shifts have occurred. Moreover, we explored evolutionary convergences to gain a deeper understanding of the evolutionary history of their beak morphology. Our results indicate that adaptive shifts in beak morphology are strongly tied to feeding ecology, with traits such as thicker, more robust beaks convergently evolving in different lineages. We identify two major convergences: one in beak shape among frugivorous and granivorous species, and another in beak size among a clade of invertebrate specialists and a nectarivorous species. Our findings reveal that the extinction of Hawaiian honeycreepers has led to a drastic reduction in the morphospace they once occupied, as peripheral species with distinct morphologies and unique adaptive peaks have been preferentially lost to extinction. This homogenization may have significant implications for ecosystem functioning, as these birds play crucial roles in ecosystem services.

2 Introduction

Bird beaks are vital for survival, and serve to perform an enormity of important tasks, including but not limited to: nest building (Sheard *et al.*, 2023), song production (Derryberry *et al.*, 2012), thermoregulation (Tattersall *et al.*, 2017), and foraging (Pigot *et al.*, 2020). So the vast morphological diversity observed among bird beaks is not surprising. From toucans with their colourful beaks that amount to one third of their body size (Tattersall *et al.*, 2009), to the needle-like beaks of Neotropical Humming birds (Missagia & Alves, 2018), beaks occupy a striking diversity of shape and size. Moreover, some of the most compelling examples of the power of natural selection in shaping variation are represented by the evolution of bird beaks, including the microevolutionary changes ob-served among Darwin's finches (Grant & Grant, 1989, 2006). Due to the diverse tasks for which they are

used, the evolution of beak morphology may be influenced by several distinct and potentially conflicting selective pressures, acting to optimize performance across different functions (Friedman *et al.*, 2019). For instance, in songbirds (Meliphagidae), while foraging ecology significantly influences beak shape, climate plays a crucial role in determining beak size (Friedman *et al.*, 2019). In passerines, diet and feeding behaviors are the primary selective force shaping beak shape evolution in many groups, such as Darwin's finches (Schluter & Grant, 1984; Grant & Grant, 1989), crossbills (Benkman, 1988), and great tits (Gosler, 1986). In fact, cranial and beak morphology in birds strongly predict dietary guild membership (Pigot *et al.*, 2016; Felice *et al.*, 2019). For example, pollinating birds often have beak shapes that match the floral morphology of the plants they pollinate, suggesting a strong constraint on pollinators' traits related to food acquisition (Abrahamczyk & Kessler, 2015).

Hawaiian honeycreepers (Aves: Fringillidae: Carduelinae) is a group of birds endemic to Hawaii, showcasing a remarkable diversity of beak shapes within a single family, even when compared to other bird groups (Lovette *et al.*, 2002; Tokita *et al.*, 2017). They also present a wide variety of foraging behaviors and diets (Pratt & Conant, 2005). For instance, this group includes species with parrot-like beaks, such as the Maui parrotbill (*Psittirostra psittacea*) (Figure 1 ID 1), warbler-like beaks, such as the Maui ʻalauahio (*Paroreomyza montana*) (Figure 1 ID 26), finch-billed species, such as the Palila (*Loxioides bailleui*) (Figure 1 ID 4), downward-curving beaks, such as the Iʻiwi (*Drepanis coccinea*) (Figure 1 ID 9), and many others, including a unique shape among birds, the akipolaau (*Hemignathus wilsoni*) (Figure 1 ID 18), a thin and curved beak with the lower bill running half the length of the upper bill. Despite originally consisting of more than 50 species, human activities including the introduction of invasive species and anthropogenic habitat loss, have severely impacted this group, leading to the extinction of approximately two-thirds of its species (Boyer, 2008; Paxton *et al.*, 2016; McClure *et al.*, 2020). Because beak shapes can define species ecological functions (Pigot *et al.*, 2016), species loss lead to the loss of unique morphological diversity and may have a substantial impact on ecosystem functioning (Ali *et al.*, 2023; Mariyappan *et al.*, 2023).

The great diversity of Hawaiian honeycreeper beak shape is thought to be the result of an explosive adaptive radiation following the initial colonization of the Hawaiian archipelago (Lovette *et al.*, 2002; Yoder *et al.*, 2010). Additionally, the existence of different non-close related species occupying the same ecological niche is commonly seen as evidence of adaptive convergence, in which species end up with very similar traits (Losos, 2011; Mahler *et al.*, 2013). In other words, convergence can be interpreted as species responding to the same selective pressures, with traits evolving to the same adaptive peaks (Mahler *et al.*, 2013). Bird communities on islands that have greater morphological similarities than expected by chance and the similarity among species is usually interpreted as a result of convergence (Triantis *et al.*, 2022). In honeycreepers, there are several compelling cases of convergence, such as in the creepers *Oreomystis baiardi* (Kauai creeper)

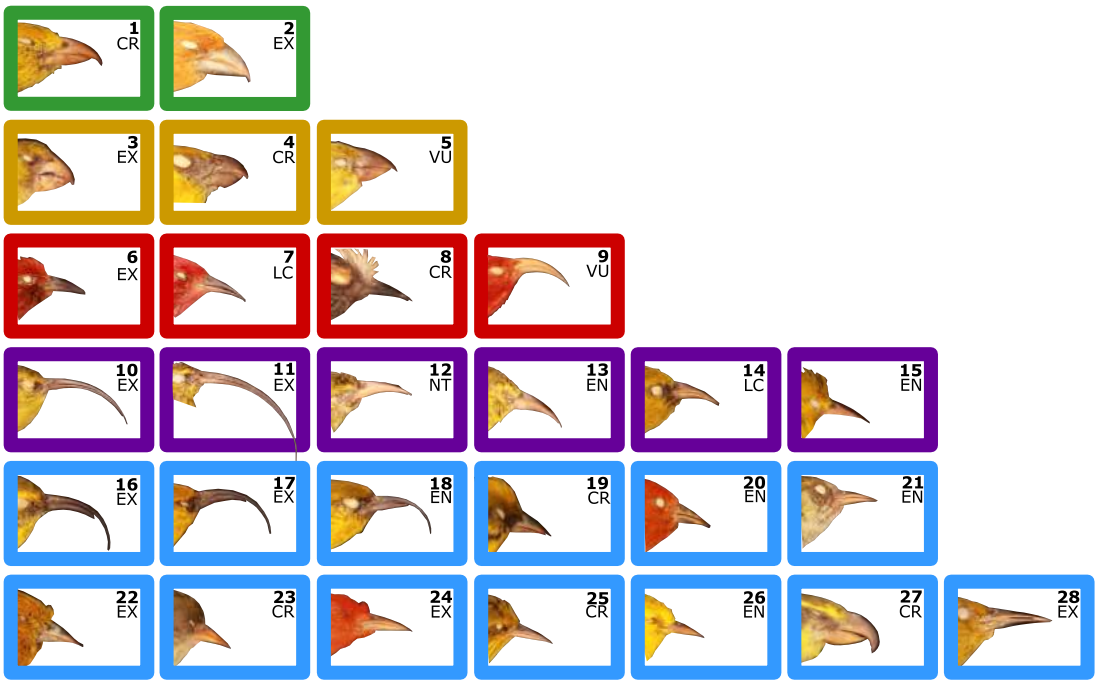

Figure 1: Diversity of beak shapes in our database of Hawaiian honeycreepers. Species within green boxes have diets based on fruits; yellow boxes on grains and fruits; red boxes on nectar; purple boxes on both nectar and invertebrates; and blue boxes on invertebrates. The species categories from the IUCN Red List of Threatened Species are also shown: EX represents extinct species; CR (critically endangered), EN (endangered), and VU (vulnerable) represent threatened species; and NT (near threatened) and LC (least concern) represent non-threatened species. 1, *Psittirostra psittacea*; 2, *Rhodacanthis palmeri*; 3, *Chloridops kona*; 4, *Loxioides bailleui*; 5, *Telespiza cantans*; 6, *Himatione fraithii*; 7, *Himatione sanguinea*; 8, *Palmeria dolei*; 9, *Drepanis coccinea*; 10, *Akialoa obscura*; 11, *Akialoa stejnegeri*; 12, *Chlorodrepanis flava*; 13, *Chlorodrepanis stejnegeri*; 14, *Chlorodrepanis virens*; 15, *Magumma parva*; 16, *Hemignathus affinis*; 17, *Hemignathus hanapepe*; 18, *Hemignathus wilsoni*; 19, *Loxops caeruleirostris*; 20, *Loxops coccineus*; 21, *Loxops mana*; 22, *Loxops ochraceus*; 23, *Oreomystis bairdi*; 24, *Paroreomyza flammea*; 25, *Paroreomyza maculata*; 26, *Paroreomyza montana*; 27, *Pseudonestor xanthophrys*; and 28, *Viridonia sagittirostris*

(Figure 1 ID 23) and *Loxops mana* (Hawaii creeper) (Figure 1 ID 21), distantly-related species, both of which characterized by short, narrow, and shallow beaks (Reding *et al.*, 2009). While these patterns are suggestive of convergence in beak morphologies, a formal test is needed, given processes other than selection can lead to the emergence of similarity between traits among distantly related species (Stayton, 2008; Losos, 2011).

Here we used phylogenetic comparative methods to provide a deeper understanding of the evolution of beak morphology in Hawaiian honeycreepers. We were especially interested in investigating patterns of convergence in beak morphology and its link to the evolution of distinct diets. Our analysis provides insight into unique adaptive peaks that might have been lost with the extinction of many species from this diverse group, both before and during recent historical extinctions. Understanding the evolutionary history of beak shape in honeycreepers sheds light on broader questions regarding how environmental pressures and divergent ecological niches can drive phenotypic diversity and speciation dynamics. First, we explored the likely ancestral states of beak morphology in Hawaiian honeycreepers. Second, we investigated whether feeding ecology is an important evolutionary force shaping beak size and shape in the group. Lastly, we examined shifts in the adaptive landscapes and whether unique adaptive peaks were lost with past extinctions.

3 Methods

3.1 Study system and morphological measurements

We examined 368 specimens from 28 different species of Hawaiian honeycreepers, representing 10 extinct and 18 extant species. The specimens used are housed in the Museum of Comparative Zoology (MCZ, Cambridge, MA), the Museum of Vertebrate Zoology (MVZ, Berkeley, CA), and the Royal Ontario Museum (ROM, Toronto, ON) collections. Because of the scarcity of some species in museum collections, we used both adult females and male specimens collected between 1880 and 1913. We included rare specimens that did not have the exact date of collection but rather the collectors' names, allowing us to infer that they were gathered during the time window assigned to other collections made by the same collector. We photographed each individual's beak in a right oriented position. Photos were then landmarked, with five landmarks and six semi-landmarks placed on each specimen (Figure S1) using the *digitize2d* function from the *geomorph* package (Adams & Otárola-Castillo, 2013) in *R* (Team, 2023). Each individual was measured twice in order to estimate landmark placement repeatability (Lessells & Boag, 1987).

We then performed a Procrustes generalized analysis (using the *geomorph* package; Adams & Otárola-Castillo, 2013) to position, scale, and rotate all specimens, thereby minimizing the square distances among landmarks and allowing a comparison of shape differences between species (Zelditch *et al.*, 2012). Using

the scaled and oriented landmarks, we performed a principal component analysis (PCA) on the superimposed data to reduce the dimensionality of shape variation. We used the first and second PC-scores (PC1 and PC2) as shape variables in subsequent analyses because they capture the largest proportions of total shape variation, providing a simplified yet informative representation of the primary axes of morphological change (Tokita *et al.*, 2017; Navalón *et al.*, 2019). The mean value for each species in PC1 and PC2 were used in the comparative analysis (Figures S2 and S3). To investigate the evolutionary history of size evolution we also used z-scored transformed mean centroid sizes (C_s) for each species, standardizing the size data to allow for comparisons across species by removing the effect of scale and highlighting relative differences from the mean.

Historical information on species' guilds was obtained from Pratt & Conant (2005). Among the 28 species used in this study, two were classified as frugivorous, three as granivorous, four as nectarivorous, six as having a mixed diet (based on invertebrates and nectar), and 13 as invertebrate feeders (Figure 1). Known dietary guilds based on historical observational accounts were then mapped onto PCA and Centroid size analyses to assess whether differences in these variables correlate with dietary specializations.

3.2 Ancestral state reconstruction

We used the most complete to date and time-calibrated phylogeny for all birds, encompassing over 9,000 species based on the Open Tree synthesis algorithm (McTavish *et al.*, 2024) We pruned this tree to obtain a phylogeny for both extant and extinct Hawaiian honeycreepers, where we retained only those 28 species for which we had gathered morphological data. The root of our Hawaiian honeycreeper pruned-tree diverged 11.38 million years ago, with the shallowest branch divergence being between *Akialoa stejnegeri* and *Akialoa obscura*, 0.37 million years ago (McTavish *et al.*, 2024).

In order to better understand the evolutionary trajectory of Hawaiian honeycreeper beaks, we first reconstructed the evolutionary history of beak shape and size in the group. Using mean species scores in PC1 and PC2 as shape variables, and the z-transformed centroid sizes as size variables, we reconstructed scaled shape and size along the phylogeny based on maximum likelihood approach for continuous traits (using the *phytools* package; Revell, 2012). We employed the REML method in the *ace* function, which first calculates the ancestral value at the root of the tree and then estimates the variance of a Brownian motion process along the evolutionary trajectory by optimizing the residual log-likelihood.

We reconstructed diet along the same phylogenetic tree to investigate its relationship with beak morphological evolution. Here, we combined the five guilds into three categories of diet: 1) fruits and grains; 2) nectar; and 3) invertebrates. In this sense, species considered to have a mixed diet of nectar and invertebrates are included in the invertebrate category. In this discrete analysis, further subdividing these categories may be prone to error, given that our tree is composed of

only 28 species. To reconstruct diet along the phylogenetic tree, we used a stochastic mapping approach (Huelsenbeck *et al.*, 2003), which estimates the transition rates between states for the trait (here the three categories of diet) and uses these rates to simulate a number of plausible evolutionary histories for the trait. We used 645 simulations premised on the "Equal Rates" (ER) model, which fits a single transition rates between all pairs combinations of character states for diet type, and 355 simulations premised on the "Symmetrical Rates" (SYM) model, which assumes that the rate of change between any two character states is the same in both directions, but each pair of states can have a unique rate. These simulations were later combined to describe the trait-to-phylogeny mapping using the complete set of simulations.

3.3 Comparative phylogenetic analyses

To explore the evolutionary processes responsible for beak shape evolution in Hawaiian honeycreepers, we used phylogenetic comparative methods to trace trait evolution over time and test different evolutionary models. Morphological data from our geometric morphometrics analysis provided observed information for the taxa defining the phylogenetic tips. By combining this data with a phylogenetic tree and utilizing statistical and mathematical models described below, we estimated patterns of evolutionary change in beak shape and size across the phylogeny.

To model a baseline evolutionary process for beak shape, we first used a standard Brownian motion (BM) approach (Felsenstein, 1985), which assumes that changes in the values of a continuous trait X are stochastic, following a random walk where each change is independent of the previous one and normally distributed with a mean of zero and a constant variance. This BM model can be treated as a null model for trait evolution, against which more complex models can be compared. The evolution of trait X over a time increment t thus follows

$$\mathrm{d}X_t = \sigma \mathrm{d}B_t, \tag{1}$$

where $\mathrm{d}B_t$ is the Gaussian white noise and σ is the magnitude of indirect, stochastic evolutionary change.

The Ornstein-Uhlenbeck (OU) model is a more complex evolutionary model than the BM framework, adding a deterministic component to the evolutionary dynamic, and introducing an adaptive optimum (θ) that traits evolve towards. The OU model is defined

$$\mathrm{d}X_t = \alpha(\theta - X_t)\mathrm{dt} + \sigma(\mathrm{d}B_t) \tag{2}$$

where B_t is as in the BM model, and α is the rate at which the trait X is pulled toward the optimum θ, and can be interpreted as strength of selection (Hansen, 1997). This standard OU model has been adapted into amultiple-optima OU models, allowing the adaptive optima to vary across multiple taxa in a phylogenetic tree (Ingram & Mahler, 2013). Using this approach, we can estimate not only the number of shifts in phenotypic optima (different θ values), but also identify

instances of convergent evolution, where traits in distantly related species converge towards the same optimal values. To choose the model that better describes the data, we used the Akaike Information Criterion, corrected for small sample size (AICc) (Anderson *et al.*, 1998), which penalizes model fits for increased numbers of parameters, with the lowest AICc value indicating the best fit.

To implement these alternative models, we used the *l1ou* package (Khabbazian *et al.*, 2016) in *R* (Team, 2023), which uses the lasso method (imposing regularization and preventing overfitting by penalizing large parameter estimates) to identify shifts in the adaptive landscape by varying θ values, while α and σ values remain fixed. To disentangle whether the BM or OU model better describes our data, we estimated phylogenetic half-life, defined as $\ln(2)/\alpha$, which represents the velocity by which a species reaches an adaptive optimum, or in other words, the average time required for a trait to reach half-way to a new θ. If the phylogenetic half-life exceeds the time marking the root of the phylogentic tree, we assumed that selection is too weak, thus approaching a BM model.

4 Results

4.1 Morphological variation and dietary guilds

The first two principal components explained a total of 89.97% of the total beak shape variation. The first principal component (PC1) accounted for 68.18% of the variation, representing shape changes moving from a thin to a curved beak (x-axis in Figure 2). For example, the genus *Akialoa* (Figure 2 ID's 10 and 11) occupies the region dominated by thin recurved beaks, while *P. psittacea* (ID 1 in Figure 2) occupies the region dominated by larger, deeper, and more robust beaks. The second principal component (PC2) explains 21.78% of beak shape variation, and captures the association between the upper and lower bill. Lower values in PC2 represent beak shapes in which the lower bill is much smaller than the upper bill, such as in *Hemignathus* (IDs 16-18 in Figure 2), whereas higher values in PC2 represents a beak shape where the upper and lower bill are nearly the same size, as with *L. mana* (ID 21 in Figure 2).

We observe beak shape to be strongly associated with dietary guilds, where most species of like guilds cluster nearby in PC space (Figure 2). Invertebrates feeders, however, are an exception, as they occupy many disjoint regions of morphospace. Nectarivorous species form the largest cluster, together with those having a mixed diet of invertebrates and nectar, alongside many invertebrate specialists. A second small cluster consists of the invertebrate/nectar-feeding genus *Akialoa*, with very thin and elongated beaks. A third cluster composed exclusively of *Hemignathus* spp. has the lowest PC2 values, with recurved and asymmetric upper and lower beaks. Finally, we observe a loosely-connected cluster composed of both granivorous and frugivorous species with high values of PC1, with shorter more robust beak shapes. Two species are highly isolated in the morphospace but are closer to the cluster composed of granivorous species, with high values of

PC1. One of these is *Pseudonestor xanthophrys* (ID 27 in Figure 2), whose diet consists of invertebrates, and the other is *P. psittacea*, a frugivorous species (ID 1 in Figure 2).

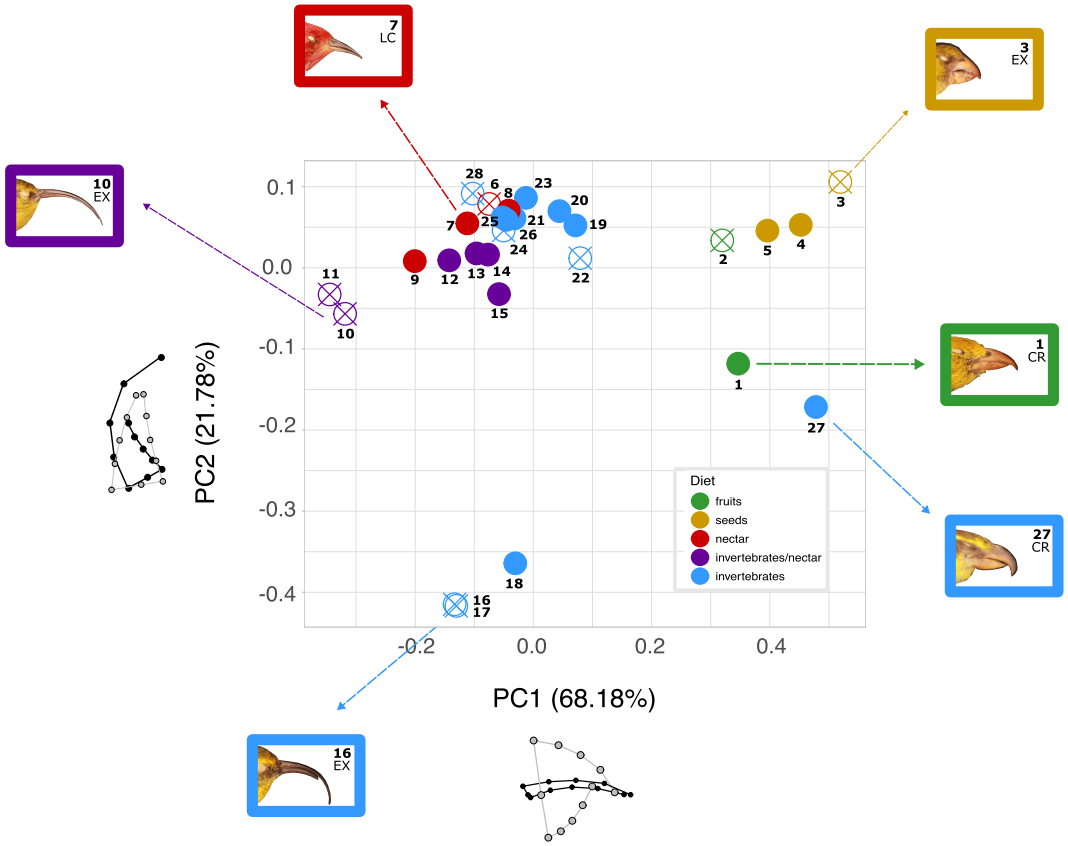

Figure 2: Principal components of beak shape using the coordinates from the Procrustes generalized analysis. Black and grey schemes show the maximum and minimum variation in each axis, respectively. Different colors represent different dietary guilds. Each point is a species and the solid and open-crossed points denote extant and extinct species, respectively. The photos show examples of beak shapes in the clusters. 1, *Psittirostra psittacea*; 2, *Rhodacanthis palmeri*; 3, *Chloridops kona*; 4, *Loxioides bailleui*; 5, *Telespiza cantans*; 6, *Himatione fraithii*; 7, *Himatione sanguinea*; 8, *Palmeria dolei*; 9, *Drepanis coccinea*; 10, *Akialoa obscura*; 11, *Akialoa stejnegeri*; 12, *Chlorodrepanis flava*; 13, *Chlorodrepanis stejnegeri*; 14, *Chlorodrepanis virens*; 15, *Magumma parva*; 16, *Hemignathus affinis*; 17, *Hemignathus hanapepe*; 18, *Hemignathus wilsoni*; 19, *Loxops caeruleirostris*; 20, *Loxops coccineus*; 21, *Loxops mana*; 22, *Loxops ochraceus*; 23, *Oreomystis bairdi*; 24, *Paroreomyza flammea*; 25, *Paroreomyza maculata*; 26, *Paroreomyza montana*; 27, *Pseudonestor xanthophrys*; and 28, *Viridonia sagittirostris*. The species categories from the IUCN Red List of Threatened Species are also shown: EX represents extinct species; CR (critically endangered), and LC (least concern) represent non-threatened species.

We observe centroid sizes to vary widely across species and across dietary guilds (Figure 3). The centroid sizes were similar for frugivorous (mean ± SD) (18.9 ± 3.33), granivorous (18.81 ± 2.91), and nectarivorous (18.22 ± 5.07). Insectivores had a slightly lower mean centroid size (14.9 ± 5.32), but with considerable within-guild variation. The nectar/invertebrate-feeding guild exhibited a higher mean centroid size (23.20 ± 18.02), largely influenced by the *Akialoa* species. To further investigate these patterns, we conducted an ANOVA to test for significant differences in centroid size between dietary guilds. The ANOVA showed significant differences in the mean values of centroid size among the different guilds ($F = 9.27$, $p < 0.05$). The *post hoc* Tukey test revealed pairwise differences only between mixed invertebrate/nectar feeders and nectarivorous species ($p < 0.05$), and between mixed invertebrate/nectar feeders and invertebrate feeders ($p < 0.05$).

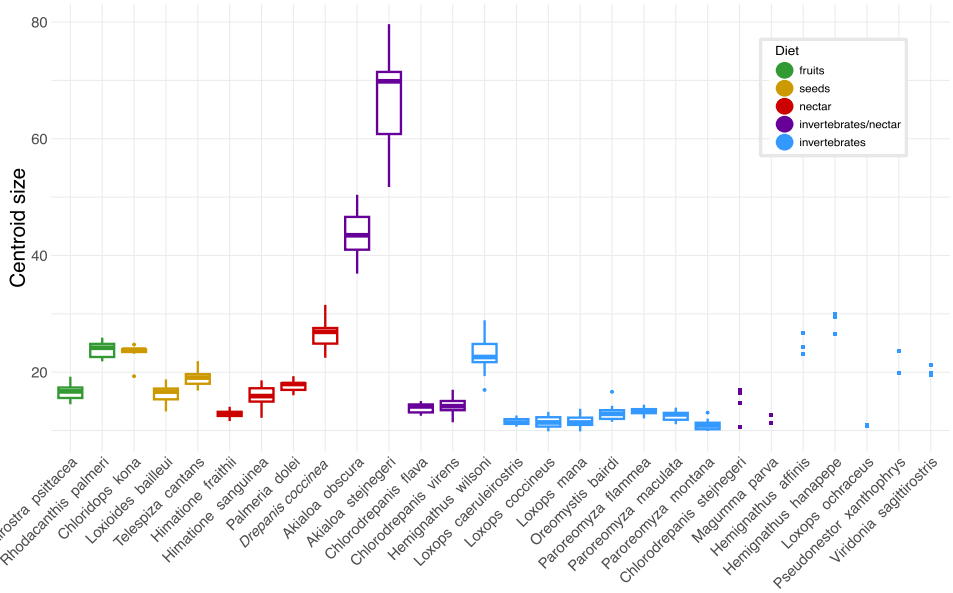

Figure 3: Boxplots showing the distribution of centroid values for different species, categorized by diet (fruits, seeds, nectar, invertebrates/nectar, and invertebrates). Each boxplot represents species with 5 or more individuals, while individual squared points represent species with fewer than 5 individuals.

4.2 Ancestral states

Beak robustness versus slenderness is captured by PC1, and using PC1 to reconstruct ancestral beak shape, we observe that distantly related clades have converged on similar PC1 values, indicating that similar beak shapes have evolved independently in these lineages (Figure 4A). For example, two distantly-related clades – on the one hand the clade including nectarivorous and invertebrate-feeding species (encompassing from *Akialoa* to *Chlorodrepanis*) and on the other hand nectarivores species (encompassing from *Palmeria* to *Himatione*) – demonstrate

lower values in PC1 (slender beaks) (Figure 4A). At the other extreme of PC1 (robust beaks), this trait appears to have evolved independently several times in the history of Hawaiian honeycreepers (e.g. *Chloridops kona*)(Figure 4A). The ancestral state reconstruction using PC2 reveals that the ancestor of *Hemignathus* underwent significant evolutionary change, resulting in the lowest values of PC2 (Figure 4B), where the lower beak is roughly half the size of the upper beak. A similar, but opposing evolutionary change is estimated for the ancestors of *Viridonia sagittirostris* and *C. kona*, which have the highest values of PC2, where upper and lower beak shapes are symmetrical Figure 4B). Our analysis of centroid size reveals beak size variation only in the *Akialoa* clade, with species exhibiting much larger beak sizes, followed by a further increase in the beak size of the ancestor of *Akialoa stejnegeri* (Figure 4C).

To further explore the relationship between beak shape evolution and feeding ecology, we performed an ancestral state reconstruction of diet (Figure 5A). The most recent common ancestor of the group has a higher probability of having been frugivorous/granivorous, even though the probability of it being insectivorous is comparable to that of being frugivorous/granivorous. Nectarivory is restricted to a small group of species, and this diet seems to have originated in the group fairly recently. Curiously, apart from three early-diverging lineages, frugivory/granivory is present in only one other pair of sister species that diverged much more recently. Nevertheless, invertebrate feeders are dominant in the dataset (19 species, compared to 5 frugivores/granivores and 4 nectarivores). This might account for the most likely ancestral state, but this would only be a bias if the species sample is somehow biased (either towards over representing invertebrate feeders or by lacking early-diverging species), which is not the case.

4.3 Evolutionary dynamics

We used maximum likelihood methods within an Ornstein-Uhlenbeck (OU) framework to estimate model parameters and identify the most likely locations of adaptive peaks, as well as shifts in optimal beak shape and size among Hawaiian honeycreepers. The total depth of the honeycreeper phylogeny is 11.38 million years, and the estimated phylogenetic half-lives for the three traits are much shorter than the total age of the group, indicating rapid adaptation and non-random evolutionary processes shaping beak morphology over time. Our analysis also reveals four shifts in PC1 (Figure 5B), three shifts in PC2 (Figure 5C), and fours shifts in centroid size, each representing distinct transitions in beak morphology across the phylogeny.

The best-fitting model, based on Akaike Information Criterion (AICc), suggests that PC1 exhibits evolutionary convergence toward two distinct adaptive peaks, corresponding to different beak morphologies (gray and red in Figure 5B). Specifically, the model indicates convergence in beak shape between *L. bailleui* and *Telespiza catan*, both of which are granivorous, with *P. psittacea*, *Rhodacanthis palmeri* and *C. kona*, which are primarily frugivorous and granivorous species,

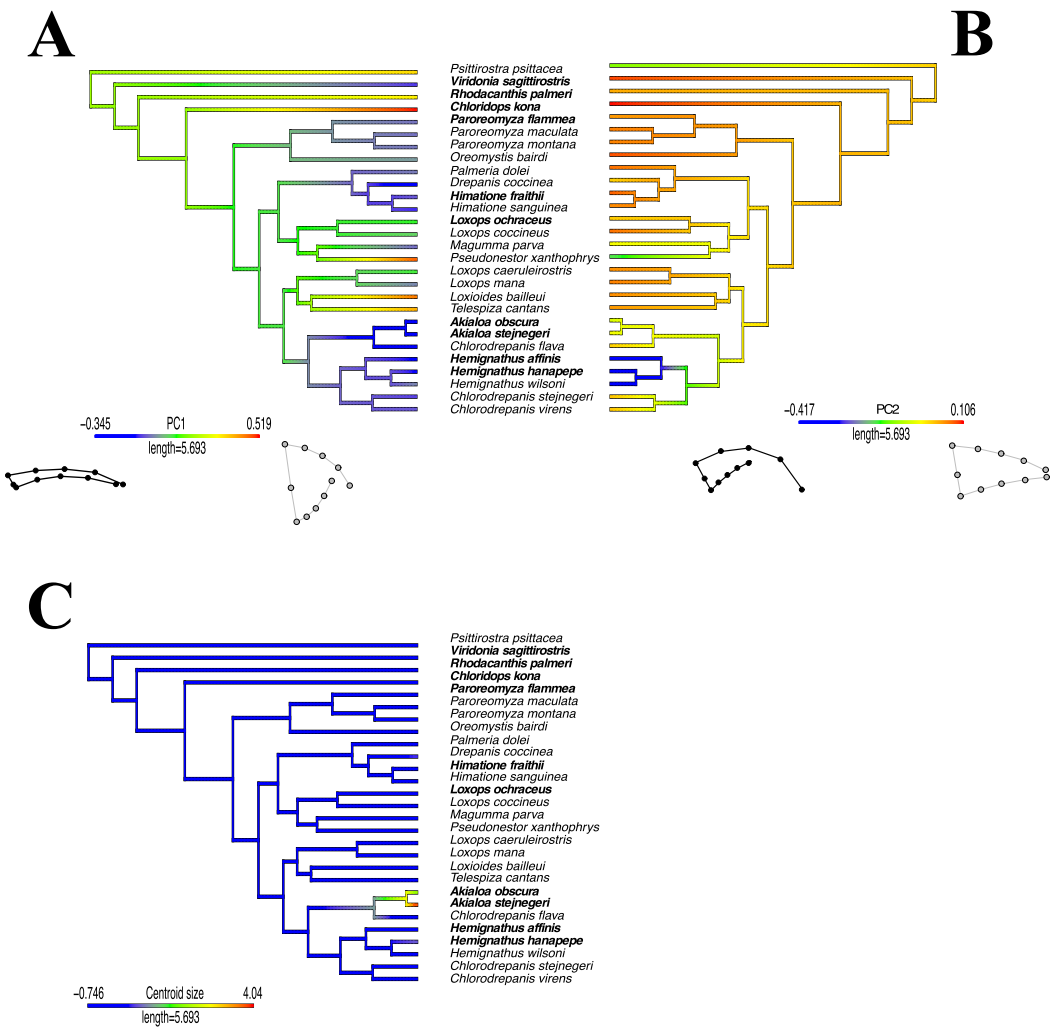

Figure 4: Reconstruction of the ancestral state of beak morphology. **A)** PC1, **B)** PC2 , and **C)** Centroid size. Phylogenies were generated using the R package Phytools (Revell, 2012).

reflecting an ancestral adaptive peak for this group (gray peak Figure 5B). Additionally, there is a convergence toward a thinner, more elongated beak morphology in *Viridonia sagittirostris* and the clade encompassing the greatest species diversity (red peak in Figure 5B). Moreover, a unique shift toward a thick, hooked beak optimal for specialized feeding is evident in the lineage of *Pseudonestor xanthophrys* (blue peak Figure 5B).

For PC2, the model does not indicate any convergence, and AICc values are similar across models ($AICc = -81.92, \alpha = 3.00, \sigma^2 = 0.008$). However, there are three shifts in the adaptive optimum, θ, each reflecting a distinct change in the relative proportions of the upper and lower beak (Figure 5C). The first shift is located at the base of the honeycreeper clade, in *P. psittacea*, indicating a broad initial diversification in beak structure (gray peak, Figure 5C). Subsequent shifts occur in the ancestor of *Pseudonestor xanthophrys*, characterized by a highly specialized bill (blue peak, Figure 5C), and within the *Hemignathus* lineage, where the lower bill becomes significantly reduced relative to the upper bill (green peak, Figure 5C).

For centroid size, the convergence model offers the best fit ($AICc = 42.22, \alpha = 0.84, \sigma^2 = 0.27$), with four notable shifts in θ. Two lineages – *Drepanis coccine* and *Hemignathus* – converge toward larger beak sizes (blue peak, Figure 5D). The remaining shifts are observed in the ancestors of *Akialoa* and the *Akialoa stejnegeri* clade, both of which exhibit an increase in beak size (red and green peaks, Figure 5 D).

4.4 The loss of uniqueness

Our results indicate a loss of unique beak morphologies in Hawaiian honeycreepers. Historically, this group occupied a broad range of morphospace, but many clades that once filled peripheral regions of this space are now extinct (Figure 2). When examining the adaptive peaks, we find that for PC1, extant species are distributed across all three peaks, yet one of these peaks (gray peak in Figure 5B), shared by five species, includes two extinct species (*R. palmeri* and *C. kona*), representing a 40% loss. For PC2, out of the four adaptive peaks identified, one (green peak in Figure 5C) is exclusively occupied by the genus *Hemignathus*, which is composed of three species, two of which are extinct. For centroid size, two of the four adaptive peaks are lost (green and red peaks in Figure 5D). Additionally, the peak characterized by convergence among the three *Hemignathus* species and *D. coccinea* (blue peak in Figure 5D), includes two extinct *Hemignathus* species.

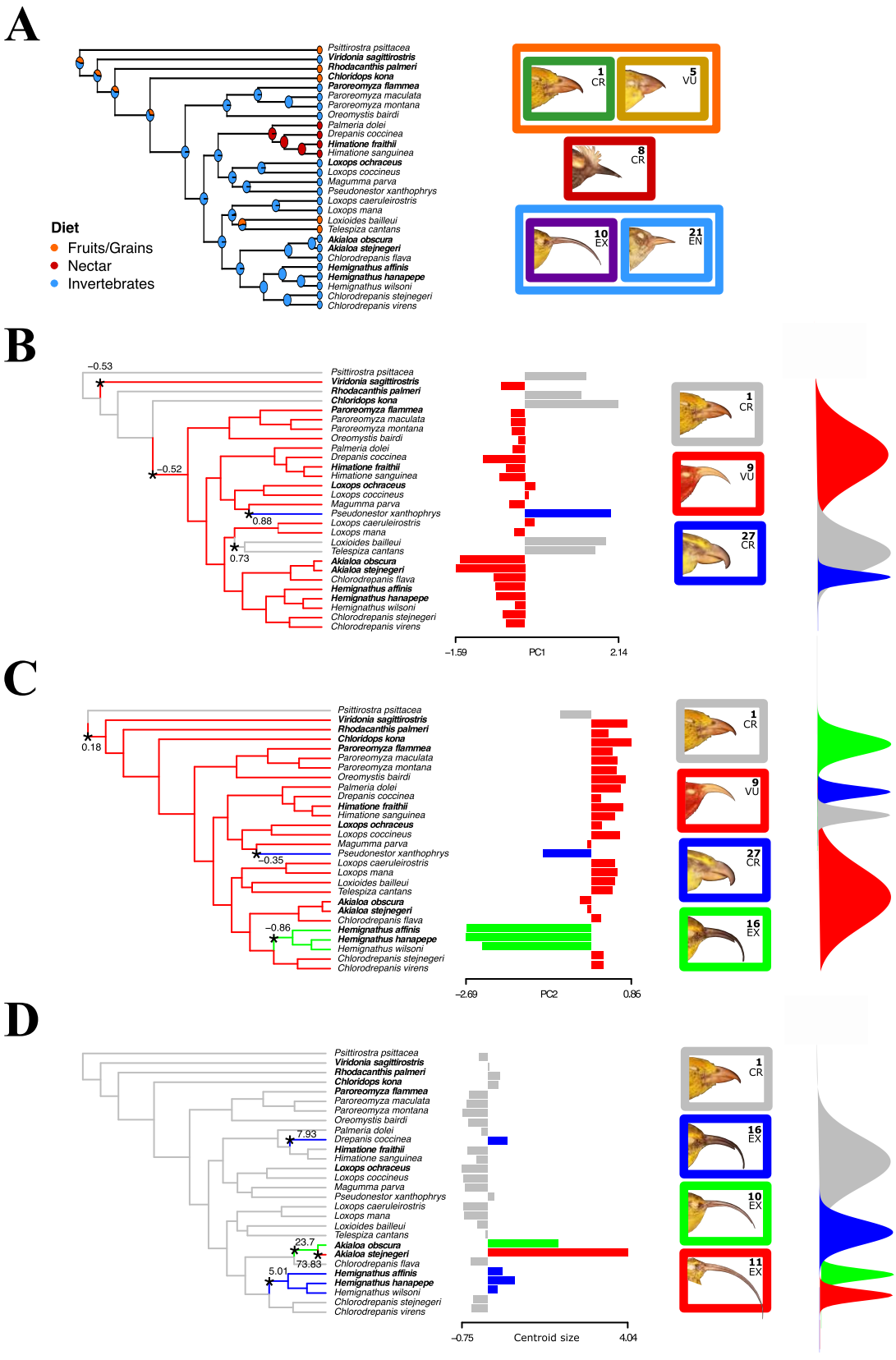
A
Psittirostra psittacea
Viridonia sagittirostris
Rhodacanthis palmeri
Chloridops kona
Paroreomyza flammea
Paroreomyza maculata
Paroreomyza montana
Oreomystis bairdi
Palmeria dolei
Drepanis coccinea
Himatione fraithii
Himatione sanguinea
Loxops ochraceus
Loxops coccineus
Magumma parva
Pseudonestor xanthophrys
Loxops caeruleirostris
Loxops mana
Loxioides bailleui
Telespiza cantans
Akialoa obscura
Akialoa stejnegeri
Chlorodrepanis flava
Hemignathus affinis
Hemignathus hanapepe
Hemignathus wilsoni
Chlorodrepanis stejnegeri
Chlorodrepanis virens
Diet
Fruits/Grains
Nectar
Invertebrates
1 CR
5 VU
8 CR
10 EX
21 EN
B
−0.53
−0.52
0.88
0.73
−1.59
PC1
2.14
1 CR
9 VU
27 CR
C
0.18
−0.35
−0.86
−2.69
PC2
0.85
1 CR
9 VU
27 CR
16 EX
D
7.93
23.7
73.83
5.01
−0.75
Centroid size
4.04
1 CR
16 EX
10 EX
11 EX

Figure 5: **A)** Phylogeny of honeycreepers displaying the distribution of trait states in the tips and the estimated states at each internal node. For this analysis, we combined the five guilds into three categories of diet: 1) fruits and grains (orange); 2) nectar (dark red); and 3) invertebrates (blue), as shown by representative species. Extinct species are shown in bold. **B-D)** Phylogenetic history of adaptive peak shifts in beak morphology. Asterisks indicate where adaptive shifts occurred in the phylogeny, with numbers representing the magnitude of the changes. Bars represent the values for each species, and species with the same color share the same adaptive peak. **B)** PC1, **C)** PC2, and **D)** centroid size. Mean shifts were estimated using a Bayesian framework for fitting the Ornstein-Uhlenbeck (OU) model. An illustration of the distribution of adaptive peaks is shown on the right, with boxes containing a representative species for each peak. Species: 1, *Psittirostra psittacea*; 5, *Telespiza cantans*; 8, *Palmeria dolei*; 9, *Drepanis coccinea*; 10, *Akialoa obscura*; 11, *Akialoa stejnegeri*; 16, *Hemignathus affinis*; 21, *Loxops mana*; 27, *Pseudonestor xanthophrys*.

5 Discussion

Hawaiian honeycreepers are a classic example of adaptive radiation, demonstrating remarkable diversity in beak morphology that surpasses that of many related and unrelated bird groups, both within Hawaii and on other islands (Lovette *et al.*, 2002; Losos & Ricklefs, 2009; Tokita *et al.*, 2017). While significant progress has been made in understanding the mechanisms driving rapid and disparate evolution in this group (Pimm & Pimm, 1982; Ricklefs & Bermingham, 2007; Navalón *et al.*, 2020b; Campana *et al.*, 2020), many aspects of their evolutionary history remain unresolved. Our study addresses some of these gaps by employing an integrative framework that combines phylogenetic comparative methods with geometric morphometrics analysis. This framework not only enhances our understanding of the evolutionary processes and selective pressures shaping honeycreeper morphology but also provides broader insights into adaptive radiation. Given the high threat status of many species within this group and the extensive extinctions that have already occurred, our findings underscore the significant loss of unique morphologies – a loss that has implications for both evolutionary biology and conservation efforts.

First, our results add to the growing body in literature showing that adaptive shifts in Hawaiian honeycreepers are linked to their feeding ecology (Tokita *et al.*, 2017; Mosleh *et al.*, 2023). For instance, thicker and more robust beaks, typically associated with frugivorous and granivorous diets, represent a convergent evolutionary peak in their evolutionary history (gray peak in Figure 5B). This adaptive peak also describes the most basal species, suggesting an ancestral origin, aligning with Lerner *et al.* (2011), who demonstrated that Hawaiian honeycreepers are derived from Eurasian rosefinches, known for their small, finch-like bill shapes,

specializing on fruits and seeds (Peiponen, 1974).

Our findings indicate that nectar specialization has played a significant role in the evolution of honeycreeper beaks, emerging as a derived trait from their invertebrate-feeding ancestors. This shift is associated with thinner and more slender beaks; however, a unique adaptive peak for this group did not develop. While recent research has demonstrated that the relationship between beak shape and feeding ecology in birds is complex—showing that diet is not always the sole evolutionary factor or the strongest influence shaping beak morphology (Bright *et al.*, 2016; Felice *et al.*, 2019; Navalón *et al.*, 2020a)—feeding ecology often becomes the dominant driver of beak shape diversification on remote islands. In such environments, it plays a crucial role in processes leading to adaptive radiation, as observed in honeycreepers (Grant & Grant, 2024). In fact, studies examining skull and upper mandible shapes across avian radiations on islands have demonstrated a strong correlation between beak shape and diet (Tokita *et al.*, 2017; Mosleh *et al.*, 2023).

A number of ingredients are required for adaptive radiation, including ecological opportunity, genetic variation, strong diversifying selection, and sufficient time (Schluter, 2000; Stroud & Losos, 2016; Meier *et al.*, 2019; Gillespie *et al.*, 2020; McGee *et al.*, 2020; Grant & Grant, 2024). Remote island systems offer prime examples of ecological opportunities, where the colonization of isolated areas and the availability of untapped resources create new diversifying evolutionary pressures (Losos, 2010; Stroud & Losos, 2016). For birds, access to these novel resources can act as a strong selective force on beak morphology, with different beak forms evolving to exploit various resources more efficiently. Indeed, there are several great examples of avian adaptive radiations in remote islands, such as the Galápagos finches, Hawaiian honeycreepers, and the vangas of Madagascar, (Jønsson *et al.*, 2012; Grant & Grant, 2024). These adaptive radiations not only lead to the evolution of distinct beak morphologies but also facilitate the filling out of morphospace, where species diversify to occupy various niches within a given morphological landscape. Our results suggest that Hawaiian honeycreepers have diversified across morphospace to exploit a range of dietary resources. And while the different beak shapes emerging from this evolutionary exploration of morphospace were likely the result of selective drivers originating from resource acquisition, we observe the ecological reality of how beak shape maps to diet to be far more complex. Here we observe that this complexity arises by the fact that similar beak shapes are found across different dietary guilds, such as granivores and frugivores, while different beak sizes can serve similar ecological roles, as seen among nectarivores and insectivores in our study.

Along these lines, convergence does not appear to be a very common outcome, with respect to beak size or shape, among Hawaiian honeycreepers, regardless of dietary guild. We documented three cases of adaptive convergence, with the first in beak shape between granivorous and frugivorous clades (*L. bailleui* and *T. catan*, alongside the basal species *P. psittacea*, *R. palmeri*, and *C. kona* - two first rows in Figure 1). Second, convergence was observed also in beak shape between

V. sagittirostris (ID 28 Figure 1) and most species in the clade (red peak - Figure 5B). Third, convergence was observed in beak size between insectivorous clades (three species of the genus *Hemignathus* - ID 16-18 Figure 1), the species of which feed by using the lower mandible to tap branches – similar to a woodpecker – and then use the upper mandible to fish out the prey and a species comprising a specialization in nectarivory *Drepanis coccinea* (ID 9 Figure 1) (Munro, 1944; Pratt & Conant, 2005). Thus, our result suggests that even different diets might lead to similar beak sizes.

Interestingly, our results do not document convergence across the suite of morphological measures for *O. baird* and *L. mana*, a pair of species commonly used as an example of convergence due to their phenotypic resemblance (Pratt, 2001; Pratt & Conant, 2005; Reding *et al.*, 2008; Tokita *et al.*, 2017). In this particular case, the morphometric landmarks that we used may miss what would be described as convergence using an alternative set of measurements, or perhaps may be due to the fact that the documented changes in shape were not strong enough to represent a new shift in adaptive peaks. We note, however, that both species do share the same adaptive peak, while this is a peak that is also shared by several other species in the clade.

While Hawaiian honeycreepers occupy a diverse morphospace, even when compared to other adaptively radiating bird groups (Tokita *et al.*, 2017; Mosleh *et al.*, 2023), much of this morphospace has been reduced with the extinction or near-extinction of species occupying peripheral regions. For example, the insectivorous cluster with the lowest PC2 values include three species of the genus *Hemignathus* (Figure 2), of which two are extinct, with the remaining species classified as endangered by the IUCN. Similarly, in the cluster containing primarily frugivorous and granivorous species, half of those are extinct, while the survivors – *L. bailleui* and *T. cantans* – are classified as critically endangered and vulnerable by the IUCN, respectively. The two species isolated in the morphospace, *P. psittacea* (ID 1 in Figure 2) and *P. xanthophrys* (ID 27 in Figure 2), are also considered threatened. *Psittirostra psittacea*, although still classified as critically endangered by the IUCN, was last observed in 1987 and is presumed extinct. *Pseudonestor xanthophrys* is classified as critically endangered, occurring in the rainforest on eastern Maui (Mountainspring, 1987). It forages by using its upper beak to split, crush, and tear bark and twigs, targeting insect larvae from mossy branches, and occasionally opens fruit to find insects (Munro, 1944; Pratt & Conant, 2005). With a 96% reduction in its effective population size over the past 110 years (Mounce *et al.*, 2015), it is an extant representative of peripheral morphospace that we know from past extinctions is perhaps prone to collapse. With the loss of these morphologically peripheral species, the remaining species are those that are most morphologically overlapping, suggesting that persistence in the face of anthropogenic disturbance favors a reversion to the mean, resulting in significant redundancy in honeycreeper beak shape.

Our study offers novel insights into the adaptive landscape of Hawaiian honeycreepers by applying an Ornstein-Uhlenbeck model to identify shifts in adaptive

peaks and the potential loss of functional diversity. These findings are essential because they show that, for example, although a species can appear distinct in the group's morphospace, such as *P. psittacea* (ID 1 in Figure 2), it can still share the same adaptive peak as other species (gray peak in Figure 5B). Beyond clustering together in the morphospace, frugivorous and granivorous species also occupy a single phenotypic optimum (gray peak in Figure 5B). As previously mentioned, these species are either extinct or on the brink of extinction, indicating that the functional traits associated with this adaptive peak are at risk of being lost. Our results shows that a special attention should be given to *P. xanthophrys*, since it exhibits a very unique adaptive peak in both PC1 and PC2, signifying a distinct functional role in the system, with the only branch that have shifts in both PCs axis (blue peaks in Figure 5B and C). The clade containing the genera *Hemignathus* and *Akialoa* also shows phenotypic peaks, and thus functional traits, that are unique and have either been threatened or lost.

Historical extinctions of Hawaiian honeycreepers have pushed the group towards increased morphological homogeneity, with the remaining species exhibiting greater similarity in their trait morphology. Extinction risk, as shown by Carmona *et al.* (2021) in a global study of over 75,000 species, is not random but clustered within specific functional spaces, resulting in a denser functional homogenization of species on a global scale. Ecosystem processes are influenced by the functional traits of species (Sodhi *et al.*, 2004; Toussaint *et al.*, 2021). Birds play a significant role in ecosystem services (Whelan *et al.*, 2008), and the loss of functionally unique species—those associated with singular functional roles—could disrupt ecosystem dynamics in unpredictable ways (Toussaint *et al.*, 2021; Ali *et al.*, 2023). Thus, species with unique traits are likely to have a more significant impact upon extinction compared to those with overlapping or redundant traits (Violle *et al.*, 2017). Moreover, Sayol *et al.* (2021) demonstrated that oceanic islands have experienced a disproportionate loss of functional diversity due to anthropogenic extinctions. Moreover, they showed that even when many species have been introduced to islands, with alien species often exceeding the number of extinct native species, they typically perform a narrower range of functional roles within the ecosystem. Thus, even though many bird species have been introduced to Hawaii (Vitousek *et al.*, 1987), the loss of these unique species will have a substantial impact not only on the biodiversity of the system but also on its ecosystem functioning. Our findings should guide future conservation efforts by highlighting the uniqueness of certain species within the group, whose loss would significantly reduce the functional trait space and potentially trigger cascading effects on Hawaii's ecosystem function. Therefore, conservation strategies should prioritize long-term objectives aimed at preserving functional diversity by focusing on a broader range of threatened species.

References

Abrahamczyk, S. & Kessler, M. (2015). Morphological and behavioural adaptations to feed on nectar: How feeding ecology determines the diversity and composition of hummingbird assemblages. *Journal of Ornithology*, 156, 333–347.

Adams, D.C. & Otárola-Castillo, E. (2013). geomorph: an r package for the collection and analysis of geometric morphometric shape data. *Methods in ecology and evolution*, 4, 393–399.

Ali, J.R., Blonder, B.W., Pigot, A.L. & Tobias, J.A. (2023). Bird extinctions threaten to cause disproportionate reductions of functional diversity and uniqueness. *Functional Ecology*, 37, 162–175.

Anderson, D., Burnham, K. & White, G. (1998). Comparison of akaike information criterion and consistent akaike information criterion for model selection and statistical inference from capture-recapture studies. *Journal of Applied Statistics*, 25, 263–282.

Benkman, C.W. (1988). Seed handling ability, bill structure, and the cost of specialization for crossbills. *The Auk*, 105, 715–719.

Boyer, A.G. (2008). Extinction patterns in the avifauna of the Hawaiian islands. *Diversity and Distributions*, 14, 509–517.

Bright, J.A., Marugán-Lobón, J., Cobb, S.N. & Rayfield, E.J. (2016). The shapes of bird beaks are highly controlled by nondietary factors. *Proceedings of the National Academy of Sciences*, 113, 5352–5357.

Campana, M.G., Corvelo, A., Shelton, J., Callicrate, T.E., Bunting, K.L., Riley-Gillis, B., Wos, F., DeGrazia, J., Jarvis, E.D. & Fleischer, R.C. (2020). Adaptive Radiation Genomics of Two Ecologically Divergent Hawai‘ian Honeycreepers: The ‘akiapōlā‘au and the Hawai‘i ‘amakihi. *Journal of Heredity*, 111, 21–32.

Carmona, C.P., Tamme, R., Pärtel, M., de Bello, F., Brosse, S., Capdevila, P., González-M, R., González-Suárez, M., Salguero-Gómez, R., Vásquez-Valderrama, M. *et al.* (2021). Erosion of global functional diversity across the tree of life. *Science Advances*, 7, eabf2675.

Derryberry, E.P., Seddon, N., Claramunt, S., Tobias, J.A., Baker, A., Aleixo, A. & Brumfield, R.T. (2012). Correlated evolution of beak morphology and song in the neotropical woodcreeper radiation. *Evolution*, 66, 2784–2797.

Felice, R.N., Tobias, J.A., Pigot, A.L. & Goswami, A. (2019). Dietary niche and the evolution of cranial morphology in birds. *Proceedings of the Royal Society B*, 286, 20182677.

Felsenstein, J. (1985). Phylogenies and the Comparative Method. *The American Naturalist*, 125, 1–15.

Friedman, N.R., Miller, E.T., Ball, J.R., Kasuga, H., Remeš, V. & Economo, E.P. (2019). Evolution of a multifunctional trait: shared effects of foraging ecology and thermoregulation on beak morphology, with consequences for song evolution. *Proceedings of the Royal Society B*, 286, 20192474.

Gillespie, R.G., Bennett, G.M., De Meester, L., Feder, J.L., Fleischer, R.C., Harmon, L.J., Hendry, A.P., Knope, M.L., Mallet, J., Martin, C., Parent, C.E., Patton, A.H., Pfennig, K.S., Rubinoff, D., Schluter, D., Seehausen, O., Shaw, K.L., Stacy, E., Stervander, M., Stroud, J.T., Wagner, C. & Wogan, G.O.U. (2020). Comparing Adaptive Radiations Across Space, Time, and Taxa. *Journal of Heredity*, 111, 1–20.

Gosler, A. (1986). Pattern and process in the bill morphology of the great tit zyxwvutsrqponm. *Ibis*, 129, 451–476.

Grant, B.R. & Grant, P.R. (1989). Natural selection in a population of darwin's finches. *The American Naturalist*, 133, 377–393.

Grant, P.R. & Grant, B.R. (2006). Evolution of character displacement in darwin's finches. *science*, 313, 224–226.

Grant, P.R. & Grant, B.R. (2024). From microcosm to macrocosm: Adaptive radiation of darwin's finches. *Evolutionary Journal of the Linnean Society*, p. kzae006.

Hansen, T.F. (1997). Stabilizing Selection and the Comparative Analysis of Adaptation. *Evolution*, 51, 1341–1351.

Huelsenbeck, J.P., Nielsen, R. & Bollback, J.P. (2003). Stochastic mapping of morphological characters. *Systematic biology*, 52, 131–158.

Ingram, T. & Mahler, D. (2013). SURFACE: Detecting convergent evolution from comparative data by fitting Ornstein-Uhlenbeck models with stepwise Akaike Information Criterion. *Methods in Ecology and Evolution*, 4, 416–425.

Jønsson, K.A., Fabre, P.H., Fritz, S.A., Etienne, R.S., Ricklefs, R.E., Jørgensen, T.B., Fjeldså, J., Rahbek, C., Ericson, P.G., Woog, F. *et al.* (2012). Ecological and evolutionary determinants for the adaptive radiation of the madagascan vangas. *Proceedings of the National Academy of Sciences*, 109, 6620–6625.

Khabbazian, M., Kriebel, R., Rohe, K. & Ané, C. (2016). Fast and accurate detection of evolutionary shifts in ornstein–uhlenbeck models. *Methods in Ecology and Evolution*, 7, 811–824.

Lerner, H.R.L., Meyer, M., James, H.F., Hofreiter, M. & Fleischer, R.C. (2011). Multilocus Resolution of Phylogeny and Timescale in the Extant Adaptive Radiation of Hawaiian Honeycreepers. *Current Biology*, 21, 1838–1844.

Lessells, C.M. & Boag, P.T. (1987). Unrepeatable Repeatabilities: A Common Mistake. *The Auk*, 104, 116–121.

Losos, J.B. (2010). Adaptive Radiation, Ecological Opportunity, and Evolutionary Determinism. *The American Naturalist*, 175, 623–639.

Losos, J.B. (2011). Convergence, Adaptation, and Constraint. *Evolution*, 65, 1827–1840.

Losos, J.B. & Ricklefs, R.E. (2009). Adaptation and diversification on islands. *Nature*, 457, 830–836.

Lovette, I.J., Bermingham, E. & Ricklefs, R.E. (2002). Clade-specific morphological diversification and adaptive radiation in Hawaiian songbirds. *Proceedings of the Royal Society B: Biological Sciences*, 269, 37–42.

Mahler, D.L., Ingram, T., Revell, L.J. & Losos, J.B. (2013). Exceptional Convergence on the Macroevolutionary Landscape in Island Lizard Radiations. *Science*, 341, 292–295.

Mariyappan, M., Rajendran, M., Velu, S., Johnson, A., Dinesh, G.K., Solaimuthu, K., Kaliyappan, M. & Sankar, M. (2023). Ecological Role and Ecosystem Services of Birds: A Review. *International Journal of Environment and Climate Change*, 13, 76–87.

McClure, K.M., Fleischer, R.C. & Kilpatrick, A.M. (2020). The role of native and introduced birds in transmission of avian malaria in Hawaii. *Ecology*, 101, e03038.

McGee, M.D., Borstein, S.R., Meier, J.I., Marques, D.A., Mwaiko, S., Taabu, A., Kishe, M.A., O'Meara, B., Bruggmann, R., Excoffier, L. *et al.* (2020). The ecological and genomic basis of explosive adaptive radiation. *Nature*, 586, 75–79.

McTavish, E.J., Gerbracht, J.A., Holder, M.T., Iliff, M.J., Lepage, D., Rasmussen, P.C., Redelings, B., Sanchez-Reyes, L.L. & Miller, E.T. (2024). A complete and dynamic tree of birds. *bioRxiv*, pp. 2024–05.

Meier, J.I., Stelkens, R.B., Joyce, D.A., Mwaiko, S., Phiri, N., Schliewen, U.K., Selz, O.M., Wagner, C.E., Katongo, C. & Seehausen, O. (2019). The coincidence of ecological opportunity with hybridization explains rapid adaptive radiation in lake mweru cichlid fishes. *Nature communications*, 10, 5391.

Missagia, C.C. & Alves, M.A.S. (2018). Does beak size predict the pollination performance of hummingbirds at long and tubular flowers? a case study of a neotropical spiral ginger. *Journal of Zoology*, 305, 1–7.

Mosleh, S., Choi, G.P., Musser, G.M., James, H.F., Abzhanov, A. & Mahadevan, L. (2023). Beak morphometry and morphogenesis across avian radiations. *Proceedings of the Royal Society B*, 290, 20230420.

Mounce, H.L., Raisin, C., Leonard, D.L., Wickenden, H., Swinnerton, K.J. & Groombridge, J.J. (2015). Spatial genetic architecture of the critically-endangered maui parrotbill (pseudonestor xanthophrys): management considerations for reintroduction strategies. *Conservation Genetics*, 16, 71–84.

Mountainspring, S. (1987). Ecology, behavior, and conservation of the maui parrotbill. *The Condor*, 89, 24–39.

Munro, G.C. (1944). *Birds of Hawaii*. Tongg Publishing Company. Honolulu, HI.

Navalón, G., Bright, J.A., Marugán-Lobón, J. & Rayfield, E.J. (2019). The evolutionary relationship among beak shape, mechanical advantage, and feeding ecology in modern birds. *Evolution*, 73, 422–435.

Navalón, G., Marugán-Lobón, J., Bright, J.A., Cooney, C.R. & Rayfield, E.J. (2020a). The consequences of craniofacial integration for the adaptive radiations of Darwin's finches and Hawaiian honeycreepers. *Nature Ecology & Evolution*, 4, 270–278.

Navalón, G., Marugán-Lobón, J., Bright, J.A., Cooney, C.R. & Rayfield, E.J. (2020b). The consequences of craniofacial integration for the adaptive radiations of darwin's finches and hawaiian honeycreepers. *Nature Ecology & Evolution*, 4, 270–278.

Paxton, E.H., Camp, R.J., Gorresen, P.M., Crampton, L.H., Leonard, D.L. & VanderWerf, E.A. (2016). Collapsing avian community on a Hawaiian island. *Science Advances*, 2, e1600029.

Peiponen, V. (1974). Food and breeding of the scarlet rosefinch (carpodacus e. erythrinus pall.) in southern finland. In: *Annales Zoologici Fennici*. JSTOR, pp. 155–165.

Pigot, A.L., Sheard, C., Miller, E.T., Bregman, T.P., Freeman, B.G., Roll, U., Seddon, N., Trisos, C.H., Weeks, B.C. & Tobias, J.A. (2020). Macroevolutionary convergence connects morphological form to ecological function in birds. *Nature Ecology & Evolution*, 4, 230–239.

Pigot, A.L., Trisos, C.H. & Tobias, J.A. (2016). Functional traits reveal the expansion and packing of ecological niche space underlying an elevational diversity gradient in passerine birds. *Proceedings of the Royal Society B: Biological Sciences*, 283, 20152013.

Pimm, S.L. & Pimm, J.W. (1982). Resource Use, Competition, and Resource Availability in Hawaiian Honeycreepers. *Ecology*, 63, 1468–1480.

Pratt, H.D. (2001). Why the hawaii creeper is an oreomystis: what phenotypic characters reveal about the phylogeny of hawaiian honeycreepers. *Studies in Avian Biology*, 22, 81–97.

Pratt, H.D. & Conant, S. (2005). *The Hawaiian Honeycreepers: Drepanidinae*. OUP Oxford.

Reding, D.M., Foster, J.T., James, H.F., Pratt, H.D. & Fleischer, R.C. (2008). Convergent evolution of 'creepers' in the Hawaiian honeycreeper radiation. *Biology Letters*, 5, 221–224.

Reding, D.M., Foster, J.T., James, H.F., Pratt, H.D. & Fleischer, R.C. (2009). Convergent evolution of 'creepers' in the Hawaiian honeycreeper radiation. *Biology Letters*, 5, 221–224.

Revell, L.J. (2012). phytools: an r package for phylogenetic comparative biology (and other things). *Methods in ecology and evolution*, pp. 217–223.

Ricklefs, R.E. & Bermingham, E. (2007). The Causes of Evolutionary Radiations in Archipelagoes: Passerine Birds in the Lesser Antilles. *The American Naturalist*, 169, 285–297.

Sayol, F., Cooke, R.S., Pigot, A.L., Blackburn, T.M., Tobias, J.A., Steinbauer, M.J., Antonelli, A. & Faurby, S. (2021). Loss of functional diversity through anthropogenic extinctions of island birds is not offset by biotic invasions. *Science Advances*, 7, eabj5790.

Schluter, D. (2000). *The ecology of adaptive radiation*. OUP Oxford.

Schluter, D. & Grant, P.R. (1984). Determinants of morphological patterns in communities of darwin's finches. *The American Naturalist*, 123, 175–196.

Sheard, C., Street, S.E., Evans, C., Lala, K.N., Healy, S.D. & Sugasawa, S. (2023). Beak shape and nest material use in birds. *Philosophical Transactions of the Royal Society B: Biological Sciences*, 378, 20220147.

Sodhi, N.S., Liow, L. & Bazzaz, F. (2004). Avian extinctions from tropical and subtropical forests. *Annu. Rev. Ecol. Evol. Syst.*, 35, 323–345.

Stayton, C.T. (2008). Is convergence surprising? An examination of the frequency of convergence in simulated datasets. *Journal of Theoretical Biology*, 252, 1–14.

Stroud, J.T. & Losos, J.B. (2016). Ecological Opportunity and Adaptive Radiation. *Annual Review of Ecology, Evolution, and Systematics*, 47, 507–532.

Tattersall, G.J., Andrade, D.V. & Abe, A.S. (2009). Heat exchange from the toucan bill reveals a controllable vascular thermal radiator. *science*, 325, 468–470.

Tattersall, G.J., Arnaout, B. & Symonds, M.R. (2017). The evolution of the avian bill as a thermoregulatory organ. *Biological Reviews*, 92, 1630–1656.

Team, R.D.C. (2023). *R: A Language and Environment for Statistical Computing*. ISBN 3-900051-07-0.

Tokita, M., Yano, W., James, H.F. & Abzhanov, A. (2017). Cranial shape evolution in adaptive radiations of birds: Comparative morphometrics of Darwin's finches and Hawaiian honeycreepers. *Philosophical Transactions of the Royal Society B: Biological Sciences*, 372, 20150481.

Toussaint, A., Brosse, S., Bueno, C.G., Pärtel, M., Tamme, R. & Carmona, C.P. (2021). Extinction of threatened vertebrates will lead to idiosyncratic changes in functional diversity across the world. *Nature communications*, 12, 5162.

Triantis, K.A., Rigal, F., Whittaker, R.J., Hume, J.P., Sheard, C., Poursanidis, D., Rolland, J., Sfenthourakis, S., Matthews, T.J., Thébaud, C. & Tobias, J.A. (2022). Deterministic assembly and anthropogenic extinctions drive convergence of island bird communities. *Global Ecology and Biogeography*, 31, 1741–1755.

Violle, C., Thuiller, W., Mouquet, N., Munoz, F., Kraft, N.J., Cadotte, M.W., Livingstone, S.W. & Mouillot, D. (2017). Functional rarity: the ecology of outliers. *Trends in Ecology & Evolution*, 32, 356–367.

Vitousek, P.M., Loope, L.L. & Stone, C.P. (1987). Introduced species in hawaii. biological effects and opportunities for ecological research. *Trends in Ecology & Evolution*, 2, 224–227.

Whelan, C.J., Wenny, D.G. & Marquis, R.J. (2008). Ecosystem services provided by birds. *Annals of the New York academy of sciences*, 1134, 25–60.

Yoder, J., Clancey, E., Des Roches, S., Eastman, J., Gentry, L., Godsoe, W., Hagey, T., Jochimsen, D., Oswald, B., Robertson, J. *et al.* (2010). Ecological opportunity and the origin of adaptive radiations. *Journal of evolutionary biology*, 23, 1581–1596.

Zelditch, M., Swiderski, D. & Sheets, H.D. (2012). *Geometric morphometrics for biologists: a primer*. academic press.

6 Supplemtary Information

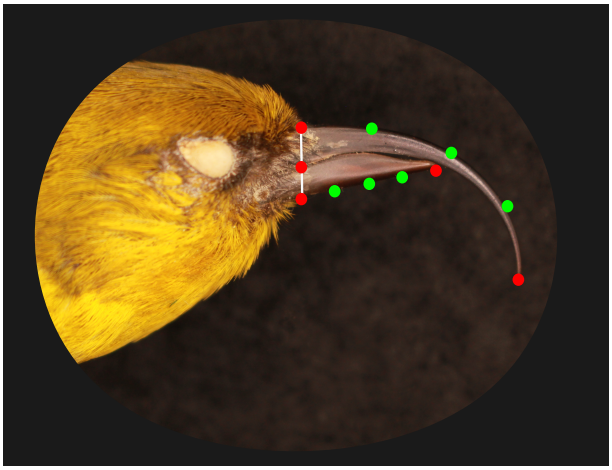

Figure S1: *Hemignathus wilsoni* with the landmarks (red) and semi-landmarks (green).

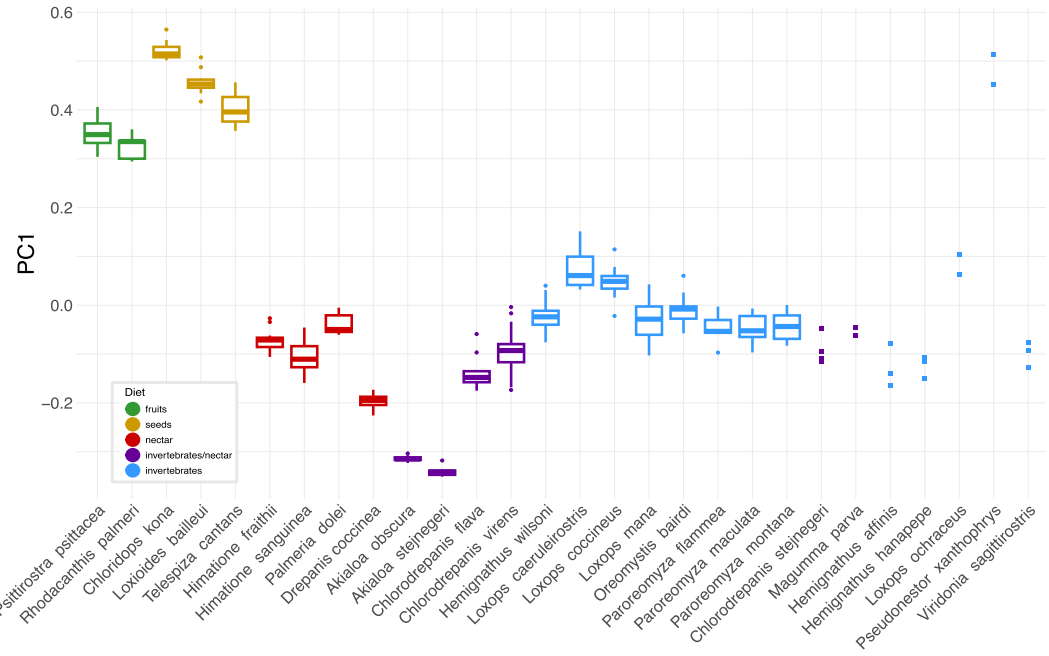

Figure S2: Boxplots showing the distribution of PC1 values for different species, categorized by diet (fruits, seeds, nectar, invertebrates/nectar, and invertebrates). Each boxplot represents species with 5 or more individuals, while individual squared points represent species with fewer than 5 individuals.

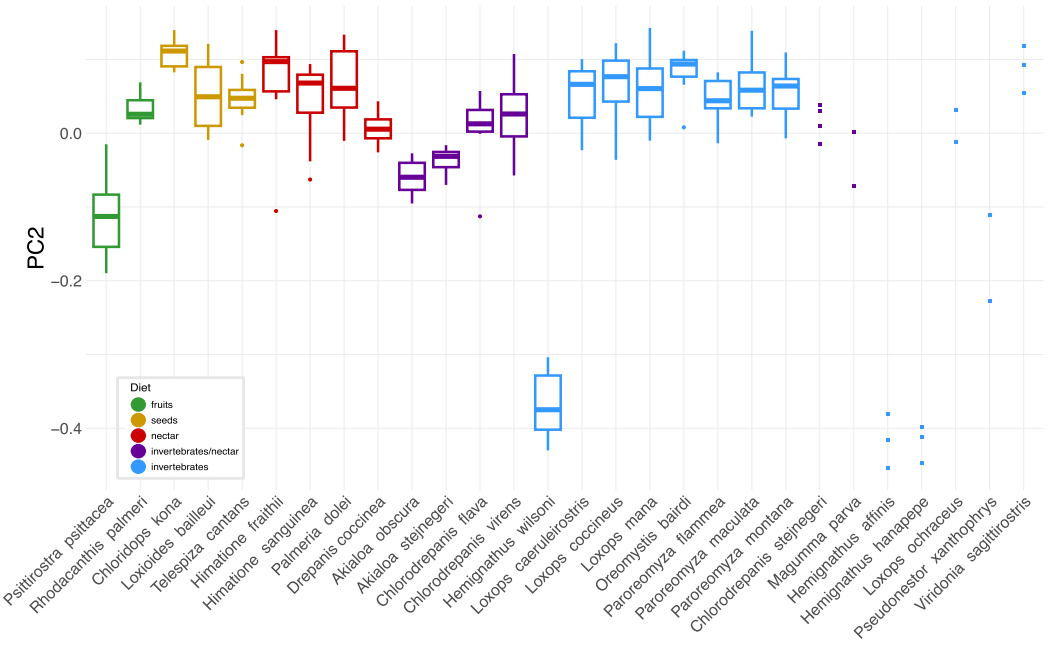

Figure S3: Boxplots showing the distribution of PC2 values for different species, categorized by diet (fruits, seeds, nectar, invertebrates/nectar, and invertebrates). Each boxplot represents species with 5 or more individuals, while individual squared points represent species with fewer than 5 individuals.

What a great adventure!